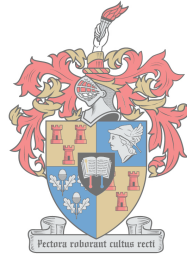


# Geometric Optimisation of Earth Retaining Quay Walls for the Marine Environment through the use of Ground Anchors

by

Alexander M. Green



UNIVERSITEIT  
iYUNIVESITHI  
STELLENBOSCH  
UNIVERSITY

*Thesis presented in fulfilment of the requirements for the degree of  
Masters in Engineering in the faculty of Engineering at Stellenbosch  
University*

Supervisor: Dr J A vB Strasheim

December 2018

# Declaration

By submitting this thesis electronically, I declare that the entirety of the work contained therein is my own, original work, that I am the sole author thereof (save to the extent explicitly otherwise stated), that reproduction and publication thereof by Stellenbosch University will not infringe any third party rights and that I have not previously in its entirety or in part submitted it for obtaining any qualification.

Date: ..... December 2018 .....

Copyright © 2018 Stellenbosch University  
All rights reserved.

# Abstract

Quay walls which accommodate the docking of marine vessels form an important part of port structures. This thesis focuses on the optimisation of precast concrete cantilever type quay walls with the incorporation of a tensioned ground anchor. With the use of this anchor concept the mass of these precast cantilever type quay walls can be optimised.

A case study of the Port of Saldanha, South Africa was used to provide design parameters such as structural loading, geotechnical information and a comparative as built design for input into the quay wall optimisation process.

The optimisation process consists of global structural system stability checks using working state design principles followed by the structural design of the precast concrete element at the ultimate limit state. A layout with a mass of 183 tons compared with the as built structure having a mass of 330 tons was determined for the equivalent 5.9m length of quay wall precast component. The required anchor force for this layout was 2752kN. This anchor force can be accommodated with a twin ground anchor system using ASDO500 M80/60 ground anchor bars manufactured by Anker Schroeder.

The mass reduction obtained will allow for the use of smaller and more readily available marine hoisting plant during the construction phase, and can markedly decrease cost of the overall port development project.

# Opsomming

Kaaimure wat die koepeering van seevarende voertuie akkommodeer, is 'n belangrike deel van hawe strukture. Hierdie tesis fokus op die optimalisering van voorafgegooide betonhoek tipe kaaimure met die gebruik van 'n grond spanningsanker. Met die gebruik van hierdie ankerkonsep, sal die massa van die betonhoek tipe kaaimure ge-optimaliseer kan word.

'n Gevallestudie van Saldanha Hawe in Suid Afrika was gebruik om die ontwerp grense, soos strukturele lading, geotegniese inligting en 'n bestaande bou ontwerp vir insette in die kaaimuur optimaliseringsproses, te verskaf.

Die optimaliseringsproses bestaan uit wereldwye strukturele sisteem stabiliteits reÃ«ls wat van werkende ontwerpbeginsele gebruik maak, gevolg deur die strukturele ontwerp van voorafgegooide beton elemente, in 'n beperkte vorm. 'n Uitleg met 'n massa van 183 ton word vergelyk met die bestaande struktuur met 'n massa van 330 ton, om die vergelykbare lengte van 5.9m vir die voorafgegooide kaaimuur te bepaal. Die nodige ankerkrag vir hierdie uitleg, was 2752kN. Hierdie ankerkrag kan bereik word met 'n dubbel anker grond sisteem wat ASDO500 M80/60 grond ankerbalke gebruik. Die balke word deur Anker Schroeder vervaardig.

Die vermindering in benodigde massa sal toelaat vir die gebruik van kleiner, maklike bekombare mariene hyserinstallasies in die konstruksie fase, wat na 'n aansienlike vermindering in die algehele hawe ontwikkelingsprojek kostes kan lei.

# Acknowledgements

- My Family for putting up with all of this over the last 18 months.
  - My Brother for always being there to distract me with a beer and drive me up the wall when I wondered to far down the rabbit hole.
  - My Dad for his words of encouragement and support along the way to my MEng and for always reminding me to read the question carefully.
  - My Mom for always being there to talk to, having a meal available whenever I wanted to come home and to check up on me to ensure I was working without her I would never have gotten this finished.
- My Grandmother for helping fund the furthering of my education.
- Dr Breda Strasheim for his guidance and wisdom while writing this paper.
- Murray and Roberts Marine, ZLH Consulting Engineers and Transnet for the use of the design documents from the Port of Saldanha expansion that formed the basis of my case study
- To the Officers, Andrew "Grumpy" Way without whom this thesis would of been finished a long time ago, Janeke "Turbo Dwarf" Volkmann for all the assistance during the first year of Masters and attempting to stop me procrastinating, Calvin "Pookie" Pagel for putting up with my rubbish for years and pushing me outside my comfort zone in our sporting endeavours.
- To the Heathens: Duaan, Ben, Shaun, Landi, Hans, Calvin, Marco, Nelia, Megs, Madrie for keeping me sane, well fed and with a drink never to far from hand, not in that particular order.
- To Brandon my oldest and least wise friend for always being up for a beer and the sharing of crazy stories.

# Contents

<b>Declaration</b>	<b>i</b>
<b>Abstract</b>	<b>ii</b>
<b>Opsomming</b>	<b>iii</b>
<b>Acknowledgements</b>	<b>iv</b>
<b>Contents</b>	<b>v</b>
<b>List of Figures</b>	<b>ix</b>
<b>List of Tables</b>	<b>xi</b>
<b>Nomenclature</b>	<b>xiii</b>
Abbreviations . . . . .	xiii
Symbols . . . . .	xiv
Roman . . . . .	xiv
Greek . . . . .	xiv
<b>1 Introduction</b>	<b>1</b>
1.1 Problem Statement . . . . .	4
1.2 Structure of this Thesis . . . . .	4
<b>2 Current Quay Wall Designs</b>	<b>6</b>
2.1 Solid Berth Designs . . . . .	6
2.1.1 Gravity Type Solid Berth Structures . . . . .	7
2.1.2 Sheet Pile Bulkheads . . . . .	10
2.1.3 Piled Structures . . . . .	11
2.2 Open Berth Designs . . . . .	12
2.3 Structures with Special Foundations . . . . .	13
2.4 Quay Wall Design Summary . . . . .	14
<b>3 Literature Review</b>	<b>15</b>
3.1 Design of Port Facilities . . . . .	15

3.2	Design of Gravity Type Quay Walls . . . . .	18
3.2.1	Cantilever Walls . . . . .	19
3.3	Design of Sheet Pile Bulkheads . . . . .	19
3.4	Structural Loading . . . . .	20
3.4.1	Lateral Earth Pressure . . . . .	21
3.5	Geotechnical Analysis . . . . .	23
3.5.1	Stability Against Sliding Failure . . . . .	23
3.5.2	Bearing Capacity . . . . .	24
3.5.3	Settlement and Tilt . . . . .	27
3.6	Lateral Support for Slope Stability . . . . .	27
3.6.1	Horizontal Anchors . . . . .	28
3.6.2	Tension Piles . . . . .	29
3.6.3	Anchors with a grout body . . . . .	30
3.6.4	Anchor Tie Details . . . . .	31
<b>4</b>	<b>Case Study: Saldanha Port Expansion</b>	<b>32</b>
4.1	Introduction . . . . .	35
4.2	Structural and Geotechnical Design Brief . . . . .	35
4.2.1	Design Parameters . . . . .	35
4.2.2	Design Loads . . . . .	36
4.2.3	Finite Element Method Analysis . . . . .	37
4.2.4	Serviceability Limit State . . . . .	37
4.3	Geotechnical Parameters . . . . .	38
4.3.1	Foundation Geology . . . . .	38
4.3.2	Back Fill Material Parameters . . . . .	40
4.4	Design Results . . . . .	41
4.4.1	Structural Design . . . . .	41
4.4.2	Geotechnical Results . . . . .	41
<b>5</b>	<b>Structural Analysis Framework and Design Assumptions</b>	<b>42</b>
5.1	Construction Methodology . . . . .	44
5.2	Design Load Cases . . . . .	46
5.2.1	Construction State . . . . .	46
5.2.2	Final State . . . . .	46
5.3	Design Assumptions . . . . .	46
5.3.1	Requirements for Stability . . . . .	46
5.3.2	Design Loads . . . . .	47
5.3.3	Geotechnical Parameters . . . . .	47
5.4	Optimisation Framework . . . . .	48
5.4.1	Optimisation Phase 1 . . . . .	48
5.4.2	Optimisation Phase 2 . . . . .	48
<b>6</b>	<b>Basic Geometric Configuration</b>	<b>49</b>
6.1	Geotechnical Limitations . . . . .	49

6.2	Inputs of Simplified Model . . . . .	51
6.2.1	Structural Configurations . . . . .	51
6.2.2	Analysis Methods . . . . .	53
6.3	Analysis Procedure of for Model Implemented using a MATLAB Script . . . . .	53
6.3.1	Computation Methodology . . . . .	57
6.4	Outputs of Simplified Model . . . . .	57
6.5	Recommendations Deduced from Analysis . . . . .	58
6.6	Configurations for Optimisation . . . . .	58
<b>7</b>	<b>Optimisation</b>	<b>59</b>
7.1	Further Reduction in Permutations . . . . .	59
7.2	Maximum Allowable Bending Moment in Section . . . . .	62
7.3	Reduction in Bending Moments Through Addition of Steel Ties . . . . .	62
7.4	Required Anchor Force for Structural Equilibrium . . . . .	64
7.4.1	Available Bar Anchors . . . . .	65
7.4.2	Required Anchor For Configuration . . . . .	66
7.5	Maximum Allowable Bending Moment Limitations . . . . .	67
7.5.1	Determination of Bending Moments for Selected Structural Configurations . . . . .	67
7.5.2	Effect of Additional Anchor Force on Bending Moments . . . . .	69
7.5.3	Final Bending Moments . . . . .	74
7.6	Cost Optimisation . . . . .	77
7.6.1	Material Costs . . . . .	77
7.6.2	Optimisation Process . . . . .	79
7.6.3	Total Cost of Each Configuration . . . . .	81
7.6.4	Additional Cost Influence: Reinforcing ties . . . . .	81
7.6.5	Cost Optimisation Conclusion . . . . .	81
7.7	Optimisation Conclusion . . . . .	82
<b>8</b>	<b>Conclusion and Recommendations</b>	<b>83</b>
8.1	Conclusion . . . . .	83
8.2	Recommendations for Further Research On Optimisation . . . . .	84
	<b>Appendices</b>	<b>85</b>
	<b>A List of Definitions</b>	<b>86</b>
	<b>B Foundation Profiles</b>	<b>89</b>
B.1	Chainages 0 to 175m; 350 to 620m . . . . .	90
B.2	Chainage 225m . . . . .	91
B.3	Chainage 375m . . . . .	92
B.4	Chainage 620m . . . . .	93
	<b>C Geotechnical Material Description and Properties</b>	<b>94</b>



## CONTENTS

viii

C.1	Marine Sands (Variably Calcretised) . . . . .	94
C.2	Residual Granite Soil . . . . .	95
C.2.1	Firm Residual Granite Soil (6m thick Layer) . . . . .	96
C.2.2	Stiff Residual Granite Soil (to bottom depth of foundation influence) . . . . .	96
C.3	Fluvial Sediments . . . . .	97
C.3.1	Fluvial Clay . . . . .	97
C.3.2	Fluvial Sand . . . . .	98
<b>D</b>	<b>As Built Counterfort Design</b>	<b>99</b>
<b>E</b>	<b>MATLAB Script Input Example</b>	<b>102</b>
<b>F</b>	<b>MATLAB Scripts</b>	<b>103</b>
F.1	Simplified Model Script . . . . .	103
F.2	Simplified Model Output Analytics . . . . .	108
<b>G</b>	<b>Full Output of Phase 1</b>	<b>110</b>
<b>H</b>	<b>Example Calculation for Moment Equilibrium</b>	<b>116</b>
<b>I</b>	<b>ASDO Bars</b>	<b>119</b>
<b>J</b>	<b>History of Port Structures</b>	<b>121</b>
<b>K</b>	<b>Maritime Transportation Vessel Details</b>	<b>123</b>
K.0.1	Transport Capacity . . . . .	123
K.0.2	Vessel Vertical Dimensions . . . . .	124
K.0.3	Vessel Horizontal Dimensions . . . . .	127
K.1	Commodities and Types of Maritime Transportation Vessels . . . . .	127
K.1.1	Conventional Cargo Vessels . . . . .	128
K.1.2	Bulk Cargo Vessels . . . . .	131
K.1.3	Container Vessels . . . . .	136
	<b>List of References</b>	<b>139</b>

# List of Figures

1.1	Example of a Port Layout Source: Google Earth(2017)	3
1.2	Location of the Port of Saldanha Source: Google Earth(2018)	5
2.1	Examples of Gravity Type Structures from Tsinker (1998)	8
2.2	Sheet Pile Bulkheads (Tsinker, 1998)	11
2.3	Relieving Platform with Front Sheet Pile Wall (Tsinker, 1998)	12
2.4	Open Berth Designs (Tsinker, 1998)	13
3.1	Design Steps for Gravity Type Walls (Tsinker, 1998)	18
3.2	Müller-Breslau solution for frictional cohesionless soil (Clayton <i>et al.</i> , 2014)	22
3.3	Types of horizontal anchorages (Centre for Civil Engineering Research and Codes, 2005)	29
3.4	Layout and cross section of tensile anchorages (Centre for Civil Engineering Research and Codes, 2005)	30
4.1	As built set of 4 precast units	33
4.2	As Built set of 4 precast units with proposed capping beam	34
4.3	Plan Showing Relevant Borehole Positions	39
5.1	Proposed Geometry of Section	43
5.2	Construction Structural State	44
5.3	Final Structural State	45
6.1	Critical global slip circle plane during the construction phase	50
6.2	The relationship between FOS and the distance of the slip plane from Wall face	50
6.3	The relationship between FOS and the distance of the slip plane from Wall face for FOS less than 1.2	51
6.4	MATLAB Analysis Procedure	54
7.1	Comparative Bending Moments at Anchor Heights 16.5m through 17.5m	61
7.2	Layout of Support ties	63
7.3	Comparative Bending Moments of Front Wall with and without ties	64
7.4	Example of 2D Frame Finite Element Model	67
7.5	Comparative Wall Bending Moments Between Lengths of Base Projection	68

## LIST OF FIGURES

x

7.6	Comparative Base Projection Bending Moments Between Lengths of Base Projection . . . . .	69
7.7	The effect of increased anchor force on the Bw9 Configuration wall bending moments . . . . .	70
7.8	The effect of increased anchor force on the Bw9 Configuration base projection bending moments . . . . .	71
7.9	The effect of increased anchor force on the Bw8.5 Configuration wall bending moments . . . . .	72
7.10	The effect of increased anchor force on the Bw8.5 Configuration base projection bending moments . . . . .	72
7.11	The effect of increased anchor force on the Bw8 Configuration wall bending moments . . . . .	73
7.12	The effect of increased anchor force on the Bw8 Configuration base projection bending moments . . . . .	74
7.13	Comparative Wall Bending Moments of Configurations Bw8, Bw8.5 and Bw9 at Anchor Force 2752kN . . . . .	75
7.14	Comparative Base Projection Bending Moments of Layouts Bw8, Bw8.5 and Bw9 at Anchor Force 2752kN . . . . .	76
B.1	Foundation Profile Design Parameters (Chainages 0 to 175m & 350 to 620m)	90
B.2	Foundation Profile Design Parameters (Chainage 225m) . . . . .	91
B.3	Foundation Profile Design Parameters (Chainage 375m) . . . . .	92
B.4	Foundation Profile Massively Calcretised Marine Sands (Chainage 620m) . . . . .	93
D.1	As Built Precast Element Design . . . . .	100
K.1	All Dimensions of Maritime Vessels (Marine Study, 2016) . . . . .	125
K.2	Layout of Plimsoll Mark (MarineWiki, 2010) . . . . .	126
K.3	General Cargo Vessel 'Sakti' (Ligteringen and Velsink, 2012) . . . . .	130
K.4	Very Large Ore Carrier (VLOC) 'Peene Ore' (Ligteringen and Velsink, 2012)	132
K.5	Very Large Crude Carrier (VLCC) 'New Vanguard' (Ligteringen and Velsink, 2012) . . . . .	134
K.6	The difference between LNG tankers and LPG tankers (Ligteringen and Velsink, 2012) . . . . .	135
K.7	The development of Liquid Gas Tankers (Ligteringen and Velsink, 2012) . . . . .	136
K.8	Jumbo container vessel " P&O Nedlloyd Southhampton" (Ligteringen and Velsink, 2012) . . . . .	138

# List of Tables

4.1	Foundations: Minimum Factors of Safety (FOS) . . . . .	41
6.1	Phase 1 Output (sample). . . . .	58
7.1	Load Factors from EN1990:2002+A1 (ENCEN, 2005) . . . . .	60
7.2	Required Anchor Forces for Structural Equilibrium for ULS design and Working States Design . . . . .	60
7.3	Required Anchor Forces for Moment Equilibrium and Resulting Maximum Bending Moment . . . . .	61
7.4	Required Anchor Forces for Moment Equilibrium at ULS compared to Chapter 6 WSD required Anchor Force . . . . .	65
7.5	Available Bar Anchor Capacities and Costs . . . . .	66
7.6	Required Bar Anchors for Design Anchor Forces . . . . .	66
7.7	Bending Moments Summary at Anchor Force 2752kN for Layouts Bw8, Bw8.5 and Bw9 in Wall . . . . .	75
7.8	Maximum Bending Moments at Anchor Force 2752kN for Layouts Bw8, Bw8.5 and Bw9 in the Base Projection . . . . .	76
7.9	Calculated Cost per Ton of ASDO500 grade material . . . . .	78
7.10	Cost per Ton of ASDO500 grade material due to inflation in South African Rand . . . . .	78
7.11	Cost of ASDO500 Bars with tensile working capacity . . . . .	79
7.12	Design Bending Moments in each Section . . . . .	80
7.13	Cost of Steel Reinforcement for Listed Configurations . . . . .	80
7.14	Cost of Concrete for Listed Configurations . . . . .	80
E.1	Phase 1 Input Example . . . . .	102
G.1	Phase 1 Outputs . . . . .	110
G.1	All Permutations for Phase 2 (cont.). . . . .	111
G.1	All Permutations for Phase 2 (cont.). . . . .	112
G.1	All Permutations for Phase 2 (cont.). . . . .	113
G.1	All Permutations for Phase 2 (cont.). . . . .	114
G.1	All Permutations for Phase 2 (cont.). . . . .	115

*LIST OF TABLES*

xii

H.1	Permutation Input Parameters . . . . .	116
H.2	Load Factors . . . . .	116
H.3	System Forces at ULS and Moment Arms . . . . .	117
H.4	System Moments at ULS . . . . .	117
H.5	Moment Equilibrium Result . . . . .	118
K.1	Types of Break-Bulk Cargo and their Handling Methods. (Ligteringen and Velsink, 2012) . . . . .	128
K.2	Bulk Carrier Types and Capacity. (Ligteringen and Velsink, 2012) . . . . .	131
K.3	Container Vessel Characteristics. (Ligteringen and Velsink, 2012) . . . . .	137

# Nomenclature

## Abbreviations

**2D** Two Dimensional

**3D** Three Dimensional

**BH** Borehole

**CD** Chart Datum

**FE** Finite Element

**FEA** Finite Element Analysis

**FEM** Finite Element Method

**FOS** Factor of Safety

**MSL** Mean Sea Level

**HDPE** High Density Polyethylene

**SLS** Serviceability Limit State

**ULS** Ultimate Limit State

**UB** Universal Beam

**WSD** Working States Design

## Symbols

### Roman

$c$  Soil Cohesion

$E$  Young's Modulus

$f$  Frictional Coefficient

$g$  Gravity ( $9.81 \text{ m/s}^2$ )

$t$  Thickness

$z$  depth of foundation

### Greek

$\alpha$  Wall Inclination

$\beta$  Backfill Slope Angle

$\gamma$  Density

$\delta$  Wall Friction Angle

$\lambda$  Soil Vertical Component Angle

$\phi$  Soil Friction Angle

$\Sigma$  Sum of

# Chapter 1

## Introduction

"Civil Engineering is the art of directing the great sources of power in Nature for the use and convenience of man."

**Thomas Tredgold**

Nowhere is the requirement for directing the great sources of power in nature more true than with the design of coastal infrastructure. This is as these structures are exposed to many more of the powers of nature while performing their duties of protecting the cities and ships that allow for maritime trade. Maritime trade has allowed the human race to expand to all corners of the globe and helped create the thriving world economy. Of these coastal infrastructure projects arguably the most vital is the port themselves.

Ports play such an important part of the world economy as maritime transport has been the least expensive option for transporting large volumes of goods and people around the world since ancient times. Therefore humans have constantly been increasing the number of ports around the world to improve the capabilities and efficiency of international maritime transport.

While over the last century aeroplanes have overtaken maritime vessels as the primary form of transporting people around the globe, these vessels still transport the majority of bulk goods. As such ports play such a vital role in world trade and a countries economy. Port infrastructure projects are often some of the most expensive projects undertaken by any country. To make these projects affordable for a country all aspects of the port are required to be optimised. The port comprises of two primary components, the breakwater that protects the port and the quay side where vessels berth and are loaded and unloaded. The breakwater is the most vital part of any port as it protects both the vessels docked within but also the infrastructure required for operation of the port. Thus the breakwater typically receives the largest portion of the budget during the construction phase of the port. While the quay side structure is not always the next most expensive component after the breakwater it does form the linchpin of the port. This is as a large portion of the operational area of the port is located behind the quay side. By designing



an optimised element for use in the quay side wall a large amount of money can be saved during construction of the port.

Throughout history various designs have been used for the construction of quay walls. While these designs vary as the site conditions for each port are different they also vary due to advances in technology that have allowed designs to be developed that could not be developed using more ancient techniques. A summary of the history of port infrastructure is given in Appendix J, while Appendix K provides details on the aspects of the vessels that make use of ports and that would influence the design of port infrastructure. A list of definitions is included Appendix A to provide detail on certain specialist terms used in coastal design.



Figure 1.1: Example of a Port Layout Source: Google Earth(2017)

## 1.1 Problem Statement

The aim of this thesis is to develop a modified cantilever type quay wall with optimised physical geometry for a section with the minimum mass, this is to allow for simplified and more rapid construction through the incorporation of tensioned ground anchors into the design. The current designs make use of a reinforced concrete counterfort to reinforce the wall of the section, the counterfort adds a considerable weight to the overall weight of the entire section, this leads to the requirement of larger plant during the construction phase. Due to the complexity of the design of marine construction projects a case study was selected to allow for comparative purposes and to provide specific values for loads and site conditions required for the design. The case study that is used for this design is the expansion of the Saldanha Bay cargo quay, the expansion for the cargo quay was completed in May 1998. The port of Saldanha Bay is located on the the west coast of South Africa, 140 km north of Cape Town. Figure 1.2(a) shows the area surrounding the Port of Saldanha whereas Figure 1.2(b) shows the current layout of the port after the expansion, the location of the current multi-purpose quay is marked.

## 1.2 Structure of this Thesis

Chapter 2 provides background information on the various types of structures that can be used as quay wall. Chapter 3 provides technical details on the methods of calculation and design used in this optimisation of the quay wall. Chapter 4 provides as designed and built details of the case study. Chapter 5 describes the methodology of optimisation and all details used. Chapter 6 describes is the first phase of optimisation and is used to determine many of the minimum design parameters required for the final optimised design. Chapter 7 describes the various methods and the process used in the determination of the final optimised design. Chapter 8 details the final optimised design and provides suggestions on further possible avenues of research and optimisation.



(a) View of Saldanha Bay



(b) Layout of Port of Saldanha

Figure 1.2: Location of the Port of Saldanha Source: Google Earth(2018)

## Chapter 2

# Current Quay Wall Designs

All ships require a berth against which to dock safely. While there are various types of berthing structures they mainly provide a vertical front against which the ships dock. The vertical fronts of these berths are constructed using one of two methods, either a solid berth structure or an open berth structure.

Open berth structures consist of slabs supported atop piers where the water is able to enter the area below the slabs, whereas solid berth structures consist of vertical front wall which is constructed to resist all horizontal loads. While this thesis will be primarily focused on solid berth structures a summary will be provided on open berth structures to allow for a full understanding of the design options for construction of berthing structures (Thoresen, 2003).

### 2.1 Solid Berth Designs

All solid berth designs can be broken down into four primary groups, gravity type structures, sheet pile bulkheads, piled structures and structures with special foundations (Tsinker, 1998). Each of these groups will be discussed in the sections below as these designs influenced the proposed design of the new element.

No two ports have the same design parameters and limitations, this results in difficulties when creating accurate guidelines for the choice of berthing structures during the design phase of the port development. These structures should be designed and built to safely resist all loads applied while attempting to minimise the cost of the structure (Thoresen, 2003). Thus a detailed background and understanding of the berthing options are required to ensure that the most cost efficient option is selected for the final design. Sections 2.1.1 to 2.1.3 provide detail on the most common berthing option designs of their type.

### 2.1.1 Gravity Type Solid Berth Structures

Gravity type quay walls make use of the element's mass and friction with the soil to ensure that the element does not displace once loads are applied. As a result of this, single elements can weigh hundreds of tons for a short length of the total quay wall length. There are various types of gravity type walls, the most common designs are given in Figure 2.1.

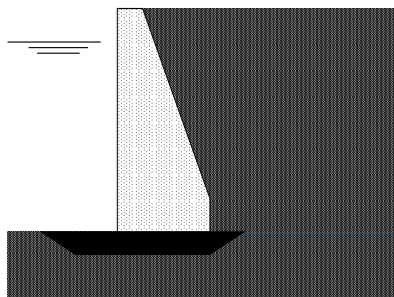
All of the designs given in Figure 2.1 have advantages and disadvantages. These would be used to influence the selection of the final design dependant on site conditions such as required loading and geotechnical limitations.

#### Cast-in-place Concrete and Masonry Walls

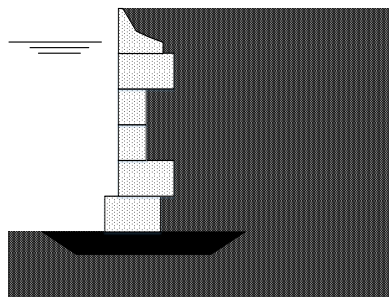
Figure 2.1(a) provides a cross section of a cast in place concrete or masonry wall, these walls are built in a dry environment which is created through the construction of a cofferdam that is then pumped dry. The primary advantage of this technique is that construction of the wall is completed using standard construction techniques which results in a better quality final structure. The disadvantage is that the construction of the cofferdam is very expensive. As a result this technique is most suitable where a short section of cofferdam wall is required to be constructed to allow for a large dry area behind the wall. An alternative method is that the entire port basin is excavated in a dry environment before being opened up to the ocean.

#### Prefabricated Concrete Blocks

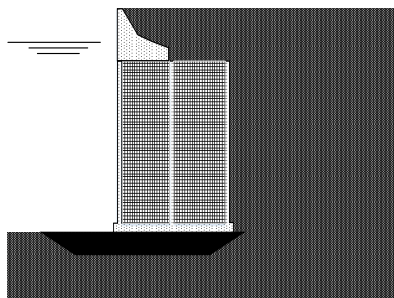
Figure 2.1(b) provides a cross section of a prefabricated concrete block wall. This is one of the oldest techniques used for construction on quay walls. This technique is the modern equivalent to the ancient method for constructing quays using large stone blocks. Quays built using this techniques are usually constructed in a wet environment where each concrete block is lowered by crane on to the block below. The advantage of this technique is that it is highly durable as often these blocks are constructed out of mass concrete and thus contain zero steel reinforcement. The primary disadvantage of this technique is the mass of each block as an individual block can weight upwards of 100 tons. A further disadvantage is that current draught of ships in operation today require many more blocks to be stack in order construct a quay wall providing sufficient depth for a vessel to dock against.



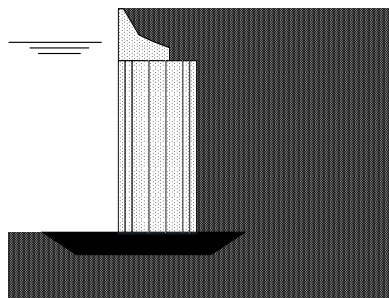
(a) Cast-in-Place Concrete or Masonry Walls



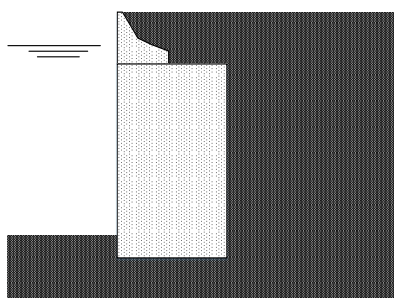
(b) Prefabricated from Concrete Blocks



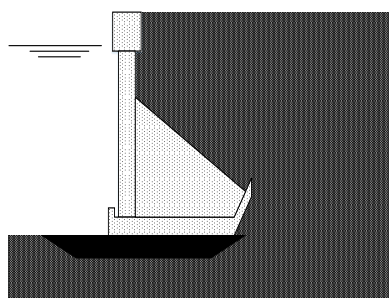
(c) Floated-in-Caissons



(d) Large Diameter Cylinders



(e) Large Diameter Sheet Pile Cells



(f) Cantilever Walls

Figure 2.1: Examples of Gravity Type Structures from Tsinker (1998)

### **Floated-in-Caissons**

Figure 2.1(c) provides a cross of a precast caisson unit. Caissons overcome many of the problems that surround the use of prefabricated concrete blocks as the caisson can be constructed to the required height for a vessel of any draught at a much lower precast element weight. The primary problem that the use of caissons overcomes, is the large weight associated with stacking the prefabricated concrete blocks. This is due to the caisson being constructed as a hollow cellular element. Thus the caisson is able to be floated or transported by ship to its final destination and then filled with rock and other loose material. The primary disadvantages of caissons are the construction of the elements is labour intensive and the transportation of these elements as they are easily damaged. Due to the ease of damage to the element, transportation can only be done in calm weather conditions. Damage caused during transportation can lead to a loss in structural integrity of the element and the requirement that the element be scrapped.

### **Large Diameter Cylinders**

Figure 2.1(d) is a version of this design where multiple smaller diameter (4-6 m) cylinders are used rather than a single large diameter (6+m) cylinder. This design is an extension of floated-in caisson design, these structures are essentially bottomless large diameter pre-cast concrete cylinders. Once in place these cylinders are filled with a granular fill which could be either dredged material or material brought from inland sources. The disadvantage of this design is that heavy lifting equipment is required for the movement of these structures both onshore and offshore. When these cylinders get to be very large they are often cut horizontally into two separate cylinders and then reconnected once in final position.

### **Large Diameter Sheet Pile Cells**

Figure 2.1(e) is an example of the structural layout for large diameter sheet pile cells. These structures are very similar to the large diameter cylinder design. Where the large diameter cylinders are made of precast concrete or welded steel, the sheet pile cell is constructed from interlocked sheet pile elements to form a cylindrical element. Once filled the interlocked sheet piles act in tension which forms a structure able to resist both lateral and vertical forces and loads. The advantage of this design is that it is lighter than a similar structure using large diameter cylinders but many of the sheet pile designs are patented which increases the cost of purchase for each pile cell, this drives up the cost of this type of structure.



### **Cantilever Walls**

Cantilever walls as shown in Figure 2.1(f) are most commonly make use of a reinforced concrete section to reinforce the wall, this reinforced concrete section is know as a counterfort. Thus this particular style of quay wall was is known as a counterfort style quay wall. These sections are mainly precast reinforced concrete monolithic elements that are then lowered into the water once the concrete has cured sufficiently. The advantage of this design is that it is a lighter element when compared to prefabricated concrete block type walls for the required height of the quay wall. The disadvantage is that due to the weight of the element and the complex geometry it results in a slower pace of construction when compared to other designs. Further details for the design of these style of walls will be provided in Section 3.2.1.

#### **2.1.2 Sheet Pile Bulkheads**

Sheet pile bulkheads are constructed from either steel or reinforced concrete piles. These elements are cantilevered out of the sea floor as shown in Figure 2.2(a), These structures make use of the stiffness of the bulkhead material and element section to distribute the loads applied to the quay wall into the sea floor. These bulkheads can be reinforced through the addition of ground anchors such as in Figures 2.2(b) and 2.2(c). The suitability of these designs are highly dependant on the geotechnical make-up of the sea floor material.

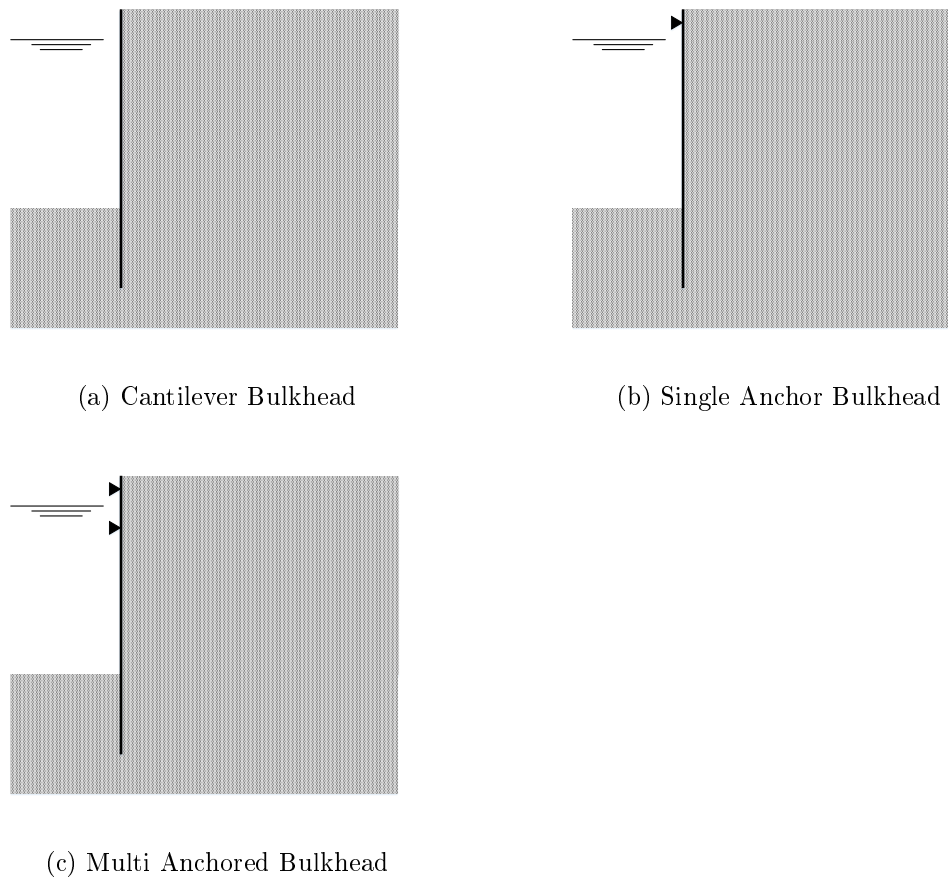


Figure 2.2: Sheet Pile Bulkheads (Tsinker, 1998)

### 2.1.3 Piled Structures

Piled structures are used for both open and solid berths, the types of piled structures used for open berths are given in Section 2.2. The stability of these types of structures is dependent on the bearing and lateral load carrying capacity of the piles used.

The layout of the piles used is dependent on the type of loads that the structure is exposed to. These include vertical and horizontal loads resulting from both live and dead loads on the structures, along with other lateral loads such as mooring loads and those induced by earth pressure resulting from the backfill material. Due to the variety of forces applied to piles there are various different materials and cross sections, the choice of which is not purely based on the loads applied but also the length of the pile and its foundation material. A further aspect that effects the choice of pile is how the pile is going to be driven into the foundation material, through methods such as hammering, vibration or the use of water jets.

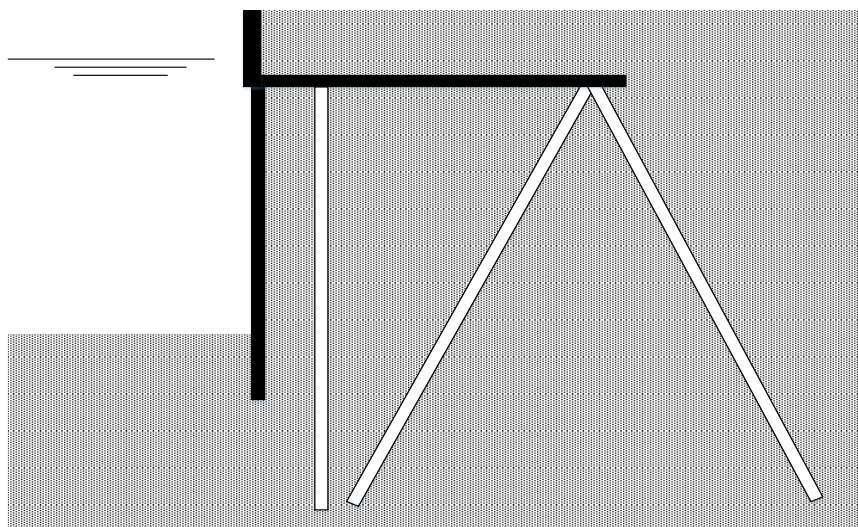
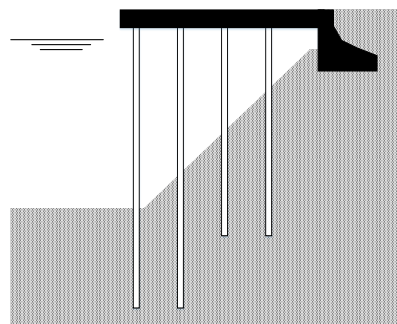


Figure 2.3: Relieving Platform with Front Sheet Pile Wall (Tsinker, 1998)

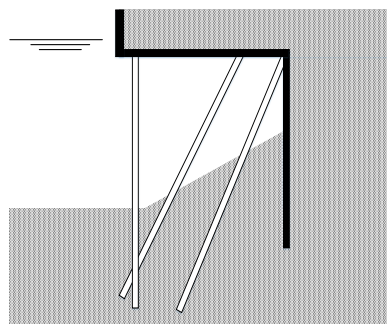
## 2.2 Open Berth Designs

This style of structure differs from the solid berth designs as the vertical distance between the seabed and the operational deck is not retained by a vertical wall but rather a slope in many cases. These structures consist of a horizontal deck that most often runs parallel to the shore or a pre-existing structure. This deck is supported on a combination of vertical and raked piles. Beneath the deck, the soil slope requires protection from the various currents, these include both those natural and artificial, that are found inside ports (Centre for Civil Engineering Research and Codes, 2005).

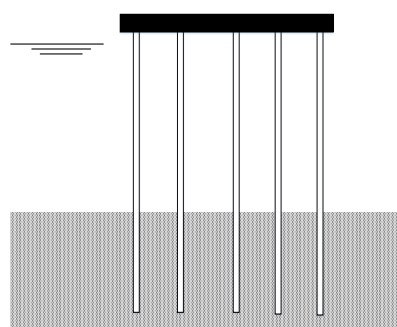
Figure 2.4(a) is an example of an open berth design supported on vertical piles where all horizontal load is transferred into the supporting earthen structure through the deck. Figure 2.4(b) provides a layout of an open berth that makes use of a relieving structure to transfer the horizontal loads into the foundation material via raked piles. Figure 2.4(c) is an example of a traditional wharf structure this structure does not make use of an earthen support at the deck level rather all loads both vertical and horizontal are carried on a combination of raked and vertical piles into the foundation material.



(a) Pile Supported Platform



(b) Relieving Platform with Rear Sheet Pile wall



(c) Wharf

Figure 2.4: Open Berth Designs (Tsinker, 1998)

### 2.3 Structures with Special Foundations

This section will cover the various special designs that are used for very specific soil conditions or vessel types. In their most basic form, these types of structures comprise a platform resting on top of some form of special foundations. There are various different types of special foundations, a few examples of the more common ones are given below:

- Steel or concrete screw piles.
- Piles with localised diameter changes.
- Deep Caissons.

Besides the types given above there are other types that are formed by combinations of open and closed berth techniques and thus these structures do not fall under the categories of either open or closed berths. An example of this is a piled structure such as those given in Figure 2.4(a), where metal sheeting is added to the external face of the piles to convert this open berth quay to a solid berth. This could have been done for a variety of reasons, such as for docking a different sort of vessel than was originally designed for or to alter the water flow patterns within the port.

## 2.4 Quay Wall Design Summary

The designs above are not a complete collection of all possible quay wall designs but a collection of the more common designs and those designs used as the basis of more complex designs. Each of these designs has their advantages and disadvantages that would influence the selection of a design for a specific site. Further detail on the parameters that influence the design of the optimised design in this research can be found in Sections 3.2 and 3.3.

## Chapter 3

# Literature Review

### 3.1 Design of Port Facilities

Prior to beginning the structural design, the primary functional requirements that the quay must satisfy are defined in consultation with the client, port operator and the manager of the quay side facilities. These requirements could change over the life span of the quay and thus consideration for future changes need to be planned during this phase. These requirements are then set down as terms of reference for the project, over the design stage period these terms of reference are refined and accurately defined as more detailed information is obtained. These terms of reference are only translated into the structural design during a later stage of the design phase. This is as the structural design is of no consequence to the operators of the completed quay facilities (Centre for Civil Engineering Research and Codes, 2005; Agerschou *et al.*, 2004).

During the planning phase of a port it is required that certain requirements need to be coordinated and harmonised by both quay operator and manager with the aim of removing impossible or conflicting situations that would have an impact on the structural design of the ports elements. The subjects that fall under this set of requirements are the following (Centre for Civil Engineering Research and Codes, 2005):

- (a) Arrangement and layout of the port.
- (b) Basis of design for front of the quay.
- (c) Determination of depth of water for operation.
- (d) Possible load combinations.
- (e) Clarity on internal interaction of forces due to external loads on the structure.

While the requirements given above would govern the basic design, consideration needs to for future actions on the structure. The quay in later in it operational life cycle could be exposed to large variations in wind, tide, currents and waves. The effect of long

term sea level rise due to climate change is consideration as this would have an impact on the currents, tidal variations and wave action within the port and surrounding areas. These variations can result in flooding, extreme low water levels, wind and wave damage, erosion and siltation. Thus quay facilities need to be designed for low probabilities of occurrence of the following:

- (a) Interruption of cargo-handling operations as a result of flooding and/or wave action.
- (b) Interruption of vessel access to the facilities or the requirement of the vessels to leave the facility due to wind, extreme water levels, currents, waves or a combination of all of these.
- (c) Damage to breakwaters and other port structures due to wave, current or wind action.
- (d) Damage to quays and other berthing platforms caused by docked ships exposed to wave, current or wind action.

This probability of occurrence should be based upon the additional economic and/or financial costs of the facilities and the economic/or financial benefits as a result of the reduction in damage and/or interruption of port operations. Thus the major design parameters which have to be chosen based upon their probability of occurrence are (Agerschou *et al.*, 2004):

- (a) Extreme high water levels causing flooding of quays leading to interruption of cargo handling along with damage to cargo and quay side infrastructure.
- (b) Extreme low water levels causing vessels to leave their berths or vessels not being able to enter the port or berth.
- (c) Extreme wind conditions causing:
  - (i) Interruption of cargo handling operations.
  - (ii) Vessels having to leave berths or not being able to dock at berth.
  - (iii) Damage to buildings and port side infrastructure.
- (d) Extreme currents causing:
  - (i) Interruptions with the arrival and departure of vessels.
  - (ii) Erosion damage to structures.
- (e) Extreme wave action causing:
  - (i) Damage to breakwaters.
  - (ii) Interruptions of cargo-handling operations.
  - (iii) Vessels having to leave berths or not being able to dock at berth.

- (iv) Siltation of berth basin and/or port access channels.
- (f) Extreme environmental occurrences causing damage to all port infrastructure such as earthquakes or tsunamis.



## 3.2 Design of Gravity Type Quay Walls

The design of quay walls is a complex procedure as along with all the requirements given in Section 3.1 there are the various other limiting factors such a geotechnical conditions that could limit the choice of designs from those given in Chapter 2. As explained in Section 2.1.1 this style of wall falls under the category of gravity style quay walls. Gravity style quay walls are usually designed according to the sequence laid out in Figure 3.1.

As the Figure 3.1 shows the design process is primarily one of iteration, to find the best and most economical solution. The best and most economical design will have to satisfy the primary functional requirements this is done by balancing various, often conflicting aspects such as durability, robustness and construction costs (Tsinker, 1998).

Prior experience gained during the construction of quay walls under similar conditions would play an important decision making input during the design process. The final result of the design process must satisfy the additional condition that the quay can be constructed in a manner that all risks are of an acceptable level and can be easily managed (Centre for Civil Engineering Research and Codes, 2005).

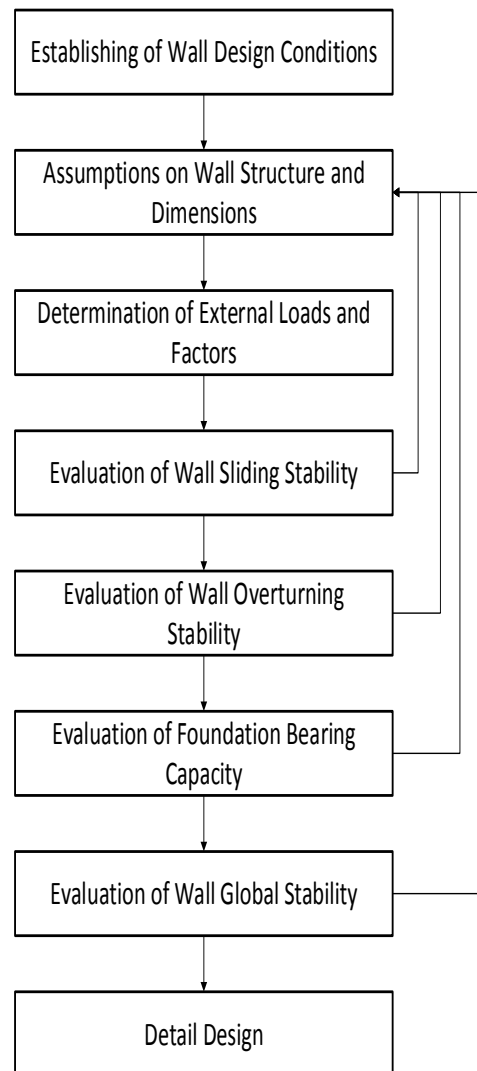


Figure 3.1: Design Steps for Gravity Type Walls (Tsinker, 1998)

### 3.2.1 Cantilever Walls

This style of wall owes its stability to the weight of the concrete structure along with the weight of the backfilled earth resting on it. The weight of the soil on the base slab helps build up the shear stresses in the subsoil to create an opposing moment to the one created by the horizontal soil pressure. This method is mainly of interest where the bearing capacity of the foundation soil is not sufficient for a heavier element such as a concrete block, as shown in fig. 2.1(b). Cantilever walls can be built in a dry construction pit or on the water side. For the first case a large construction pit is required with a dewatering system that is able to keep the construction area dry. In the second case, the structural elements are prefabricated in a construction yard and transported to site. These precast elements are then placed using heavy lifting equipment from either the water's edge or from a floating platform. The costs for both of these cases is high and thus this style of wall is only used for long quay walls where the design of each element is replicated many times. To ensure that washing out of backfill material is prevented the joints between elements must be sealed, this is done by inserting a grout sock which is inserted between the elements thus forming the seal (Centre for Civil Engineering Research and Codes, 2005).

## 3.3 Design of Sheet Pile Bulkheads

Sheet pile bulkheads are commonly used in marine engineering as they have proven to be a viable and economic option for waterside construction, provided the required wall height does not exceed 20m. This system requires that the seabed allows for the driving of piles while still being capable of resisting the loads applied to the sheet pile system. The wall is treated as a flexible element and is distinguished by the material of the sheet pile (steel, wood or concrete), the method of support for the sheet pile and the construction sequence of the wall.

The type of sheet piling selected for each project is primarily based upon the structural and economic aspects of the project. Other parameters that need to be taken into account during the design phase such as the pile driving conditions, allowable wall deflections, water tightness of the wall, required durability of the wall and resistance to loads created while the vessel is berthed this includes both berthing and mooring loads (Tsinker, 1998).

These bulkheads are distinguished as either cantilevered (Figure 2.2(a)) or anchored (Figures 2.2(b) and 2.2(c)). The anchored systems are then further classified according to the type of anchor system used to support the bulkhead. Detail on the various anchorage systems is given in Section 3.6.

### 3.4 Structural Loading

The various loads that can be applied to marine structures can be defined in four basic categories:

- Loads from the water side of the structure.  
These loads are primarily those resulting from environmental factors such as waves, wind, currents and ice.
- Loads from the landward side of the structure.  
These loads are typically include the weight of the structure, the vertical and horizontal components of the soil pressure, as calculated in Section 3.4.1 and hydrostatic pressure resulting from the groundwater behind the structure.
- Loads resulting from port operation.
  - Vessel berthing and mooring forces along with the effects of wind, waves and currents on these loads.
  - Vertical and horizontal friction forces between the vessel and fenders during berthing operations when the vessel has some velocity as changes in water level caused by tidal change.
  - Operation loads such as the moving of cargo and mobile cargo handling equipment.
- Loads due to environment effects.
  - The loads created by temperature fluctuations can have a substantial effect on the spacing of expansion joints.
  - Environmental loads such as those created by a tsunami or a seismic event.

The loads on marine structures are classified in a similar manner as those loads on more common inland structures, these load classifications are *permanent*, *temporary* and *special*.

The *permanent loads* on the structure include not only the weight of the structure but also the weight of all permanent structures situated on or near the marine structure. These permanent structures include warehouses, administration offices and fixed cargo handling equipment such as conveyor belts.

The *temporary loads* on the structure include those that result from dock operation and those arising from environmental factors. The dock operation loads include those from the operational surcharge, resulting from tidal lag and the forces from vessels berthing and any mooring loads induced by the vessels once berthed.

*Special loads* are used to classify loads that fall outside of normal operations this includes accidental loads, such as those from a vessel crashing into the structure or loads resulting from some natural phenomenon such as an earthquake or tsunami or loads resulting from the use of a specialist piece of equipment that is not required for normal operations (Tsinker, 1998).

### 3.4.1 Lateral Earth Pressure

Lateral earth pressure is defined as the pressure exerted by the soil against a surface surrounded by a mass of soil. The magnitude of the soil pressure is dependant on the properties of the soil, geometry of the surface and the type of soil-structure interaction that occurs such as the displacement of the surface.

The relationship between lateral earth pressure and wall displacement is defined as *at rest*, *active* or *passive*. Active or passive soil pressures occur where the relative displacement between the soil and the structure may cause the soil to expand forcing the structure away from its original position, known as active pressure, or loads causing the soil to contract such as caused by a vessel pushing up against the quay wall during berthing operations, known as passive pressure. At rest pressure occurs where no deformations or displacements of the structure occurs, this is viewed as a highly conservative design option (Tsinker, 1998).

Various theories have been developed for the calculation of the lateral earth pressures most notably those developed by Coulomb(1776) and Rankine(1857). These theories are effective for regular retaining wall but for cantilevered retaining walls the assessment of the design parameters and mechanisms is more complicated. This complexity is a result of the length of the cantilever base, with a shorter cantilever base the stresses on the virtual back of the wall could not be considered similar to those obtained using Rankine's theory. As a result of this a different theory is used, the Müller-Breslau solution allows for the computation of these stresses acting on the virtual back of wall (Clayton *et al.*, 2014). Equations (3.4.1) and (3.4.2) provide the Müller-Breslau solution equations for the calculation of  $K_{ah}$  and  $K_{ph}$ , with parameters and parameter details given in Figure 3.2.

$$K_{ah} = \frac{\cos^2(\phi + \alpha)}{\cos^2\alpha \left[ 1 + \sqrt{\frac{\sin(\phi + \delta)\sin(\phi - \beta)}{\cos(\alpha - \delta)\cos(\alpha + \beta)}} \right]^2} \quad (3.4.1)$$

$$K_{ph} = \frac{\cos^2(\phi - \alpha)}{\cos^2\alpha \left[ 1 + \sqrt{\frac{\sin(\phi + \delta)\sin(\phi + \beta)}{\cos(\alpha + \delta)\cos(\alpha + \beta)}} \right]^2} \quad (3.4.2)$$

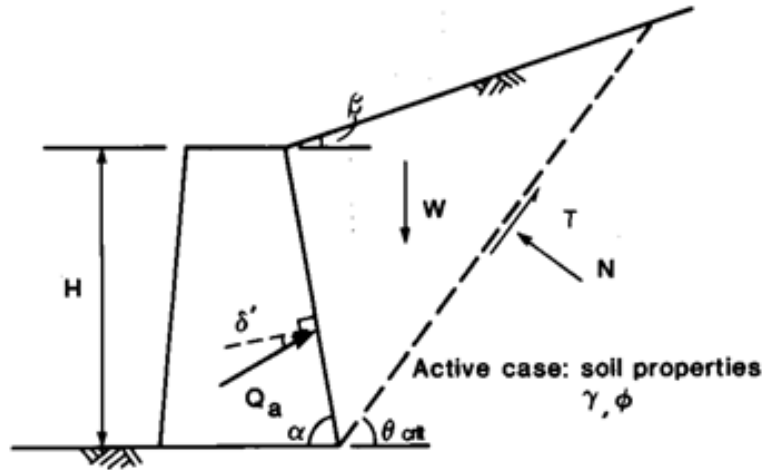


Figure 3.2: Müller-Breslau solution for frictional cohesionless soil (Clayton *et al.*, 2014)

Where:

- $\phi$ : Friction Angle
- $\alpha$ : Wall Inclination (Angle -  $90^\circ$ )
- $\beta$ : Backfill Slope
- $\delta$ : Wall Friction ( $\frac{2}{3}\phi$ )

The horizontal earth pressure resulting from an additional surcharge is calculated according to Equation (3.4.3), where  $K$  is either the  $K_{ah}$  or  $K_{ph}$  value calculated depending on relationship between the soil and the structure,  $q$  is the pressure of the additional surcharge. This pressure has a rectangular distribution.

$$\text{SurchargePressureHorizontal} = K * q \quad (3.4.3)$$

The horizontal earth pressure resulting from the mass of soil behind the wall is calculated using Equation (3.4.4), where  $K$  is the same as for the horizontal surcharge load  $\gamma$  is the density of the soil and  $h$  is the depth of the soil at the point calculated. This pressure has a triangular distribution.

$$\text{EarthPressureHorizontal} = K * \gamma * h \quad (3.4.4)$$

The vertical component angle ( $\lambda$ ) of the horizontal force is obtained from Equation (3.4.5).

$$\lambda = \alpha + \delta \quad (3.4.5)$$

The vertical component of both the surcharge and earth pressure is given in Equations (3.4.6) and (3.4.7) and is taken by multiplying the results of Equations (3.4.3) and (3.4.4) by  $\tan(\lambda)$ .

$$\text{SurchargePressureVertical} = \text{SurchargePressureHorizontal} * \tan(\lambda) \quad (3.4.6)$$

$$\text{EarthPressureVertical} = \text{EarthPressureHorizontal} * \tan(\lambda) \quad (3.4.7)$$

### 3.5 Geotechnical Analysis

The methods detailed below are used to determine the stability of quay wall system against sliding and bearing capacity failure. Rotational failure is often considered when discussing the stability of retaining walls, in discussion with Professor P. Day (Day, 2018) it was decided to excluded rotational failure in the basic stability checks of this research. As for rotational failure to occur an infinitesimal area of soil is required to yield at the point of rotation, this is considered unrealistic and conservative and thus was not considered in this research.

#### 3.5.1 Stability Against Sliding Failure

The quay wall is required to provide adequate stability against the sliding mode of failure, which is calculated using the following ratio.

$$F_{sl} = \frac{\text{Sum of Resisting Forces}}{\text{Sum of Driving Forces}} \quad (3.5.1)$$

Where  $F_{sl}$  is the factor of safety against the element sliding.

Driving loads normally include lateral earth pressure, unbalanced hydrostatic pressure and in the case of quay walls mooring loads, the former and the latter were discussed in detail in Section 3.4. The buoyancy of the wall and its backfill material is typically included in the calculation of the wall resisting forces.

The wall is susceptible to extreme driving loads such as earthquakes, heavy waves and extreme winds. Special purpose rarely used heavy cargo handling and hauling equipment, that might be required to load/unload a specialist product also constitutes an extreme load. Normally these extreme loads are not combined with each other as this is deemed very conservative for design purposes.

Thus numerically, the sliding stability of the quay wall can be expressed as:

$$F_{sl} = \frac{(\Sigma V - \Sigma U)f}{\Sigma H} \quad (3.5.2)$$

Where:

$F_{sl}$  = Safety factor.  $F_{sl}$  should not be less than 1.5 for normal loading and no less than 1.25 for a combination of extreme loads. The required safety factors varies by project and is dependant on both the structure's design and the site's geotechnical conditions.

$\Sigma V$  = Sum of all vertical loads acting on the base projection of the base.  $\Sigma V$  often includes the vertical component of the lateral soil pressure, this is dependant on the geotechnical method chosen to calculate the lateral soil pressure as discussed in Section 3.4.1.

$\Sigma U$  = Uplift(Buoyancy) force, seawater has a density of  $1025kg/m^3$ .

$\Sigma H$  = Sum of all horizontal driving forces.  $\Sigma H$  typically includes the horizontal component of the lateral soil pressure, the unbalanced hydrostatic load and an mooring forces.

$f$  coefficient of friction. For a concrete structure located on top of a rockfill mattress the coefficient of friction  $f$  of 0.5 - 0.65 is usually used. The friction coefficient between rubble mattress and foundation soil is usually assumed to be  $t.g(\frac{2}{3}\phi)$ , where  $\phi$  is the angle of internal friction of material used for the wall rockfill mattress or foundation soil. For whichever provides the smaller value of  $f$ . The upper limit of the coefficient of friction is  $f = t.g\phi$ .

Note that  $(\Sigma V - \Sigma U)$  represents the effective weight of the structure. It should also be noted that the passive pressure of the water is not included in the calculation of the resisting forces.

### 3.5.2 Bearing Capacity

Bearing Capacity ( $q_f$ ) is defined as the pressure at which shear failure of the supporting soil immediately below and adjacent to the foundation begins (Knappett and Craig, 2012). Exceeding the bearing capacity leads to foundation collapse and in the case of quay walls bulging of the soil mass on the side of the footing. In general, computation of the ultimate load represents a problem of elastic-plastic equilibrium which can be solved in plain-strain and axisymmetric geometries. In the case of gravity-type quay walls the resultant force is inclined in relation to the cantilever base and is eccentric from the centre of the cantilever base.

It should be noted that one of the earliest set of recommendations on soil bearing capacity was proposed by Terzaghi (1943) which was further developed by Meyerhof (1951, 1963) amongst others.

The factor of safety for bearing pressure is determined using:

$$F_b = \frac{q_f}{q} \quad (3.5.3)$$

Where:

$F_b$  = Factor of safety against bearing.  $F_b$  is usually taken as 2.0 for normal loading and is reduced to 1.5 for extreme loading.

$q_f$  = Bearing capacity of the foundation material in Pa.

$q$  = Bearing pressure of the quay wall and the weight of soil resting on the wall base.

As a result of the large volume of research into the bearing capacities of foundations there are various methods for determination of the bearing capacity. From personal correspondence with Day (2018) it was recommended that the bearing capacity of the foundation material be calculated using the method laid out in Eurocode 7 (BSI, 2004), as given below.

### 3.5.2.1 Undrained Conditions

The design bearing resistance may be calculated from:

$$R/A' = (\pi + 2)c_u \cdot b_c \cdot s_c \cdot i_c + q \quad (3.5.4)$$

With the dimensionless factors for:

- The inclination of the foundation base:

$$b_c = 1 - \frac{2\alpha}{(\pi + 2)} \quad (3.5.5)$$

- The shape of the foundation:

$$s_c = 1 + 0.2(B'/L') \quad \text{for a rectangular shape} \quad (3.5.6)$$

$$s_c = 1.2 \quad \text{for a square or circular shape} \quad (3.5.7)$$

- The inclination of the load, caused by horizontal load H:

$$i_c = \frac{1}{2} \left( 1 + \sqrt{1 - \frac{H}{A'c_u}} \right) \quad (3.5.8)$$

with  $H \leq A'c_u$



### 3.5.2.2 Drained Conditions

The design bearing resistance may be calculated from:

$$R/A' = c'N_c(b_c s_c i_c) + q'N_q(b_q s_q i_q) + 0.5\gamma' B' N_\gamma(b_\gamma s_\gamma i_\gamma) \quad (3.5.9)$$

With the design values of dimensionless factors for:

- The bearing resistance:

$$N_q = e^{\pi \tan(\phi')} \tan^2(45 + (\phi'/2)) \quad (3.5.10)$$

$$N_c = (N_q - 1) \cot \phi' \quad (3.5.11)$$

$$N_\gamma = 2(N_q - 1) \tan \phi' \quad (3.5.12)$$

- The inclination of the foundation base:

$$b_q = b_\gamma = (1 - \alpha \tan \phi')^2 \quad (3.5.13)$$

$$b_c = b_q - (1 - b_q)/(N_c \tan \phi') \quad (3.5.14)$$

- The shape of the foundation:

$$s_q = 1 + (B'/L') \sin \phi' \quad \text{for a rectangular shape} \quad (3.5.15)$$

$$s_q = 1 + \sin \phi', \quad \text{for a square or circular shape} \quad (3.5.16)$$

$$s_\gamma = 1 - 0.3(B'/L') \quad \text{for a rectangular shape} \quad (3.5.17)$$

$$s_\gamma = 0.7 \quad \text{for a square or circular shape} \quad (3.5.18)$$

$$s_c = (s_q N_q - 1)/(N_q - 1) \quad \text{for rectangular, square or circular shape} \quad (3.5.19)$$

- The inclination of the load, caused by a horizontal load H:

$$i_q = [1 - H/(V + A' \cot \phi')]^m \quad (3.5.20)$$

$$i_c = i_q - (1 - i_q)/(N_c \tan \phi') \quad (3.5.21)$$

$$i_\gamma = [1 - H/(V + A' \cot \phi')]^{m+1} \quad (3.5.22)$$

Where:

$$m = m_B = \frac{[2 + (B'/L')]}{[1 + (B'/L')]} \quad \text{when H acts in the direction of B';} \quad (3.5.23)$$

$$m = m_L = \frac{[2 + (L'/B')]}{[1 + (L'/B')]} \quad \text{when H acts in the direction of L'.} \quad (3.5.24)$$

### 3.5.3 Settlement and Tilt

Noticeable settlement of gravity walls on non bedrock foundations may be expected therefore an analysis is required to determine immediate, long-term and differential settlement and that the settlement is within tolerable limits for the overall stability of the quay wall.

A reliable prediction of the various types of settlement and tilt requires a thorough understanding of the soil properties and subsurface soil variations along the wall length. To ensure this comprehensive testing of quality samples is necessary to properly understand the stress history, time-rate consolidation, Youngs modulus and the effects of cyclic loadings on the design parameters of the foundation soils.

Quay walls built upon dense granular soil would undergo the majority of the expected settlement by the time construction of the wall and backfill is completed. As a result the long term settlement is negligible, the granular foundation material allows for rapid dissipation of the pore water pressure resulting in little settlement as all pore water is dissipated by the time construction is complete.

For quay walls built on cohesive soils that have consolidation potential, settlement will continue for a some time after the construction phase of the project is complete. This is as the cohesion of the soil leads to a much lower rate of dissipation of the pore water pressure (Centre for Civil Engineering Research and Codes, 2005).

Where the quay wall is built on soils that vary in type and consistency along the wall, differential settlement may result between adjacent units.

## 3.6 Lateral Support for Slope Stability

A wide variety of systems, both temporary and permanent have been developed to stabilise slopes. The primary aim of these systems is to ensure the stability of the supporting structure and all retained materials. This includes any adjacent structures and services on the surface or buried within the backfill material that could the affect structure (SAICE Geotechnical Division, 1989). This thesis focuses on anchored wall systems and thus the other methods of slope stabilisation will be ignored.

These anchored wall systems are also referred to as tieback wall systems. The mechanism with which anchored wall systems resist the earth pressures is complex, as the soil, wall, free and fixed anchor lengths all interact to resist this pressure which develops not only during construction but during the service life of the structure (Boyce, 1996).

Anchored walls make use of a "tie" system to transfer the lateral forces to a zone behind any potential slip plane. These "ties" can be divided into three main groups:

- Horizontal anchorages: bar anchors, cable anchors and screw anchors.
- Tension Piles: steel tubular piles, H piles and MV-piles.
- Anchors with a grout body: grout anchors and screw injection anchors.

The tensile capacity of the anchor is expressed as  $F_{a,max}$  = which is maximum tensile strength of the anchor in direction of the tension element. The capacity of each anchor system is:

Horizontal Anchors:	100 to 4000 kN
Tension Piles:	100 to 6000 kN
Anchors with a grout body:	300 to 2000 kN

It is necessary to take the following aspects into account when selecting the type of anchorage used (Centre for Civil Engineering Research and Codes, 2005):

- Horizontal anchorages and tension piles at an inclination of less the 45° have the greatest stiffness.
- Horizontal anchorages are mainly used in sandy cohesionless soils.
- Existing structures, paved areas, excavation and drainage that could interfere with the path of the anchorage system.
- Anchors with a grout body that are made of prestressed steel tendons have low stiffness, require protection from corrosion, careful and skilled execution and usually have to be further prestressed once installed in the structure.
- MV-piles and anchors with grout injection; the tensile capacity is highly dependant on the quality of the installation work. It is recommended that tests of each anchor are preformed.

### 3.6.1 Horizontal Anchors

Traditional horizontal anchors consist of a deadman anchorage that is connected to the sheet pile structure by a tie with an anchor head. The selection of horizontal anchor type is highly dependant on the soil conditions in which the anchorage is situated. Rock bolts can be used for anchorages in rocky conditions while in softer soils an anchor trestle can be used, the layout of these anchor types is given in Figure 3.3. The deadman often consists of a vertical wall constructed a calculated distance behind the wall. The tie takes the form of either a bar or a cable, these are discussed further in Section 3.6.4.

Conventional horizontal anchors are constructed in situ. With the selected method of anchorage being situated at a distance behind the wall such that the active soil pressure zone acting on the back of the wall does not interfere with the passive soil pressure zone acting the front of the anchorage system.

- **Bar Anchors:**  
A bar anchor is a traditional anchor system consisting of a threaded steel bar and anchor block. The passive earth pressure required to stabilise the wall is obtained from a vertical anchor wall which can be constructed from wood, concrete, steel or pile trestles depending on the structural loads and the soil conditions.
- **Cable Anchors:**  
This system is very similar to the system used for bar anchors but these anchors make use of unbonded prestressed composite tensioned cables rather than a solid bar. This system is more complex as the system needs to be gradually tensioned as the backfill material is added to limit deformations of the wall (Centre for Civil Engineering Research and Codes, 2005).

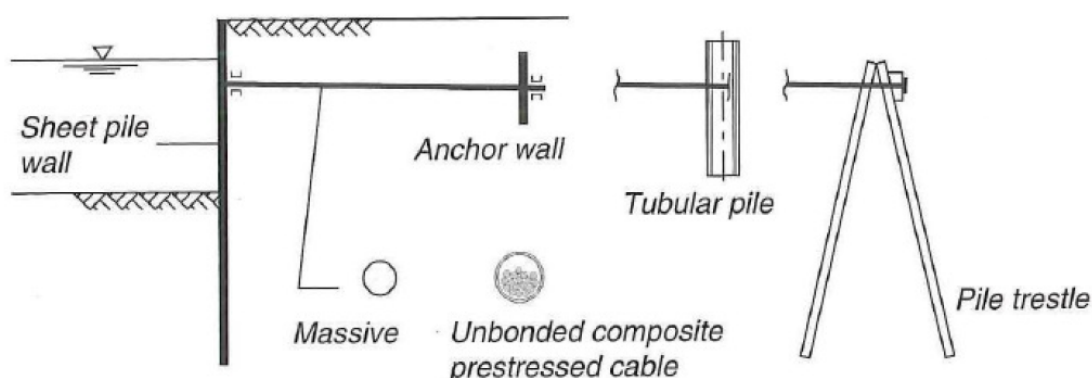


Figure 3.3: Types of horizontal anchorages (Centre for Civil Engineering Research and Codes, 2005)

### 3.6.2 Tension Piles

Sheet pile walls can be anchored through the use of either a pile trestle or a tension pile connected directly to the sheet pile wall. There are various types of piles used for this form of anchorage, the most common are closed precast concrete piles, steel H-piles, open tubular piles and MV-piles which consist of an H-pile with grout injected around it during the driving of the pile. The tensile capacity of these piles is supplied by the skin friction along the pile length. Figure 3.4 provides the basic layouts and cross sections of the piles used for these anchorages.

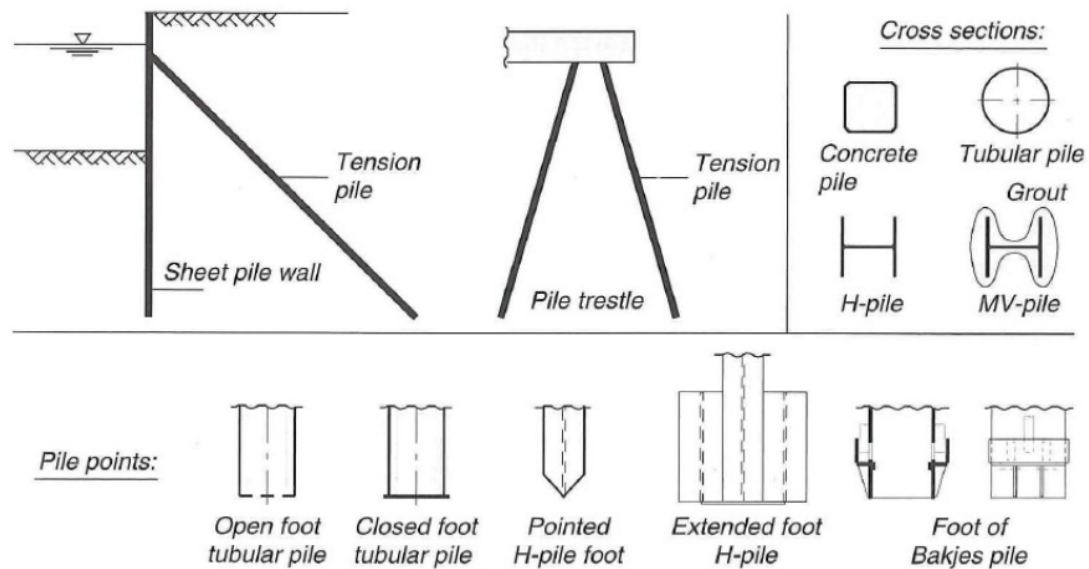


Figure 3.4: Layout and cross section of tensile anchorages (Centre for Civil Engineering Research and Codes, 2005)

### 3.6.3 Anchors with a grout body

This system of anchorage consists of in-situ cast cement grout elements. The most common of these are the use of grout anchors and screw injection anchors.

- **Grout Anchors.**  
This is a prestressed anchor system consisting of an anchor head and a tendon. Part of the tendons length is bonded to the ground by grout injected into the soil under pressure. The bar tendon is fitted with trapezoidal screw threads along its entire length. These anchors are required to be pretensioned as to minimise deformations of the sheet pile walls. The tensile capacity is obtained from the friction between the soil and the grouted section.
- **Screw Injection Anchors.**  
This anchor system is constructed using a hollow stem auger with a perforated tube that is a few meters in length. During the drilling process a grout mixture is forced out through the perforations into the soil forming a layer of higher strength material. The of the anchor body is similar in size to that of the auger.

### **3.6.4 Anchor Tie Details**

#### **3.6.4.1 Bar Anchors**

These types of ties are round steel bars, the ends of which have a screw thread. The bar diameter is often increased to compensate for any weakness caused by the screw thread in these areas. Details on diameters, steel qualities, couplings, hinges, end fittings and corrosion protection can be found in the product catalogues of manufactures.

#### **3.6.4.2 Cable Anchors**

Cable anchors are mainly composed of stands of high strength steel. The unbonded composite prestressed cables are built up of multiple strands. Each strand is composed of seven wire coated in grease and encased in a HDPE sheath with a minimum thickness of 1.2mm. The strands are then installed inside a larger HDPE tube, once prestressing of the cable is completed the remaining space within the HDPE tube is filled with grout. This results in the cable having two layers of protection from corrosion.

#### **3.6.4.3 Connections between Anchor and Sheet Pile Wall**

The primary consideration when designing the connection of the anchor to a sheet pile wall is the differential settlement that can occur. The soil below the anchor and anchorage is likely to settle more than the sheet pile wall due to the material on which the elements are founded upon. This is of more concern when the anchorage is constructed on top of uncompacted backfill material. This is necessary as to avoid the anchor tendon being overloaded by shear forces and bending moments. For bar anchors a hinged connection is suggested with a second hinge situated 2m behind the sheet pile wall.

## Chapter 4

# Case Study: Saldanha Port Expansion

This chapter provides a review of the structural and geotechnical analysis and design of the reinforced concrete counterfort units used for the general cargo quay extension of the Port of Saldanha. These design requirements and parameters will be used to inform the optimisation procedure. All information was provided by Murray and Roberts Marine, which traded under the name Lama International Contractors Ltd. for this project. All design requirements and loads were determined and provided by Protekon, which is the engineering division of Transnet.

A set of four of the basic reinforced concrete units is given in Figure 4.1, with Figure 4.2 gives the units with a proposed capping beam. Each of the units has the following parameters:

- Mass: 330 tons.
- Nominal Plan Dimensions of Base: 5900 x 15800mm.
- Wall Height : 17500mm.
- Foundation Bed : 450mm thick layer of crushed stone.
- Spacing between expansion joints: 4 units.
- Vertical grouted connection between each of the precast concrete units.
- Units support a reinforced concrete capping beam extending from a level of +1.9m Chart Datum(CD) to +5.1m CD\*.
- Total Retained Height: 20.8m (includes height of capping beam)
- MSL location: +0.9m CD

\*Final Capping beam was designed by Protekon, and was not included in case study documents, thus exact design is unknown.

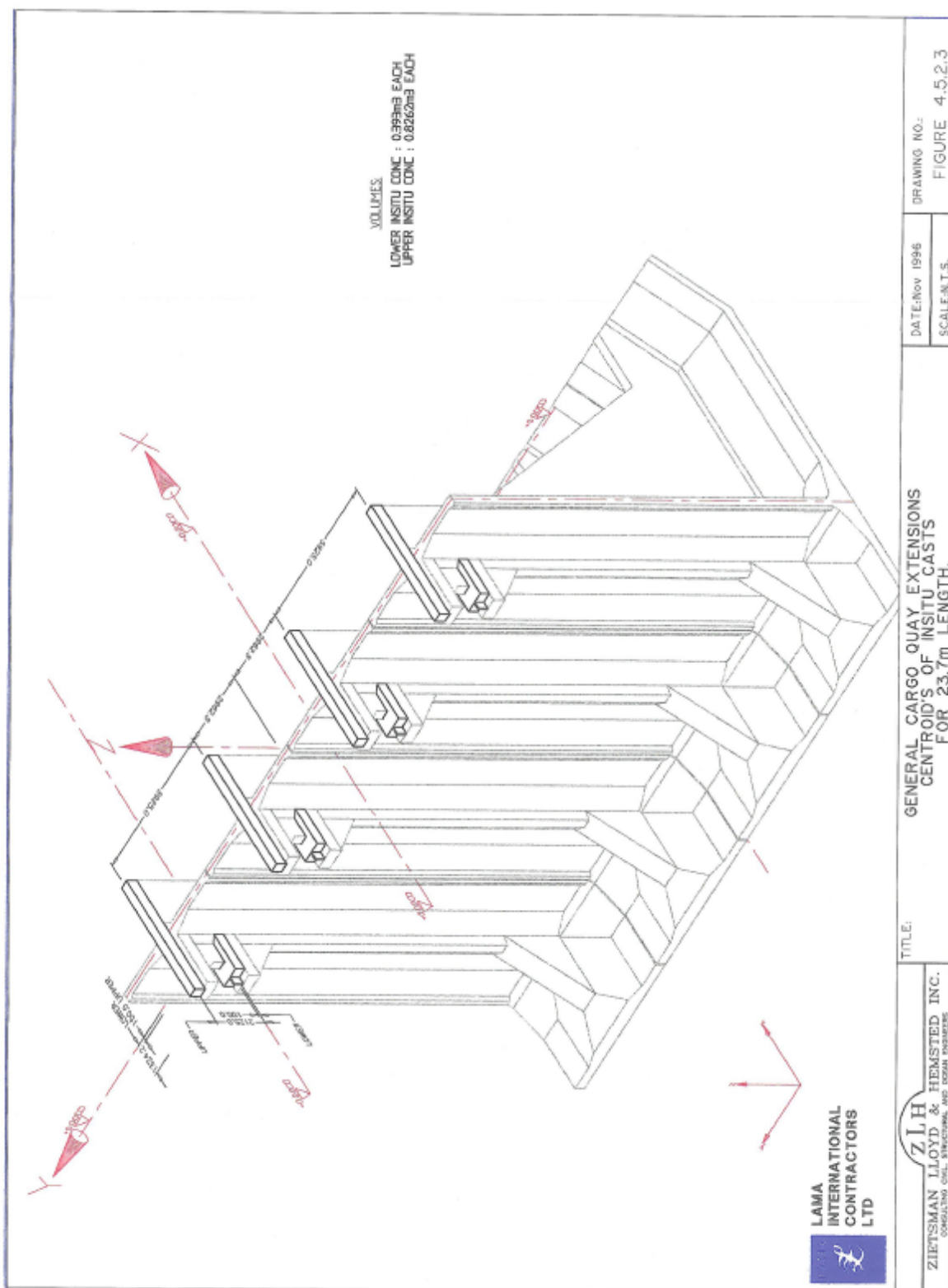


Figure 4.1: As built set of 4 precast units



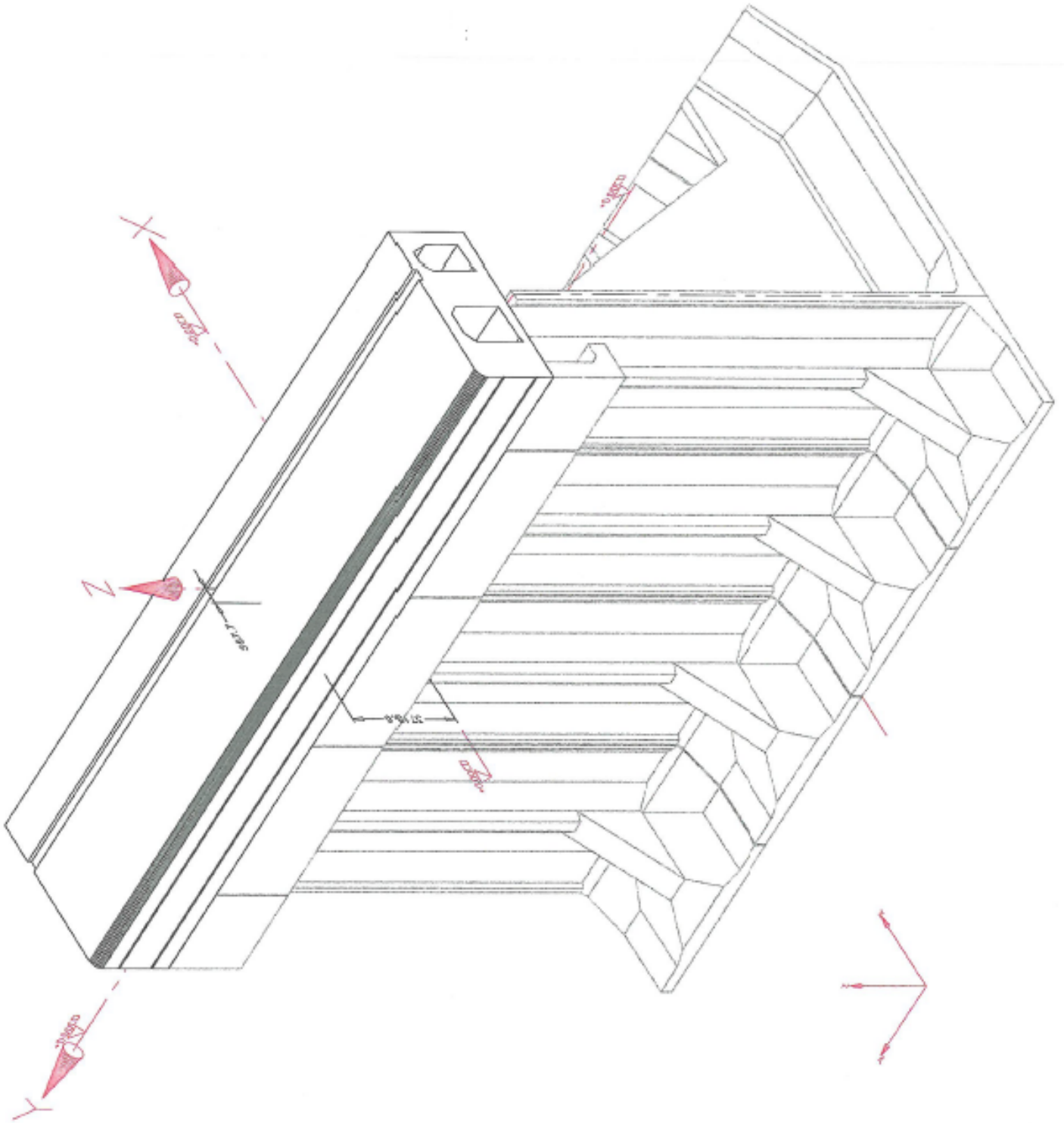


Figure 4.2: As Built set of 4 precast units with proposed capping beam

## 4.1 Introduction

The anchorage at Saldanha Bay was first discovered in 1601 and remains the largest and deepest natural port in the southern hemisphere, it is speculated that the reason this never became the first major port along the South African coast was due to the lack of fresh drinking water (Transnet National Ports Authority, 2010). The port grew only in modern times as it was required to export iron ore from Sishen in the Northern Cape Province of South Africa. The first deliveries of iron ore were exported in 1976. The iron ore from Sishen is delivered to the port via a dedicated ore railway. This railway is also used to deliver iron ore to the Saldanha Steel Mill located near the port. The steel products manufactured at the mill are also exported from the port of Saldanha.

The port of Saldanha is a multi purpose port, with capabilities for handling dry and liquid bulk, containers and break bulk goods as are the rest of the ports in South Africa. The port is owned and operated by the Transnet Port Authority and operates 24 hours a day 365 days a year. The port comprises of a 990m long pier containing two iron ore berths which is linked to the shore along a 3.1km long causeway/breakwater. The port also comprises a 874m long multi-purpose quay, comprised of three berths, for the handling of break-bulk cargo and a 365m tanker berth at the end of the ore pier. The two iron ore berths have an allowable draughts of 21.25m, the multi-purpose berths have a maximum draught of between 12 and 13.4m that varies across the three berths, the tanker berth has a maximum draught 21.5m (africaports.co.za, 2016). Many of these facilities were built as part of the same port expansion project that included the of the expansion multi-purpose quay.

## 4.2 Structural and Geotechnical Design Brief

This section will be summarising all relevant geotechnical and structural aspects and requirements used to design the as built precast elements used in the port expansion.

### 4.2.1 Design Parameters

This section details all relevant material properties, stability requirements and design vessels that impact the structural design of the precast elements.

#### 4.2.1.1 Reinforced Concrete Properties

Reinforced concrete used in the counterfort units has the following properties:

Minimum 28 day cube strength:	45 MPa
Elastic Modulus (instantaneous):	31 GPa
Partial Material Factor:	1.5
Cover to reinforcement:	60mm

The reinforcing steel has the following properties:

High Tensile Y Bars:	450 MPa
Mild Steel R Bars:	250 MPa
Partial Material Factor:	1.15

#### 4.2.1.2 Requirements for Stability

The minimum factors of safety are the following:

Against Sliding:	2.0
Bearing Capacity:	2.0
Slip Circle Failure:	1.4 *

\*Using Bishop's Method

#### 4.2.1.3 Design Vessel

The design vessel used for the design of the quay walls for this case study is not specified but rather a bollard load and bollard loading scheme were provided by the client. The details are given in Section 4.2.2.1.

### 4.2.2 Design Loads

The loads summarised below were supplied to Lama International Contractors by Protekon.

#### 4.2.2.1 Bollard Pull

The bollard pull loads are applied 0.3m above the cope level and are as follows:

- 800 kN per bollard applied at any horizontal angle and at a vertical angle of up to 30° above or below the horizontal.
- 4 consecutive bollards are to be taken under load simultaneously.

#### 4.2.2.2 Berthing Impact

The berthing impact loading was calculated according to BS 6349 (BSI, 1984) using the following information:

- Ship Size: 65 000 tonne (Deadweight)
- Berthing Energy: 48 tonne/m
- Maximum Hull Pressure: 450 kPa

#### 4.2.2.3 Uniformly Distributed Live Load

A pressure of  $40\text{kN}/\text{m}^2$  was applied from the cope line landward continuously or in part so as to induce the most adverse vertical and horizontal loading on the structure.

#### 4.2.2.4 Container Crane Wheel Loading

The wheel load for the crane is distributed along a crane rail running parallel to the quay side.

- 8 000 kN distributed along the carriage length of the crane. The length of the crane carriage was not included in the design documents obtained.

#### 4.2.2.5 Point Loading

The following loads were used for the design of local elements and were not considered to act concurrently with other loads.

- 2 000 kN outrigger load applied on an area of 1.2 x 1.6m such as from outriggers on a mobile crane.

#### 4.2.2.6 Tidal Lag

A  $10\text{kN}/\text{m}^2$  uniform horizontal pressure has been applied to the rear of the wall to simulate a 1.0 m tidal lag.

#### 4.2.2.7 Earth Pressures

The backfill earth pressures was calculated using the backfill material information given in Section 4.3.2. The method to determine the earth pressures for the expansion of the multi-purpose quay is unknown.

#### 4.2.2.8 Cyclic and Earth Loading

No cyclic loading due to wave action or earthquake loads had been specified by the client and thus were not taken into account during the design process.

### 4.2.3 Finite Element Method Analysis

A three dimensional finite element method structural analysis of the counterfort units was performed using thick shell and three dimensional continuum elements.

### 4.2.4 Serviceability Limit State

For all SLS calculations the crack width was limited to 0.1mm in the splash zone and tidal zone and to 0.3mm below CD.

### 4.3 Geotechnical Parameters

These geotechnical parameters are based on borehole and laboratory test data provided by Protekon. Along with the results of the laboratory test estimations of material parameters where obtained from previous experience, as similar material had been revealed at an adjacent site the was used for the construction of the Mossgas natural gas platform. During the planning phase of the quay expansion boreholes were drilled into the ocean bed to determine the geotechnical details for use in the design of the final structure. The location of the various boreholes are given in Figure 4.3. All further geotechnical information is given in Appendix C.

#### 4.3.1 Foundation Geology

The foundation profile along the length of the quay wall extension is relatively uniform and consists of two primary materials types as shown in Figure B.1. A breakdown of these two materials is given below.

##### Marine Sands

- Variably calcretised
- Average Layer Thickness: 5.5m
- Layer Thickness Range: 4.8m to 6.2m
- Details of this material parameters are given in Appendix C.1.

##### Residual Granite Soil

- Layer thickness extends to beyond depth of foundation influence ( $\pm 25\text{m}$ )
- Details of this materials parameters are given in Appendix C.2

Between chainages 175m and 350m spanning a length of 175m, or about 30 precast counterfort units, a third material is found between the marine sands and residual granite soil Refer to Figure 4.3. This material is a deposit of fluvial sediments (defined in Appendix C.3) and was found with a typical layer thickness of 4m. Figure B.2 is an example of a soil borehole profile taken in this area, the borehole found a fluvial layer thickness of 2.5m in this area.

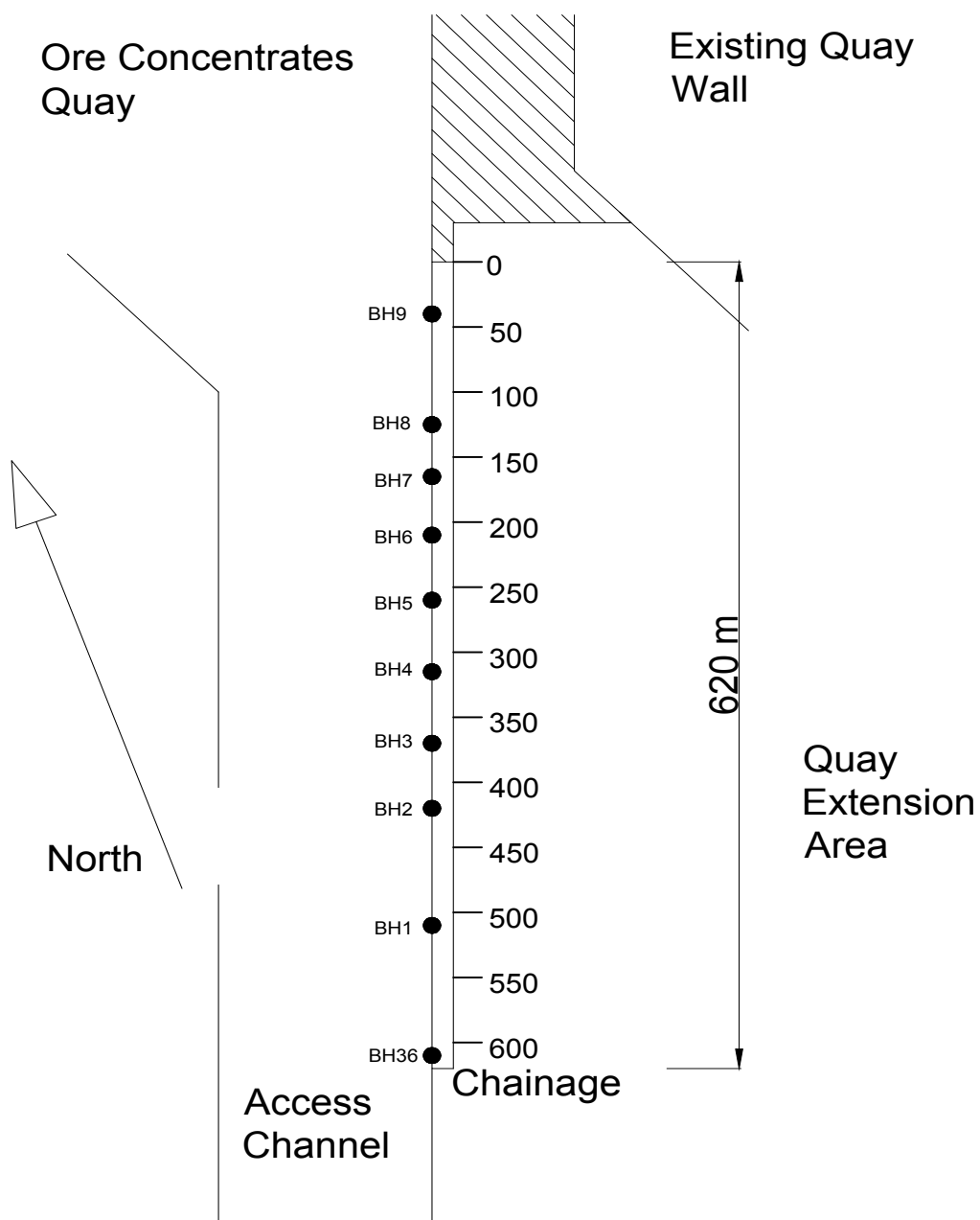


Figure 4.3: Plan Showing Relevant Borehole Positions

The project geotechnical engineers determined that this layer of fluvial sediments has a small effect on the settlement of the counterfort units and a minor impact on the bearing capacity of the foundation geology in this area. The fluvial sediments were deemed to have no effect on the sliding or global slip circle stability of the units. Figures B.3 and B.4 provide additional profiles on the foundation geology that were used to determine the foundation geology for the final structural analysis and design.

### 4.3.2 Back Fill Material Parameters

The backfill material selected comprised a dredged sand/calcrete gravel mix, with such segregation that lenses of sand, calcrete gravel and gravel/sand mixes will occur throughout the backfill profile.

The backfill material will be dredged and deposited into a water depth of 16.6m such that a very loose material condition should initially prevail ( $\pm 10\%$  of the relative density). The maximum vertical effective stress in the fill will only be in the order of 20kPa so that the limited time related compaction would be anticipated around  $\pm 20\%$  of the relative density. Above MSL the ease of compaction of the backfill material will result in higher compaction and consequently higher shear strength parameters.

The backfill parameters used for design purposes are as follows:

#### Beneath MSL

- $\gamma$  submerged : 8 kN/m<sup>3</sup>
- $\phi'$  : 27°
- $c'$  : 0 kPa
- Elastic Modulus (E) : 5 MPa

Assuming  $\pm 10\%$  relative density for a 20% gravel, 80% fine sand mix.

#### Above MSL

- $\gamma$  saturated : 20 kN/m<sup>3</sup>
- $\phi'$  : 34°
- $c'$  : 0 kPa
- Elastic Modulus (E) : 50 MPa

## 4.4 Design Results

### 4.4.1 Structural Design

The results the structural analysis resulted in the final design given in Figure 4.1 with the details given at the beginning of this chapter. Appendix D provides detailed technical drawings of the final as built design.

### 4.4.2 Geotechnical Results

Using the information provided in Section 4.3, a review of all geotechnical information was carried out. From this review the bearing capacity, slip circle and sliding calculations were completed. Using the minimum factors of safety (FOS) specified in Section 4.2.1.2 the results summarised in Table 4.1 were obtained for bearing capacity, global slip circle stability and sliding stability.

Table 4.1: Foundations: Minimum Factors of Safety (FOS)

	Required Minimum FOS	Computed FOS
1. Sliding	2.0	2.19
2. Slip Circle	1.4	1.41
3. Bearing Capacity	2.0	3.68



## Chapter 5

# Structural Analysis Framework and Design Assumptions

The structural configuration to be considered for optimization incorporates the use of a ground anchor as used for the quay wall designs given in Figure 2.2. Ground anchors are used in quay wall construction mainly in conjunction with steel and concrete sheet pile walls and not with the heavier monolithic concrete elements. The ground anchor is used to resist much of the lateral pressure applied behind the quay wall by the earthen backfill material. This leads to the weight of the concrete elements being less critical to the overall stability of quay wall. The overall height of the proposed quay wall ( $H_{wall}$ ) design will remain constant throughout the optimisation process as it is the primary factor determining what vessels are able to dock against the quay without striking the seabed within the port. The dimensions of the structural parameters to be optimised are given in Figure 5.1 and the tension in the ground anchor needs to be determined for the development of an optimised structure while still maintaining the stability requirements given in Section 4.2.1.2. Descriptions of each parameter are provided below Figure 5.1.

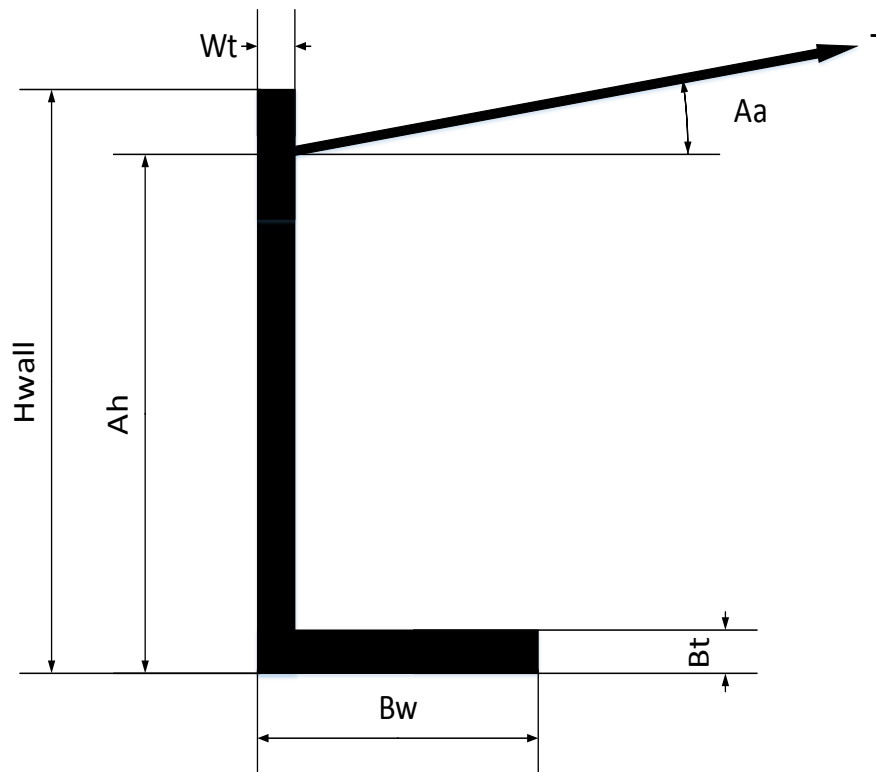


Figure 5.1: Proposed Geometry of Section

Where:

- **H<sub>wall</sub>** is the fixed height of the quay wall for all proposed sections. This will be determined for the largest ships that could be docked against this quay wall.
- **W<sub>t</sub>** is the thickness of the vertical wall of the quay wall.
- **B<sub>t</sub>** is the thickness of the base on the quay wall.
- **B<sub>w</sub>** is the width of the base of the quay wall or base projection of the quay wall.
- **A<sub>h</sub>** is the distance from the bottom of the structure to where the ground anchor attaches to the quay wall.
- **T** is the tension applied to the ground anchor to ensure stability of the structure.
- **A<sub>a</sub>** is the angle at which the ground anchor is acting at.

## 5.1 Construction Methodology

The addition of an external ground anchor to the precast quay wall implies that two structural configurations need to be considered in the analysis of the proposed design i.e. with and without the ground anchor and additional surcharge loading. The external ground anchor will be installed above MSL, this is to allow for easier installation as most installation work will be completed in a dry conditions.

The first structural configuration, referred to as the construction state, is prior to the ground anchor being installed and being tensioned. In this state backfill material extends up to MSL or 0.9m below the top of the 17.5m precast wall. A 10kPa imposed load is applied to simulate possible loadings during the backfilling operation along with any vehicle loads during construction. A full layout is provided in Figure 5.2.

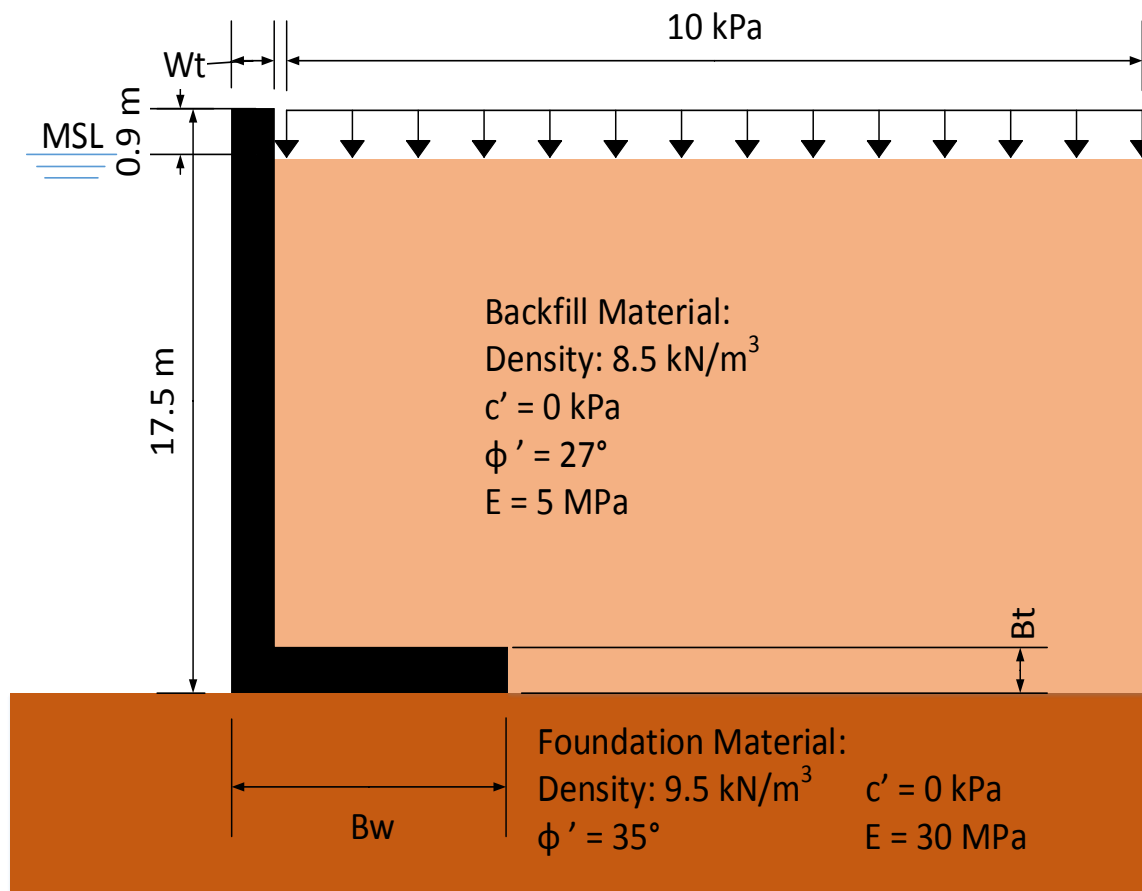


Figure 5.2: Construction Structural State

The second structural configuration, referred to as the final state, will have the backfill completed to a level of 5.1m CD. All permanent and imposed loads as given in Section 5.2.2 will then be applied. Figure 5.3 provides a layout of the surcharge and earth pressure loads during this final state.

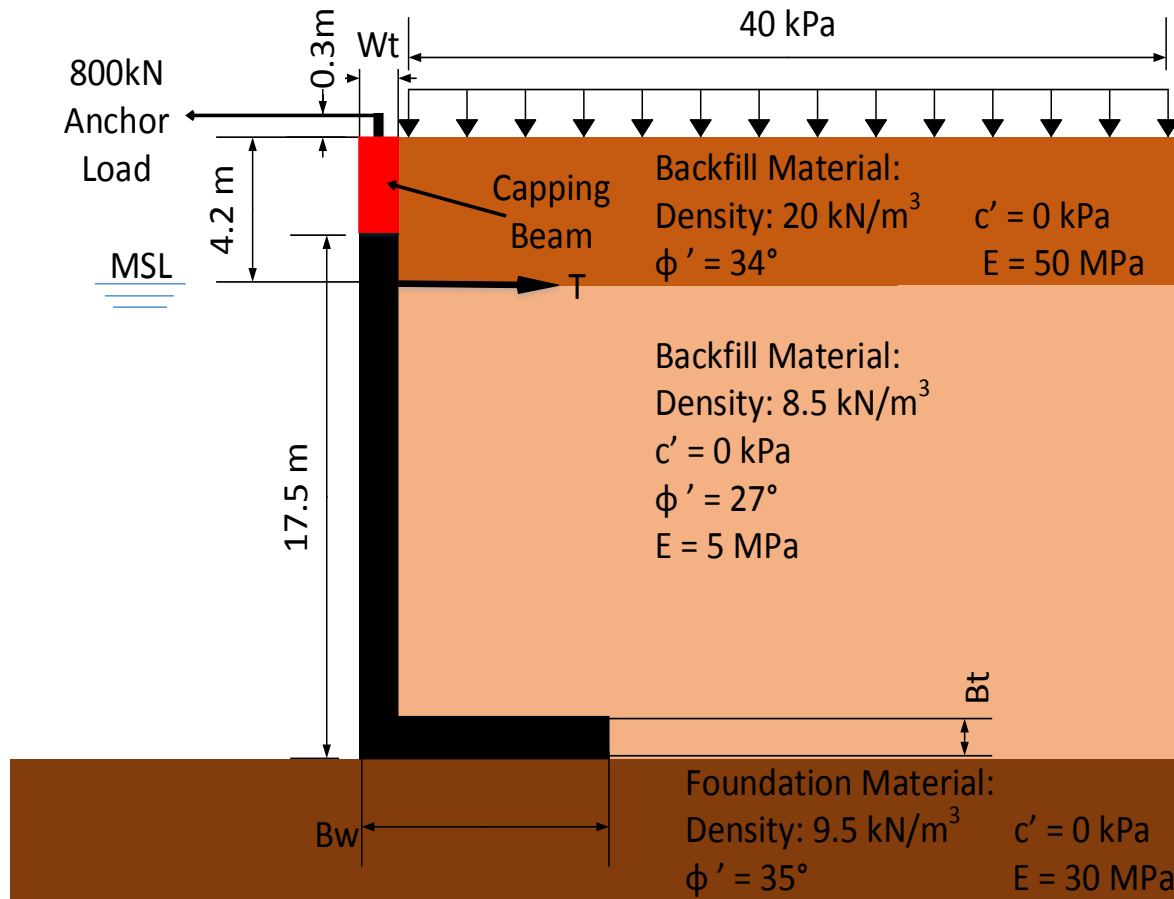


Figure 5.3: Final Structural State

## 5.2 Design Load Cases

This section details the loading on each of the two structural configurations.

### 5.2.1 Construction State

The only load case considered during the construction state was with the backfill material to a level of +0.9m CD (16.6m vertically from the base of the structure). Along with the backfilled material a 10kPa load was applied to simulate the loading effect due to construction operations. Other loads cases that would require consideration with the final for construction design are the lifting and moving of the section into place, the ability of the precast element to withstand wind and wave loads prior to the backfilling beginning.

### 5.2.2 Final State

The load case that was used for the final state of the optimised design was selected as the load case creating the largest horizontal load acting away from the wall as this was expected to require the largest tensile force in the ground anchor to resist. The other load cases were ignored in order to streamline the optimisation process as they were expected to require a lower tensile force in the ground anchor. Thus the structure in the final phase was subjected to the full bollard load (800kN) acting between 30° below to 30° above the horizontal along with the full operational surcharge (40kPa) and a pressure due to the tidal lag (10kPa) acting on the back of the precast wall sections. This load case is needed to simulate the structural loading effect during port operations with high offshore winds after high tide when the tidal lag is greatest. As the design of the capping beam is unknown the mass of the beam was ignored in Chapter 6 for the stability calculation but the height of the capping beam was included as this influences the lever arm of the moments applied to the structure. In Chapter 7 the capping beam was modelled as a simple rectangular block to allow for transfer of moments and forces in the FEM model further detail on the capping beam is given in Section 7.1.

## 5.3 Design Assumptions

This section will detail all parameters used from those provided in Chapter 4 along with any assumptions made during the design process of the optimised design, as not all required information was included in the documents used for the case study.

### 5.3.1 Requirements for Stability

Due to differences between the as built design as given in Chapter 4 and the design of the optimised section, the methodology for the determination of system stability varies. The methodology used to determine the global system stability is given below.

### 5.3.1.1 Global Slip Circle

Due to the two phases of the design resulting from the addition of the ground anchor two factors of safety (FOS) for the global slip circle stability are required. In Section 4.2.1.2 of the case study a FOS of 1.4 was specified for the final design. Through discussion with Professor P. Day (Day, 2018) a lowered FOS of 1.2 was selected for the construction phase of the design. The lowering of the FOS was selected as the loading during construction is temporary and this could lead to an over conservative design, impacting the ability to optimise the structure.

Once the tensioned ground anchor is installed the confinement of the backfill material would force the slip circle to pass behind the deadman of the anchor resulting in a greater FOS. The length of the anchor tie is determined to ensure that the deadman anchorage of the anchor tie is situated behind the slip circle with a FOS of 1.4 with all loads applied to the soil excluding the ground anchor. A further limit on the length of the anchor tie is the minimum distance such the active soil pressure on the back of the precast wall does not interfere with the passive soil pressure acting on the deadman anchorage.

### 5.3.1.2 Sliding Resistance

The FOS for sliding resistance was taken as 1.2 for the construction state. The FOS for the final state was maintained as 2.0 as specified in the case study (Section 4.2.1.2).

### 5.3.1.3 Bearing Capacity

The bearing capacity FOS was reduced to 1.75 for the construction state while 2.0 was used as specified in the case study (Section 4.2.1.2) for the final state.

## 5.3.2 Design Loads

Further detail on the loads used for the design of the optimised section in the final state can be found in Section 4.2.2.

## 5.3.3 Geotechnical Parameters

The geotechnical information provided in Section 4.3 was used in the determination of the optimised section.

## 5.4 Optimisation Framework

The optimisation of the quay wall design and the determination of ground anchor tension, was done in two primary phases as given below. The results of each phase were used to guide the optimisation during the following phase.

### 5.4.1 Optimisation Phase 1

The first phase of optimisation was used to determine many of the minimum values used for optimisation in phase 2. This phase was completed using a custom Matlab script (Appendix F) and the use of geotechnical analysis package GeoSlope 2016. After the analysis, the outputs from the MATLAB script were then further reduced. The reduced outputs were then passed to phase 2.

### 5.4.2 Optimisation Phase 2

The second phase of optimisation was used to determine the final optimised design. Determination of which was completed using a comparative structural analysis of the precast element using finite element methods. The cost of each possible configuration was also used as a parameter for optimisation. From these the final optimised structural configuration was determined.

## Chapter 6

# Basic Geometric Configuration

### 6.1 Geotechnical Limitations

The primary global stability parameter that is independent of the structural configuration of the precast element is the global slip circle as this is based on the site specific geotechnical conditions. The determination of the FOS was done using Bishops Method as this is the same method as used in the case study (Section 4.2.1.2). The analysis was completed using the Slope\W package from GeoSlope (GEOSLOPE), using all the loads as prescribed for the construction state (Section 5.2.1).

The critical slip circle FOS was determined as 0.985 with the slip plane passing 0.24m behind where the face of the quay wall would be located. Figure 6.1 shows the slip plane of the critical slip circle.

The relationship between the distance of the slip plane from the face of the quay wall and the associated FOS was determined for all remaining FOS obtained from the analysis. Refer to Figure 6.2. The maximum distance from the wall face for an FOS of less than 1.2 was determined as 3.412m as highlighted in Figure 6.3. This value of 3.412m will be used as the minimum base projection of the proposed design for the model inputs given in Section 6.2.1.



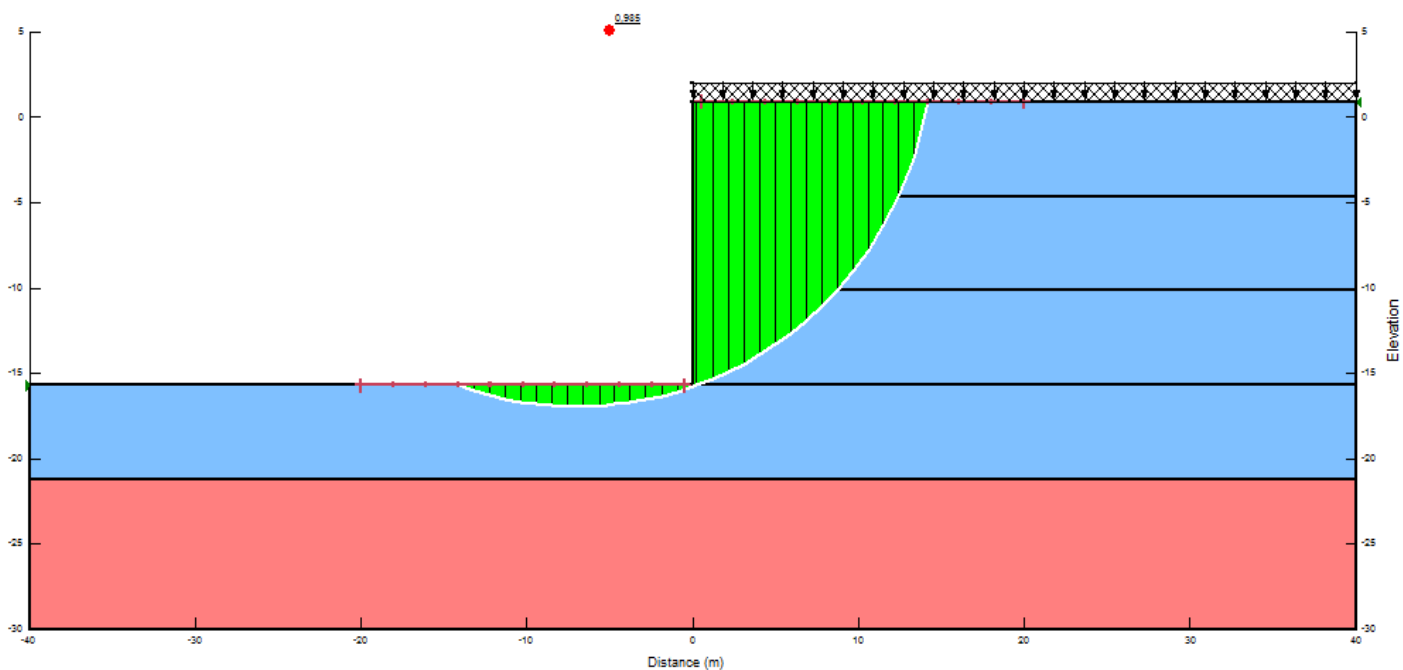


Figure 6.1: Critical global slip circle plane during the construction phase

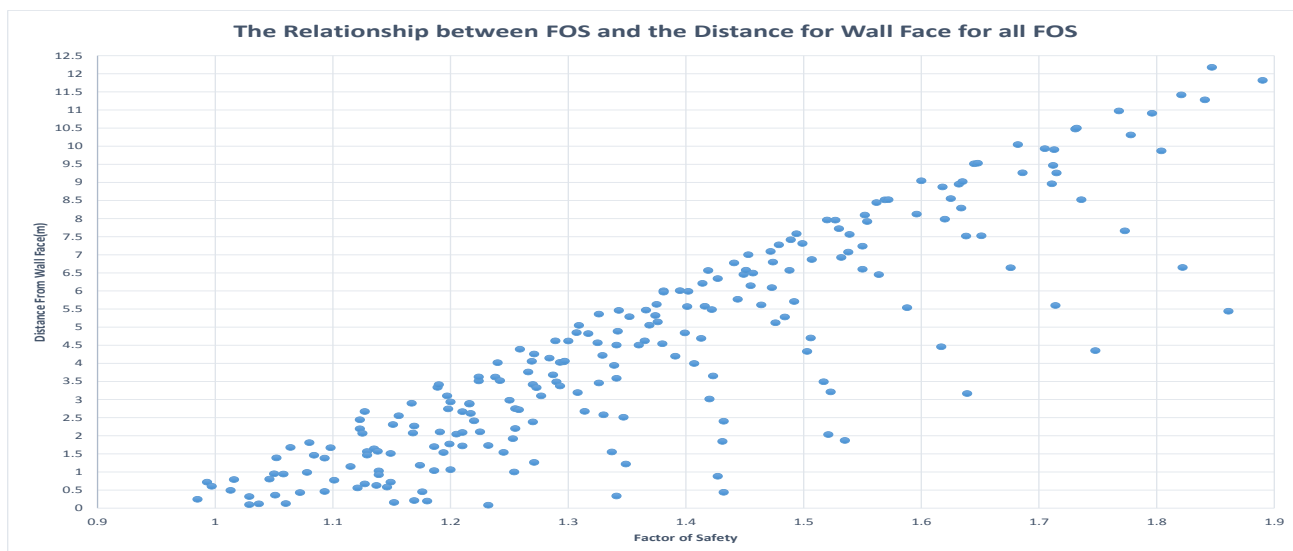


Figure 6.2: The relationship between FOS and the distance of the slip plane from Wall face

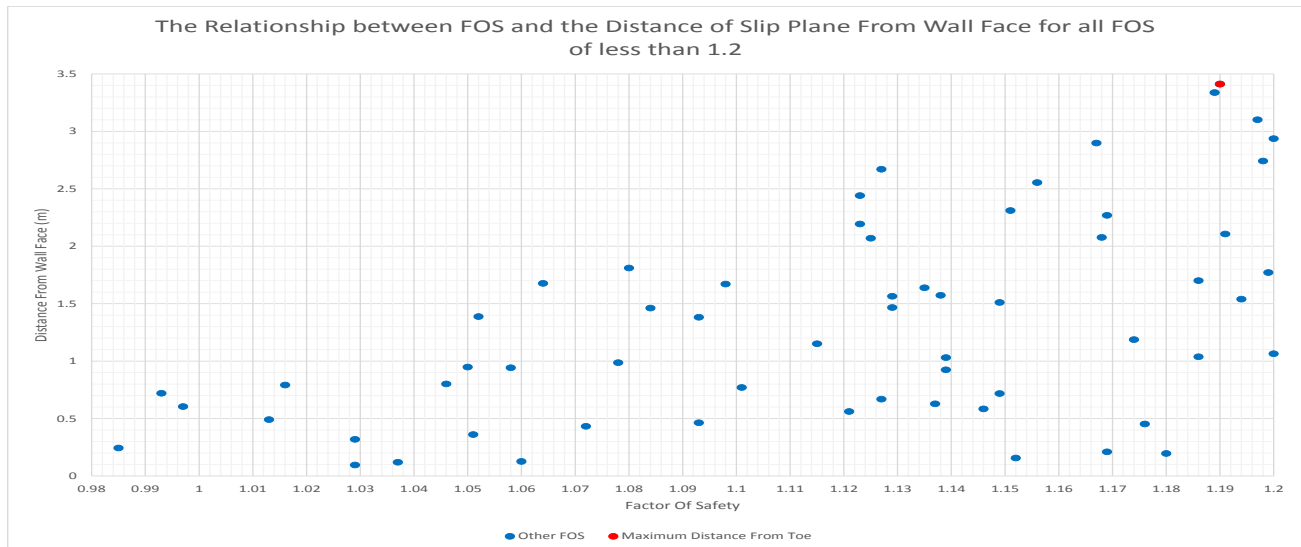


Figure 6.3: The relationship between FOS and the distance of the slip plane from Wall face for FOS less than 1.2

## 6.2 Inputs of Simplified Model

A custom MATLAB script was created to perform the analysis for global stability of the quay wall, this section details all inputs and analysis methods used in the model.

### 6.2.1 Structural Configurations

As a result of the varying of the parameters given below a total of 17920 configuration permutations were analysed. Examples of various configurations are provided in Appendix E. The height of the capping beam and the backfill material retained by this beam are included in the calculation as shown in Appendix F.1 but are not considered inputs to the structural configurations of the precast elements.

#### 6.2.1.1 Wall Height

The wall height was kept constant at 17.5m for all configuration to ensure that the design vessel selected by the client would be able to berth against the optimised structure. Refer to Section 4.2.1.3.

#### 6.2.1.2 Base Projection

The minimum base projection was determined to be 3.412m a given in Section 6.1 this was rounded up to 3.5m. The base projection was increased in increments of 0.1m from 3.5m up to and including 9m.

### 6.2.1.3 Base Thickness

The base thickness was varied for each possible configuration with thicknesses of 0.5m, 0.6m, 0.8m and 1m.

### 6.2.1.4 Wall Thickness

The wall thickness was varied for each possible configuration with thicknesses of 0.5m, 0.6m, 0.8m and 1m.

### 6.2.1.5 Anchor Height

The height of the ground anchor above the base of the precast wall was varied between 16.5m and 17.5 in increments of 0.25m for each possible configuration. These heights were selected to allow the installation of the anchor and the construction of the dead man to be performed above MSL and to allow for easier monitoring of the anchor once installed.

### 6.2.1.6 Anchor Angle

The angle of the ground anchor was varied for each possible configuration at an angle of between 0° and 15° above the horizontal in increments of 5°.

### 6.2.1.7 Designation of Structural Configurations

The designation of each configuration is a concatenation of all parameters and their labels. An example is

**Wt1 \_ Bw3.5 \_ Bt1 \_ Ah16.75 \_ Aa0**

Where:

- **Wt1** is a wall thickness of 1m
- **Bw3.5** is a base projection of 3.5m
- **Bt1** is a base thickness of 1m
- **Ah16.75** is an anchor height of 16.75m
- **Aa0** is an anchor angle of 0°

## 6.2.2 Analysis Methods

The section details the specific methods used within the MATLAB script to determine required FOS for the configurations determined above.

### 6.2.2.1 Sliding Resistance

The sliding resistance of the entire quay wall system was determined using Equation (3.5.2), this method as described in Section 3.5.1 provides a horizontal equilibrium check for the entire structure. The value of the coefficient of friction,  $f$  was taken as 0.5 to be conservative as the value used in the case study is unknown.

### 6.2.2.2 Bearing Capacity

The bearing capacity of the foundation material below each configuration was determined using the method given in Section 3.5.2 for the undrained condition. The base of the quay wall was determined to be resting on top of the foundation material for the analysis and thus  $z = 0$  where  $z$  is the depth of the base projection below the surface of the foundation material.

## 6.3 Analysis Procedure of for Model Implemented using a MATLAB Script

The steps of the procedure for the determination of the minimum ground anchor tension is given in Figure 6.4. Each step is explained in detail below. The full MATLAB script developed to do the optimisation is included in Appendix F.1.

### Step 1: Input Design Constants

In this step all parameters that remain constant during the analysis are added. These include:

- Height of the wall ( $H_{wall}$ )
- Segment Length
- Operation Surcharge
- Construction Surcharge
- Mooring Loads
- Tidal Lag
- Material Properties
- Cope Height

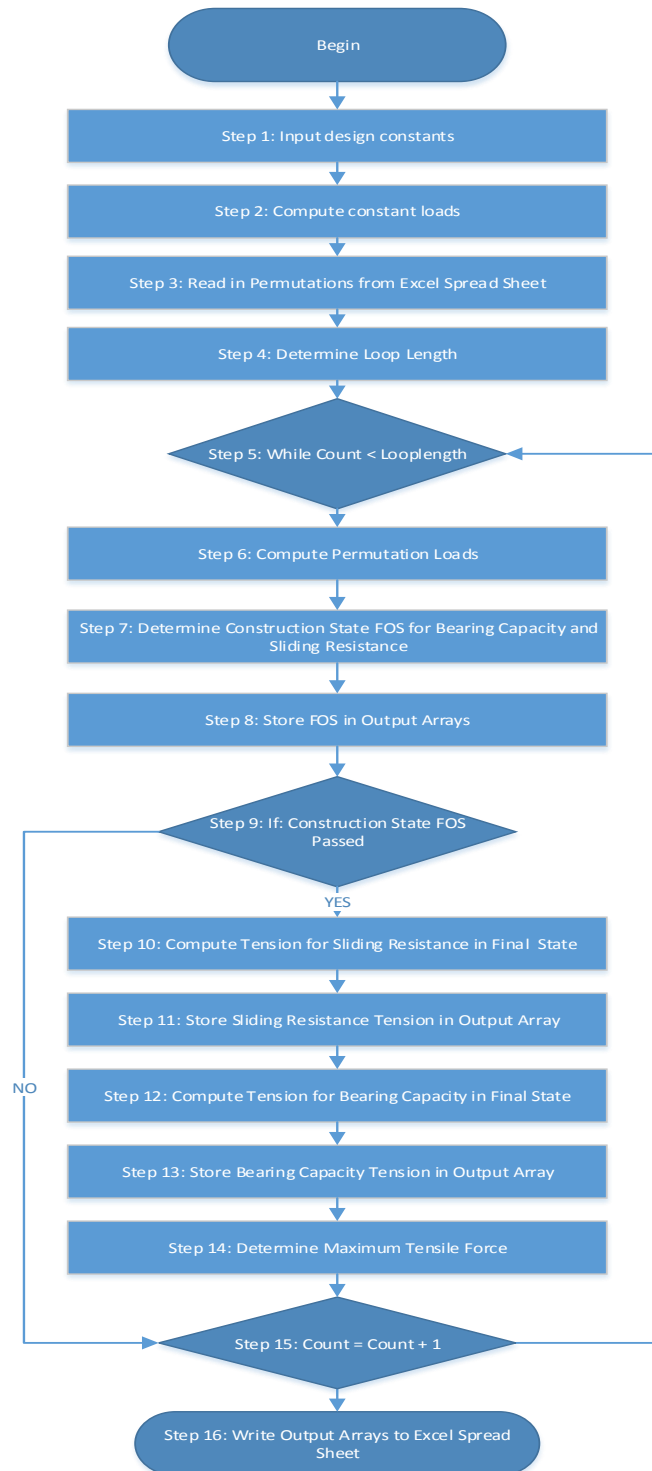


Figure 6.4: MATLAB Analysis Procedure

**Step 2: Compute Constant Loads**

All loads that remain constant throughout the analysis are calculated in this step, these loads are the horizontal force and moment created by the pressure from the tidal lag and the mooring loads acting between  $30^\circ$  below to  $30^\circ$  above the horizontal in  $15^\circ$  increments.

**Step 3: Read in Permutations from Excel Spreadsheet**

The parameters associated with all the structural configuration permutations set out in Section 6.2.1 are read in from an Excel spreadsheet into MATLAB. The parameters of each permutation was then stored in a parameter type array. The collection of arrays is used for the rest of the calculations, the arrays in the order they are read in are:

- Designation of Structural Configuration
- Wall Thickness (m)
- Base Projection (m)
- Base Thickness (m)
- Anchor Height (m)
- Anchor Angle ( $^\circ$ )

**Step 4: Determine Loop Length**

Determine the maximum number of iterations from the length of the Designation of Structural Configuration array.

**Step 5: While Count < Loop Length**

A while loop that iterates through each permutation while incrementing a counter until the counter reaches the maximum number of iterations as determined in Step 4. Within this loop all calculations are performed.

**Step 6: Compute Permutation Loads**

All loads that vary with each permutation are computed in this step using information from the parameter arrays created in Step 3. Along with the loads the lever arm of the force and the resulting moment are calculated. These loads are:

- Vertical and Horizontal Earth Pressures
- Mass of the Structure
- Vertical and Horizontal Surcharge Pressures
- Mass of soil resting on top of base projection.

**Step 7: Determine Construction State FOS for Bearing Capacity and Sliding Resistance**

This step determines the FOS for bearing capacity and sliding resistance using the loads computed in steps 2 and 6 and using the methods specified in Sections 3.5.1 and 3.5.2.

**Step 8: Store FOS in Output Arrays**

The calculated FOS of bearing capacity and sliding resistance for all permutations are stored in an output array.

**Step 9: If Construction State FOS Passed**

If the FOS calculated in step 7 exceeds 1.75 for bearing capacity and 1.2 for sliding resistance then steps 10 through 14 are calculated. If not then the counter is incremented (step 15) and the next permutation begins analysis at step 6.

**Step 10: Compute Tension for Sliding Resistance in Final State**

The tensile capacity of the ground anchor is determined for sliding resistance by using the appropriate loads calculated in steps 2 and 6 and the correct method (Section 3.5.1). The tensile force required was determined for each of the angles of mooring load as calculated in Step 2. The maximum of these tensile forces was selected as the minimum required anchor force for sliding resistance for a FOS of 2.0.

**Step 11: Store Sliding Resistance Tension in Output Array**

Store the tensile ground anchor force determined in Step 10 in an output array.

**Step 12: Compute Tension for Bearing Capacity in Final State**

The required tensile capacity of the ground anchor for bearing capacity is determined through the loads calculated in steps 2 and 6 and the method in Section 3.5.2. As with step 10 it was determined for all angles of mooring load with the maximum being selected as the required tensile force for bearing capacity with a FOS of 2.0.

**Step 13: Store Bearing Capacity Tension in Output Array**

Store the tensile ground anchor force determined in Step 12 in an output array.

**Step 14: Determine Maximum Tensile Force**

Determine the maximum tensile force when comparing the required tension for sliding resistance and bearing capacity. The maximum required tension will be the governing force of this permutation. Store this value in an output array.

**Step 15: Count = Count + 1**

Increment the counter and begin computation of the next permutation from step 5. Once the counter has reached the maximum number of iterations determined in step 4 proceed to step 16.

**Step 16: Write Output Arrays to Excel Spreadsheet**

The MATLAB scripts writes the following arrays out to an Excel spreadsheet using existing MATLAB commands in the following order:

- Permutation Designation of Structural Configuration
- Permutation Mass
- Construction State FOS: Sliding
- Construction State FOS: Bearing
- Ground Anchor Tension: Sliding
- Ground Anchor Tension: Bearing
- Ground Anchor Tension: Maximum.

**6.3.1 Computation Methodology**

The input parameter file created in Section 6.2.1 was divided into five separate parts. This was to allow for the analysis of all permutations to be completed more rapidly. This decrease in computation time resulted from each of the five parts begin able to be analysed simultaneously on separate workstations. Each of the five separate parts followed the analysis method laid out above. The input parameter file was separated into the five parts according to anchor heights with a file for each of the anchor heights 16.5m through 17.5m.

**6.4 Outputs of Simplified Model**

After the completion of the analysis of each of the five parts, the output files of each were combined to form an output of the entire permutations file using the MATLAB script included in Appendix F.2. The computation time for each of the five workstations for the analysis was  $\pm 15$  hours, for a total computation time of  $\pm 75$  hours.

The MATLAB script used for merging the separate output files was also used to rank the permutations. Prior to ranking the permutations all permutations that failed the construction state FOS check were removed from the output file. The number of permutations that passed the construction phase FOS check was 12 880. The remaining permutations were then ranked according to permutation mass and required anchor tension. The rankings for each permutation are summed together to determine a final score for each permutation. The ranking of mass and anchor tension where given equivalent weighting when summed. The final scores were then sorted from lowest to highest to determine the optimal sections.



## 6.5 Recommendations Deduced from Analysis

The results of the ranked analysis show that ground anchors with an angle other than  $0^\circ$  required a higher anchor force than those at an angle of  $0^\circ$ , at the same anchor height. Thus for the further phases of optimisation non horizontal ground anchors were ignored.

The permutations with wall thickness of 0.5m and base thickness of 0.5m provided the lightest sections for every base projection thus permutations with wall and base thickness of 0.6 to 1m where ignored in the further optimisation.

Due to the required tensile anchor loads, the use of horizontal anchor bars, with deadman anchor where selected as the preferred anchorage method over the use of unbonded composite prestressed cables. This is as the bars allow for easier construction and are more commonly used in practice. The bars selected for use in this thesis are manufactured by Anker Schroeder but other manufacturers produce similar products.

## 6.6 Configurations for Optimisation

From the recommendations in Section 6.5 the number of permutations was reduced to a total of 190 from the 12 880 that passed the construction state FOS check. All 190 permutations and their analysis output are given in Appendix G. A sample of these outputs is provided in Table 6.1. See Section 6.2.1.7 for detailed breakdown on the Designation of Structural Configuration.

Table 6.1: Phase 1 Output (sample).

Designation of Structural Configuration	Mass (t)	Construction State		Final State Tensile Force (kN)		
		Sliding FOS	Bearing FOS	Sliding	Bearing	Maximum
Wt0.5_Bw5.3_Bt0.5_Ah16.5_Aa0	164.5	1.209	5.553	2231.4	1231.7	2231.4
Wt0.5_Bw5.3_Bt0.5_Ah16.75_Aa0	164.5	1.209	5.553	2231.4	1205.1	2231.4
Wt0.5_Bw5.3_Bt0.5_Ah17.25_Aa0	164.5	1.209	5.553	2231.4	1177.1	2231.4
Wt0.5_Bw5.3_Bt0.5_Ah17.5_Aa0	164.5	1.209	5.553	2231.4	1175.6	2231.4
Wt0.5_Bw5.3_Bt0.5_Ah17_Aa0	164.5	1.209	5.553	2231.4	1203.6	2231.4
Wt0.5_Bw5.4_Bt0.5_Ah16.5_Aa0	165.2	1.228	5.812	2191.2	1199.5	2191.2
Wt0.5_Bw5.4_Bt0.5_Ah16.75_Aa0	165.2	1.228	5.812	2191.2	1173.8	2191.2
Wt0.5_Bw5.4_Bt0.5_Ah17.25_Aa0	165.2	1.228	5.812	2191.2	1147.4	2191.2
Wt0.5_Bw5.4_Bt0.5_Ah17.5_Aa0	165.2	1.228	5.812	2191.2	1146.7	2191.2
Wt0.5_Bw5.4_Bt0.5_Ah17_Aa0	165.2	1.228	5.812	2191.2	1173.1	2191.2
Wt0.5_Bw8.9_Bt0.5_Ah16.5_Aa0	191.0	1.881	17.890	784.7	-490.7	784.7
Wt0.5_Bw8.9_Bt0.5_Ah16.75_Aa0	191.0	1.881	17.890	784.7	-477.4	784.7
Wt0.5_Bw8.9_Bt0.5_Ah17.25_Aa0	191.0	1.881	17.890	784.7	-479.2	784.7
Wt0.5_Bw8.9_Bt0.5_Ah17.5_Aa0	191.0	1.881	17.890	784.7	-469.1	784.7

## Chapter 7

# Optimisation

Due to the large number of possible structural configurations determined in Chapter 6 resulting from the global system analysis and working states design (WSD), a further reduction in structural configurations was necessary along with the determination of the structural suitability of each of the configurations. This section will make use of the structural analysis of each configuration at the ultimate limit state (ULS) to determine which of the configurations would allow for practical structural design. From this the lightest final design would be determined.

### 7.1 Further Reduction in Permutations

An analysis of a single configuration was selected to determine the effect of the anchor height on the bending moments in the structure at ULS for the structures final load case. The configuration selected was **Wt0.5\_Bw9\_Bt0.5**. Due to the differences between working states design and ultimate limit states design the required anchor tension for structural equilibrium was determined. EN1990:2002+A1 (ENCEN, 2005) provided the required ULS load factors for this computation as give in Table 7.1. Table 7.2 provides both the required anchor tension at ULS and the anchor tension required for WSD for the chosen configuration, the calculation of the required tension at ULS is given in Appendix H. For this configuration the required anchor tension for WSD exceeds that of ULS design, this is not true of all configurations as shown in Section 7.4. Thus the anchor force required for WSD was used for further analysis of this configuration. The capping beam was modelled as having the same wall thickness (0.5m) as the precast element this was to allow for easier computation within the FEM model, while the density of the concrete used in the capping beam was double to simulate a thicker section.

Table 7.1: Load Factors from EN1990:2002+A1 (ENCEN, 2005)

Load Factors ULS (BS)		
Permanent Loads	Self Weight	1.35
	Soil parameters	1.35
	Prestressed Tendons	1
Variable Loads	Imposed Loads	1.5
	Loads from fluids that vary with time	1.5

Table 7.2: Required Anchor Forces for Structural Equilibrium for ULS design and Working States Design

Anchor Height (m)	Required Force ULS (kN)	Required Force WSD (kN)
17.5	0	744.5
17.25	0	744.5
17	0	744.5
16.75	0	744.5
16.5	0	744.5

Each of the configurations with base projection 9m, at anchor heights 16.5m through 17.5m were analysed using a basic 2D frame Finite Element Model (FEM) in Abaqus (Dassault Systems) to determine the bending moments and the resulting bending moment diagrams for each anchor height. The maximum bending moment determined from this analysis is given in Table 7.3. The entire 5.9m section of the quay wall was reduced to a 2D frame model, this was to allow for easier determination of the structure's bending moments. The resulting bending moments are given in Figure 7.1, the maximum bending moment calculated is for the entire 5.9m width of the section.

Figure 7.1 provides a comparative plot of the bending moment diagrams obtained from the frame model analysis, from the results given in Tables 7.2 and 7.3 and Figure 7.1 it can be seen that the effect of the ground anchor has a minimal impact on the bending forces within the range of 16.5m to 17.5m. The range of the difference at the base of the wall was  $\pm 745\text{kNm}$ . Thus all further optimisation was completed using a fixed anchor height of 17.5m. This has the additional advantage that for the installation of the ground anchor, much of the work will be completed in a dry environment as the anchor is situated 0.9m above MSL.

Table 7.3: Required Anchor Forces for Moment Equilibrium and Resulting Maximum Bending Moment

Anchor Height (m)	Anchor Force (kN)	Max Bending Moment (kNm)
17.5	744.5	73 380
17.25	744.5	73 567
17	744.5	73 753
16.75	744.5	73 939
16.5	744.5	74 125

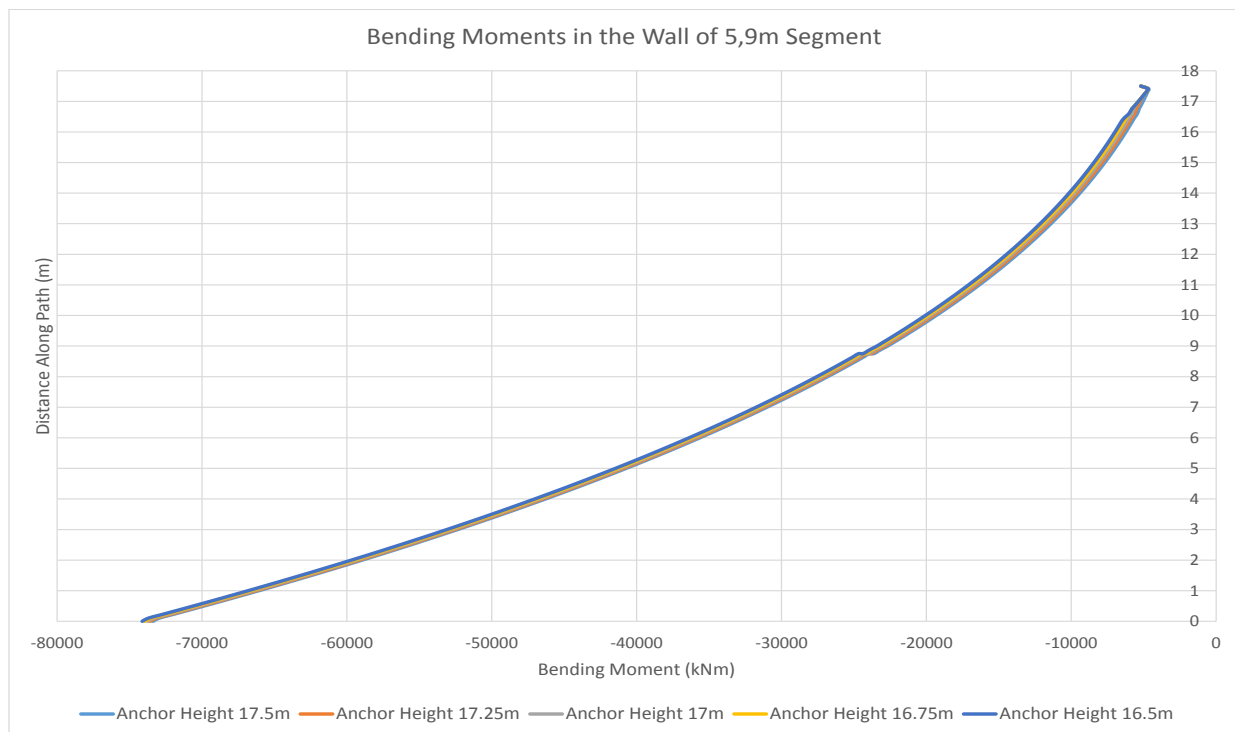


Figure 7.1: Comparative Bending Moments at Anchor Heights 16.5m through 17.5m

Due to the large bending moments obtained, in the range of  $\pm 73\,380\text{kNm}$  to  $\pm 74\,125\text{kNm}$  from the analysis it was recommended to include a set of steel ties to support the wall and reduce the bending moments within the wall.

## 7.2 Maximum Allowable Bending Moment in Section

A minimum rebar spacing of 120mm was decided upon to allow for easier placement of concrete. The easier placement minimises the risk of poor concrete quality that could negatively effect the overall durability of the overall structure. The primary concerns are segregation of the concrete mix due to the tight mesh of steel rebar, this spacing also ensures that vibrating pokers are able to be used to ensure proper compaction of the placed concrete.

The spacing of 120mm was selected as to allow for the use of 40 mm diameter bar as the primary vertical reinforcement elements without the openings in the reinforcement mesh being less than 80mm. From this and the use of SABS 0100-1 (SABS, 2000) the maximum achievable bending moment using Y40 bars at a spacing of 120mm is 8020kNm for the entire 5.9m section.

Smaller spacing between rebar could be obtained through the use of a concrete mix that makes use of smaller stone aggregate or a self compacting concrete as these mixes have a reduced chance of segregation which would result in better quality of concrete when used in the smaller mesh. Through the use of these measures a greater maximum bending moment could be achieved. Both of these measures would increase the price of the concrete used in each segment. The focus of this research is on the structural optimisation of each segment and thus optimisation of the materials and the effect of such optimisations have been ignored.

## 7.3 Reduction in Bending Moments Through Addition of Steel Ties

The maximum bending moment obtained in the 2D frame analysis was  $\pm 73\,500\text{kNm}$  in the front wall for the entire 5.9 m section. This bending moment exceeds the maximum bending moment calculated in Section 7.2, thus the addition of steel ties was selected to reduce this bending moment.

The ties were selected to be situated at 8.75m from the base of the front wall, this is the midspan point on the wall and would join the base of the structure 0.5m from the end of the base projection. The distance from the end of the base projection was selected to ensure the most gradual slope of the tie member while minimising the stress concentration in the concrete at the end of the base projection.

The steel section selected for use in the tie was a UB 254x146x37. Three(3) ties were selected to provide an even distribution of support. The ties are located 0.95m from the edge of the structure with 2m centres. This spacing ensures that the spacing between ties, including ties on adjacent sections is  $\pm 2\text{m}$  allowing for the unsupported horizontal length to not exceed 2m. Figure 7.2 shows the layout of these ties on the final structure,

the configuration shown is **Wt0.5\_Bw9\_Bt0.5\_Ah17.5\_Aa0**, referred to as Bw9.

The effect of these ties on the bending moment is given in Figure 7.3. The bending moment was computed using a basic 2D frame model with a mesh size of 100mm. While using a 2D frame model for a structure that has geometric differences along its out of plane dimension is not recommend, it does provide an indication of the effect of the ties on the bending moments within the structure. Figure 7.3 provides a comparison between the unsupported wall and the wall supported with ties, using the Bw9 configuration as used in the previous section. The discontinuity in the bending moments at the height of 8.75m is due to the additional stiffness due to the addition of the steel ties. From this it shows that the tie greatly reduces the maximum bending moment from  $\pm 73\ 500\text{kNm}$  to  $\pm 23\ 600\text{kNm}$  for th entire 5.9m section. This value of 23 600kNm still exceeds the maximum allowable bending moment of 8020kNm obtained in Section 7.2 it is hypothesised that through the increasing the anchor tension the bending moment within the structure will be reduced to meet the maximum allowable bending moment.

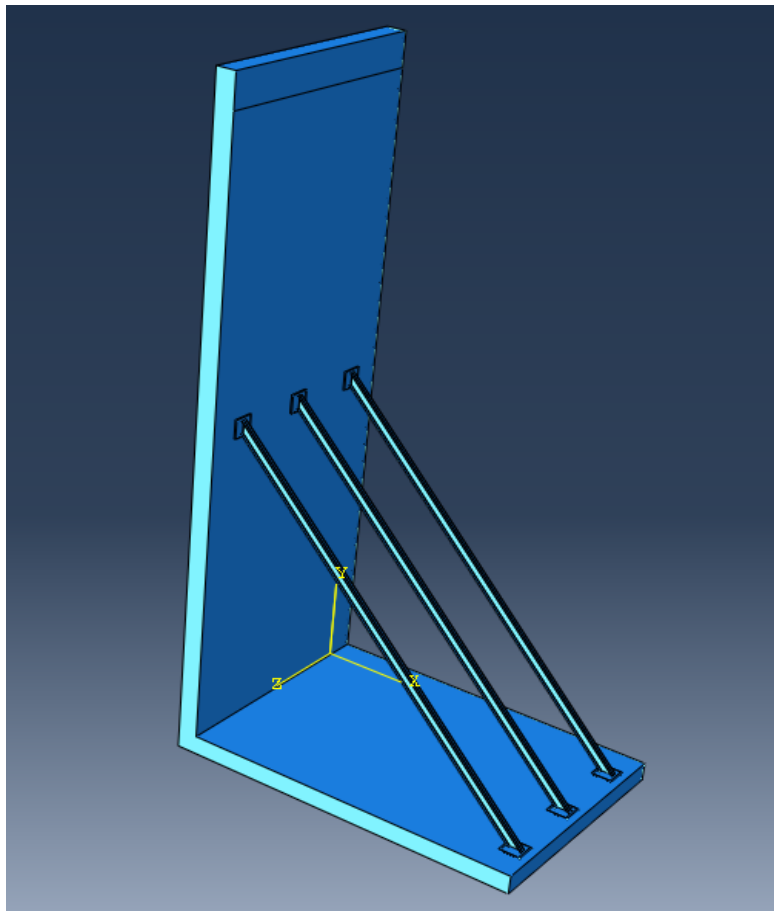


Figure 7.2: Layout of Support ties

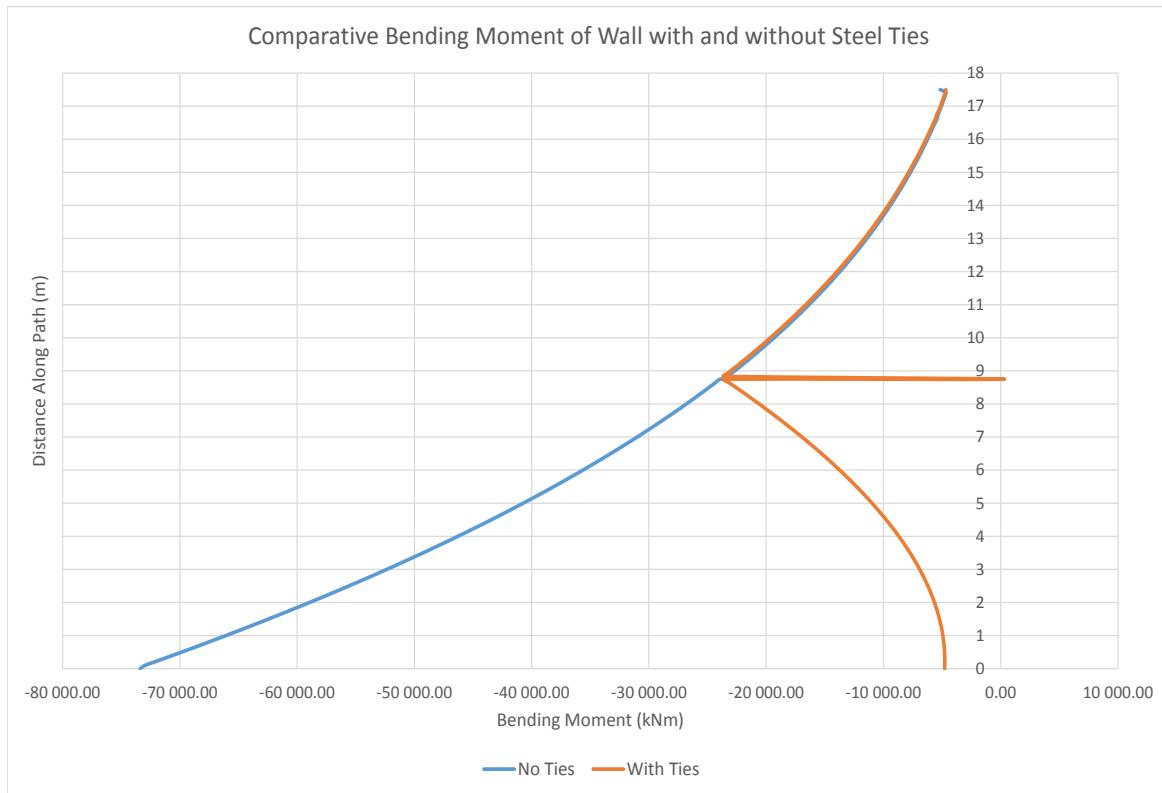


Figure 7.3: Comparative Bending Moments of Front Wall with and without ties

## 7.4 Required Anchor Force for Structural Equilibrium

As with the Bw9 configuration used in Section 7.1 the required anchor force for moment equilibrium at ULS of the structure with each of the base projection lengths was determined, these required anchor forces are given in Table 7.4. The maximum required anchor force computed in Chapter 6 is also given, the maximum of the required anchor forces will be used as the design anchor force for further optimisations.

Table 7.4: Required Anchor Forces for Moment Equilibrium at ULS compared to Chapter 6 WSD required Anchor Force

Base Projection (m)	Required Force ULS (kN)	Required Force WSD (kN)	Design Anchor Force (kN)
5.3	3168	2231.4	3168
5.5	3031	2151.0	3031
6	2666	1950.1	2666
6.5	2269	1749.2	2269
7	1841	1548.2	1841
7.5	1382	1347.3	1382
8	891	1146.4	1146.4
8.5	368	945.4	945.4
9	0	744.5	744.5

From the required anchor forces given in Table 7.4 it was found that the WSD anchor force does not always provide the required anchor force for design purposes. Only configurations with base projections greater than 7.5m require the use of the WSD anchor force computed for final design while configurations with base projections less than 7.5m require the use of the anchor force computed at ULS for design purposes.

#### 7.4.1 Available Bar Anchors

The selected bar anchors for use in this optimisation are ASDO500 anchor bars produced by Anker Schroeder. These bars were selected as the cost of these bars was readily available, see Section 7.6.1.3 for further details on the costs of the bars. Anker Schroeder also produce bars of higher tensile yield capacities but the price of these was unknown during the research and thus was ignored. Various other manufactures produce similar products and thus the ASDO500 bar could be replaced with an equivalent product. Table 7.5 provides the working tensile capacities of various single and twin anchor set-ups along with the associated costs, the working tensile capacity of a single bar is specified in Appendix I .



Table 7.5: Available Bar Anchor Capacities and Costs

Anchor Code	Bar Diameter (mm)	Working Capacity		Costs	
		Single Anchor (kN)	Twin Anchor (kN)	Single Anchor (R)	Twin Anchor (R)
M64/48	48	848	1696	R 34 722	R 69 443
M72/52	52	1062	2124	R 40 750	R 81 499
M76/56	56	1232	2464	R 47 260	R 94 520
M80/60	60	1376	2752	R 54 252	R 108 505
M85/65	64	1559	3118	R 61 727	R 123 454
M90/68	68	1771	3542	R 69 684	R 139 369
M95/72	72	1987	3974	R 78 124	R 156 247
M100/76	76	2216	4432	R 87 045	R 174 090
M105/80	80	2457	4914	R 96 449	R 192 898
M110/85	85	2710	5420	R 108 882	R 217 763
M120/90	90	2976	5952	R 122 068	R 244 136
M125/95	95	3544	7088	R 136 008	R 272 016

#### 7.4.2 Required Anchor For Configuration

Table 7.6 provides the cheapest possible bar anchor set-up for the required design anchor force, the final column specifies if a twin bar anchor set-up is used.

Table 7.6: Required Bar Anchors for Design Anchor Forces

Base Projection (m)	Design Anchor Force (kN)	Anchor Code	Twin Anchor
5.3	3168	M125/95	No
5.5	3031	M85/65	Yes
6	2666	M80/60	Yes
6.5	2269	M76/56	Yes
7	1841	M95/72	No
7.5	1382	M85/65	No
8	1146.4	M76/56	No
8.5	945.4	M72/52	No
9	744.5	M64/48	No

## 7.5 Maximum Allowable Bending Moment Limitations

### 7.5.1 Determination of Bending Moments for Selected Structural Configurations

Using the design anchor force computed in Section 7.4 the bending moment for each of the possible configurations was determined, this was completed using a similar basic Finite Element (FE) 2D Frame Model as used in Section 7.3 with only the length base projection and location of the tie connection on the base projection varied. An example of the FE model is given in Figure 7.4, the configuration given in the example is Bw9. The resulting bending moment diagrams for the wall and the base projection are given in Figures 7.5 and 7.6 respectively, included in each figure, the 8020kNm maximum allowable bending moment in the section is plotted as calculated in Section 7.2.

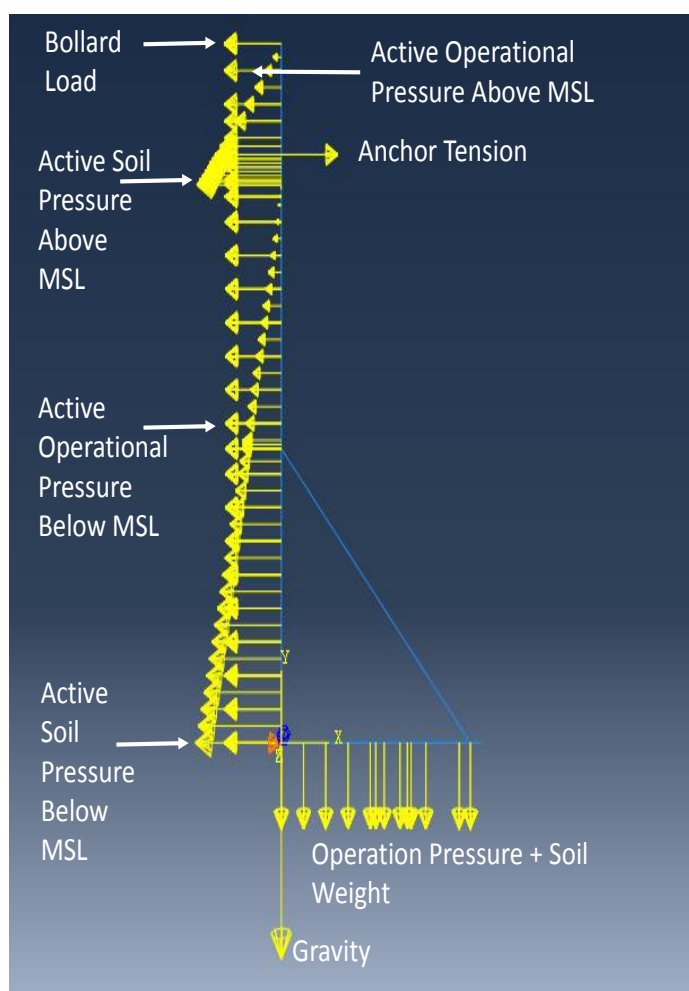


Figure 7.4: Example of 2D Frame Finite Element Model

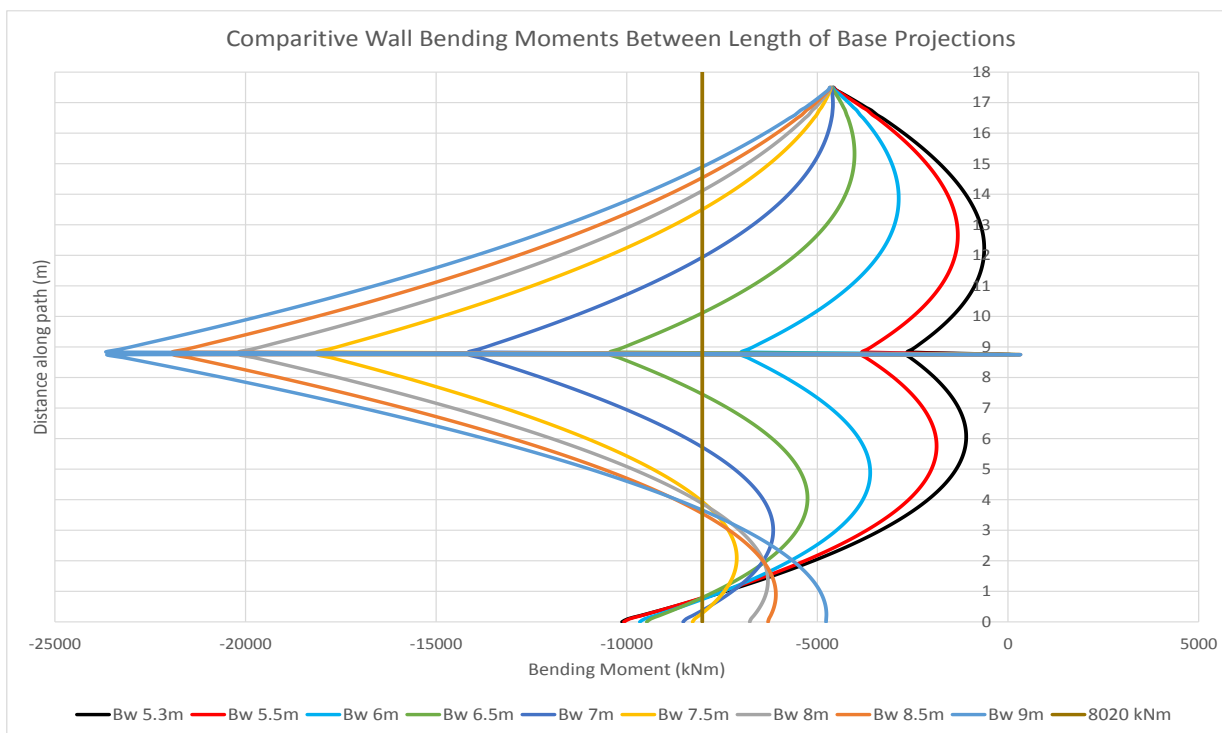


Figure 7.5: Comparative Wall Bending Moments Between Lengths of Base Projection

From Figure 7.5 it was determined that only configurations with base projections of greater than 7.5m have bending moments at the base of the wall of the structure that did not exceed the computed maximum allowable bending moment in the section, the rest of the configurations failed the check in this portion of the wall. Above the height of  $\pm 3\text{m}$  to a height of  $\pm 15\text{m}$  the configurations with base projections greater than 7.5m also fail the maximum allowable bending moment check, while the configurations with base projections of between 5.3m and 6m do not in the same portion of the wall. From this it was determined that the increased anchor force that the structures with smaller base projections require for structural equilibrium decreases the maximum bending moments between the wall heights of  $\pm 1.5\text{m}$  and  $17.5\text{m}$  while increasing the the maximum bending moment in the base of the wall, between  $0\text{m}$  and  $\pm 1.5\text{m}$ .

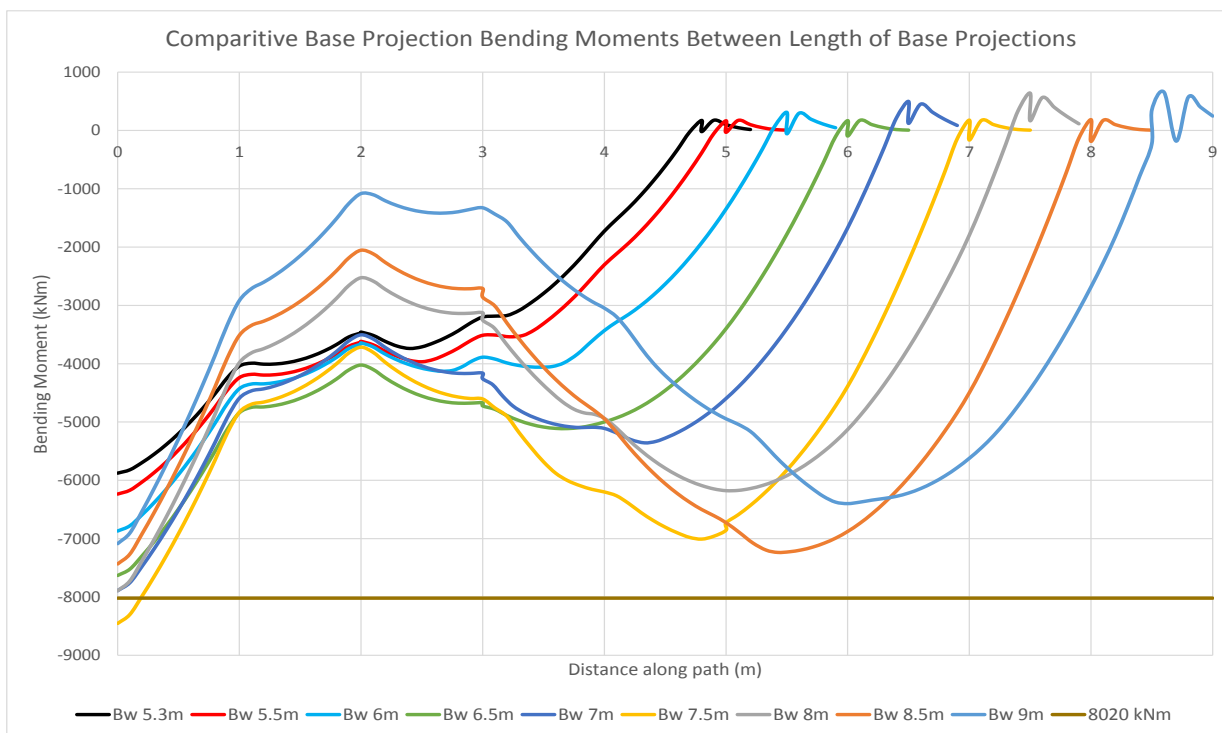


Figure 7.6: Comparative Base Projection Bending Moments Between Lengths of Base Projection

Figure 7.6 shows that all possible configurations do not exceed the maximum allowable bending moment barring the configuration with a base projection of 7.5m (referred to as Bw7.5), this is most likely due to the minor difference between the required ULS anchor force and WSD anchor force. The Bw7.5 exceeds the maximum allowable bending moment in the section by  $\pm 435\text{kNm}$ . Unlike with the bending moments induced in the wall, the increased anchor force reduced the maximum bending moments in the base projection apart from the Bw7.5 configuration which is due to the factors mentioned above.

### 7.5.2 Effect of Additional Anchor Force on Bending Moments

The configurations with base projections greater than 7.5m were the only sections where there was available bending moments capacity in the section to allow for an increased anchor force that would reduce the bending moment in the wall between the heights of  $\pm 1.5\text{m}$  and  $17.5\text{m}$ . By increasing the anchor force the bending moment at the base of the wall would increase. Thus an anchor force that would reduce the maximum bending

moment in the wall while not exceeding the maximum allowable bending moment at the base of the wall would be required. By increasing the anchor force a reduction in the maximum bending moment within the base projection is expected.

Using the configurations with base projections between 8m and 9m as modelled in Section 7.5.1, the anchor force was increased to match the capacities of various single or twin ground anchors as given in Section 7.4.1, until a suitable anchor force was determined. In the keys of all figures in Sections 7.5.2.1 to 7.5.2.3 all anchor forces that require the use of twin anchors have *twin* in parenthesis adjacent to the anchor force.

### 7.5.2.1 Base Projection: 9m

Using the Bw9 configuration, the bending moments in the structure for anchor forces between 744.5kN and 3118kN. Figure 7.7 provides the resultant bending moments, as shown the minimum anchor force that produces a maximum bending moment at midspan and a moment at the base of the wall of less the 8020kNm is 2752kN. The resulting moment at midspan is  $\pm 6250$ kNm with a moment at the base of  $\pm 6260$ kNm. Figure 7.8 provides the bending moments within the base projection, the anchor force of 2752kN produces a maximum bending moment of  $\pm 2420$ kNm versus the  $\pm 7090$ kNm when an anchor force of 744.5kN is used.

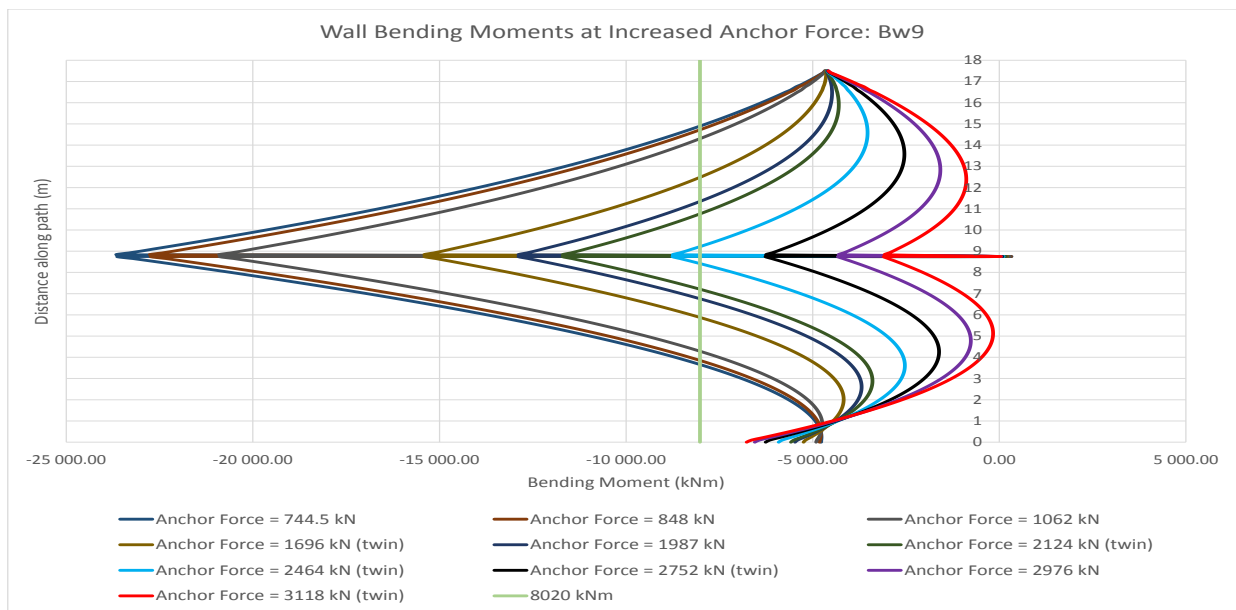


Figure 7.7: The effect of increased anchor force on the Bw9 Configuration wall bending moments

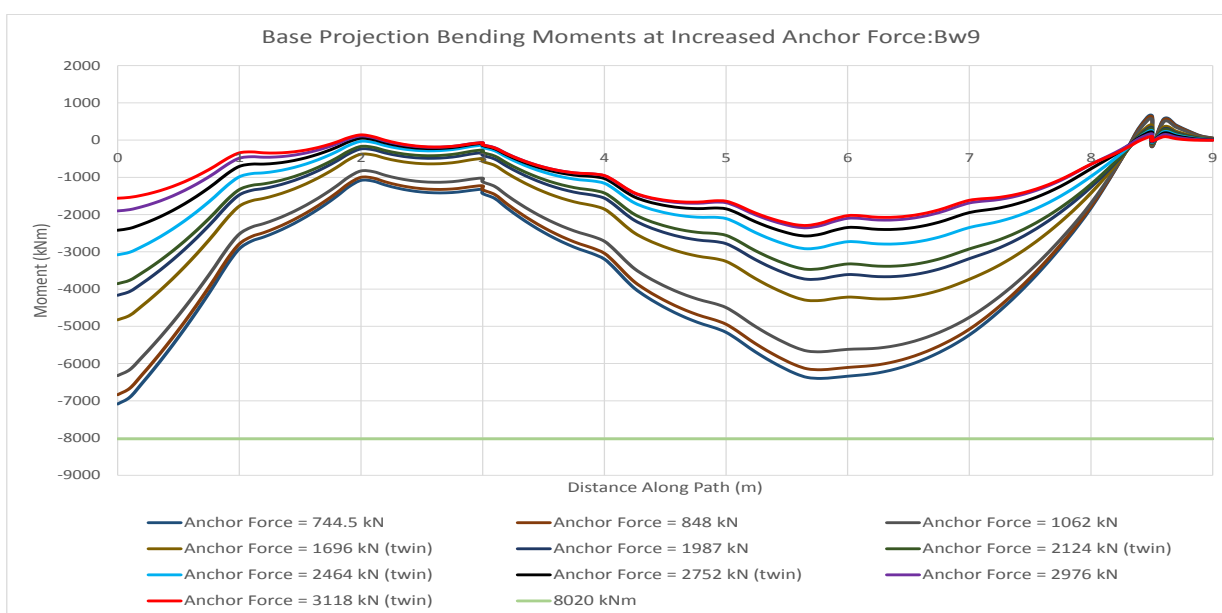


Figure 7.8: The effect of increased anchor force on the Bw9 Configuration base projection bending moments

### 7.5.2.2 Base Projection: 8.5m

From Figure 7.7 it was determined that a suitable anchor force lies between 2464kN and 2752kN. Thus for the **Wt0.5\_Bw8.5\_Bt0.5\_Ah17.5\_Aa0** configuration, referred to as Bw8.5, the bending moments for these anchor forces were determined. The resultant bending moments in the wall are given in Figure 7.9 and the moments in the base projection are given in Figure 7.10. As in Section 7.5.2.1 the anchor force of 2752kN provides a suitable bending moment in the wall,  $\pm 6245\text{kNm}$  at midspan and  $\pm 6580\text{kNm}$  at wall base, while ensuring suitable bending moments in the base projection.

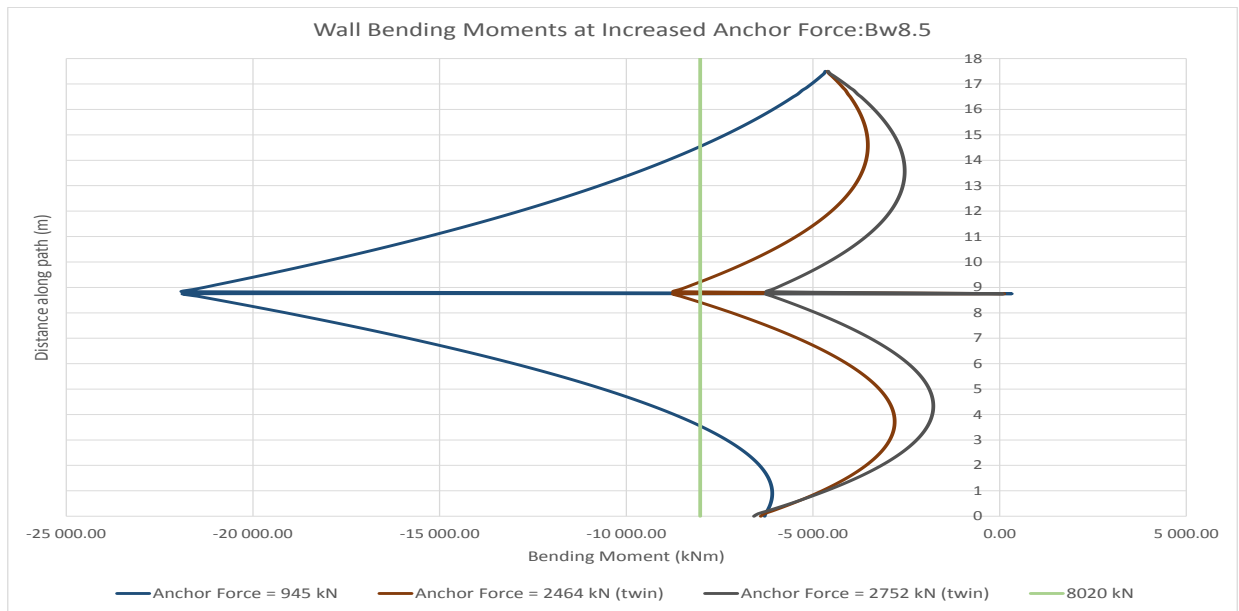


Figure 7.9: The effect of increased anchor force on the Bw8.5 Configuration wall bending moments

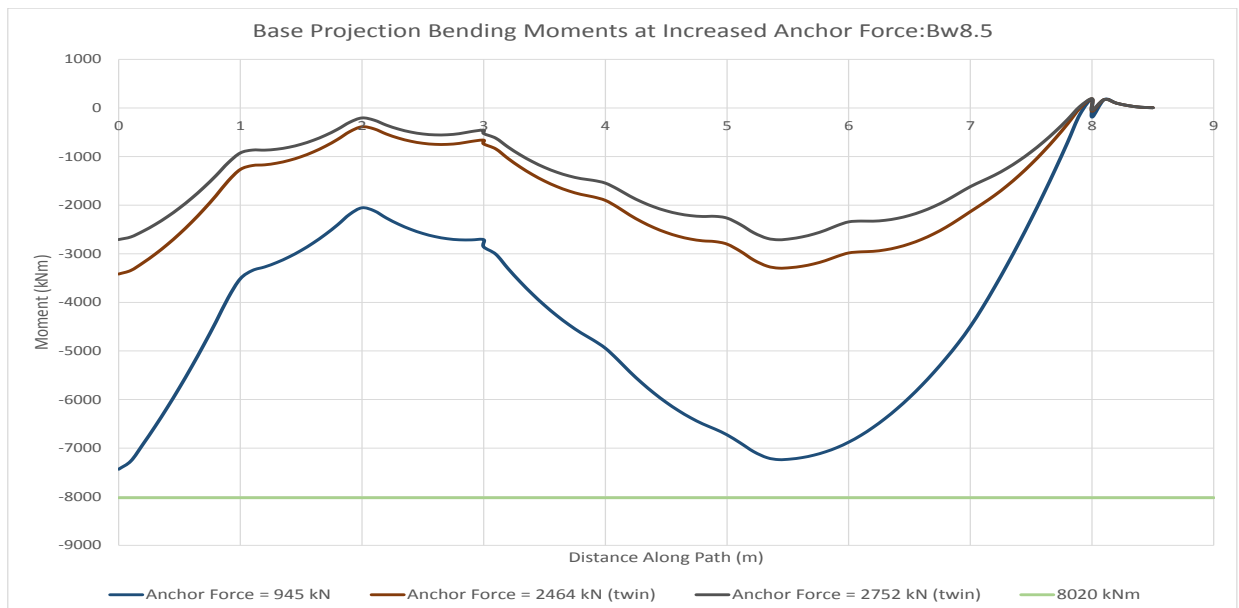


Figure 7.10: The effect of increased anchor force on the Bw8.5 Configuration base projection bending moments

### 7.5.2.3 Base Projection: 8m

Using the same increased anchor forces as in Section 7.5.2.2 on the **Wt0.5\_Bw8\_Bt0.5\_Ah17.5\_Aa0** configuration, referred to as Bw8, the bending moments were determined. The resultant bending moments in the wall are given in Figure 7.11 and the moments in the base projection are given in Figure 7.12. As in Section 7.5.2.1 the anchor force of 2752kN provides a suitable bending moment in the wall,  $\pm 6246\text{kNm}$  at midspan and  $\pm 6985\text{kNm}$  at wall base, while ensuring suitable bending moments in the base projection.

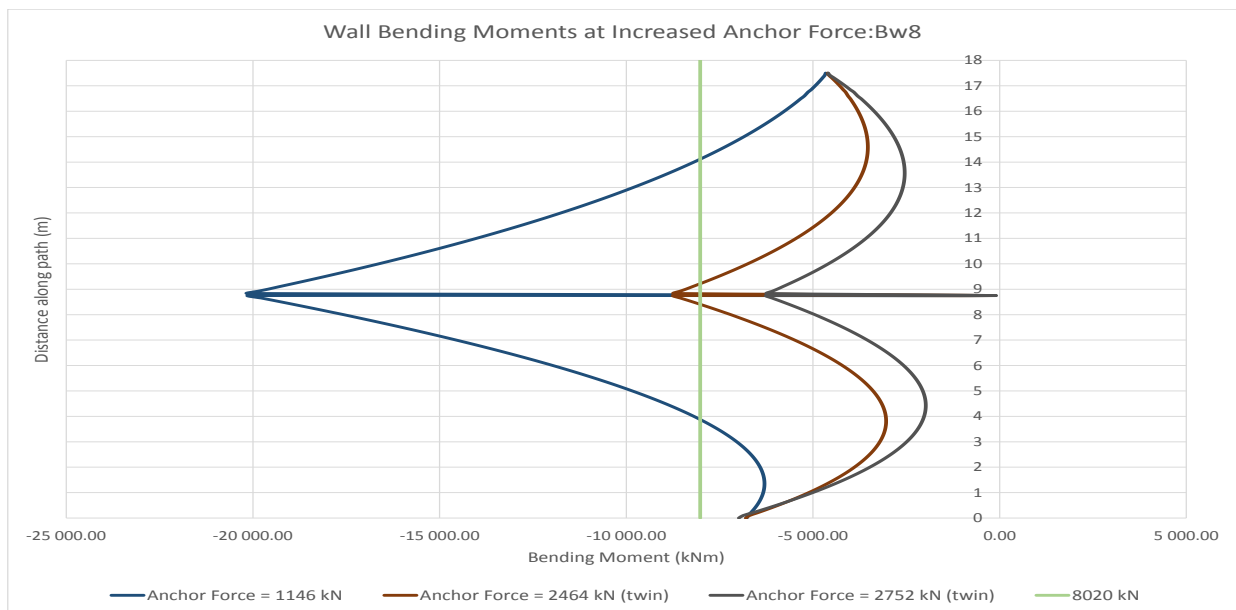


Figure 7.11: The effect of increased anchor force on the Bw8 Configuration wall bending moments



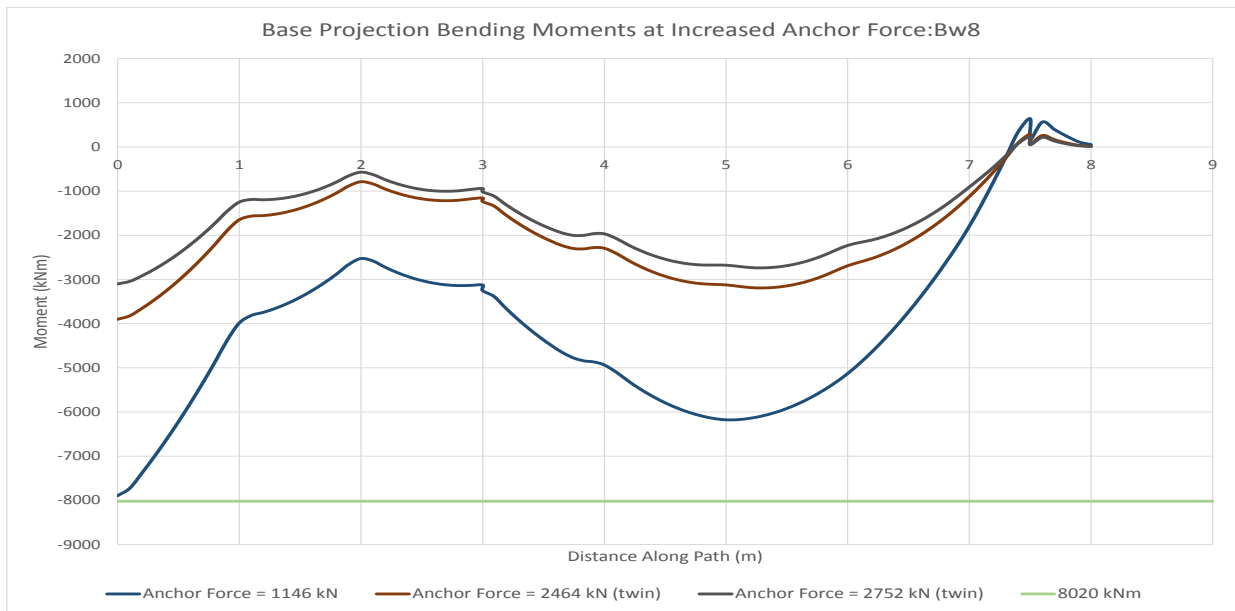


Figure 7.12: The effect of increased anchor force on the Bw8 Configuration base projection bending moments

### 7.5.3 Final Bending Moments

From the results obtained in Section 7.5.2 the anchor force of 2752kN was selected for the Bw8, Bw8.5 and Bw9 configurations. The comparative bending moments are plotted in Figure 7.13 for the wall and Figure 7.14 for the base projection. From these comparative bending moments, envelopes of possible bending moments were determined for all configurations with base projections between those computed.

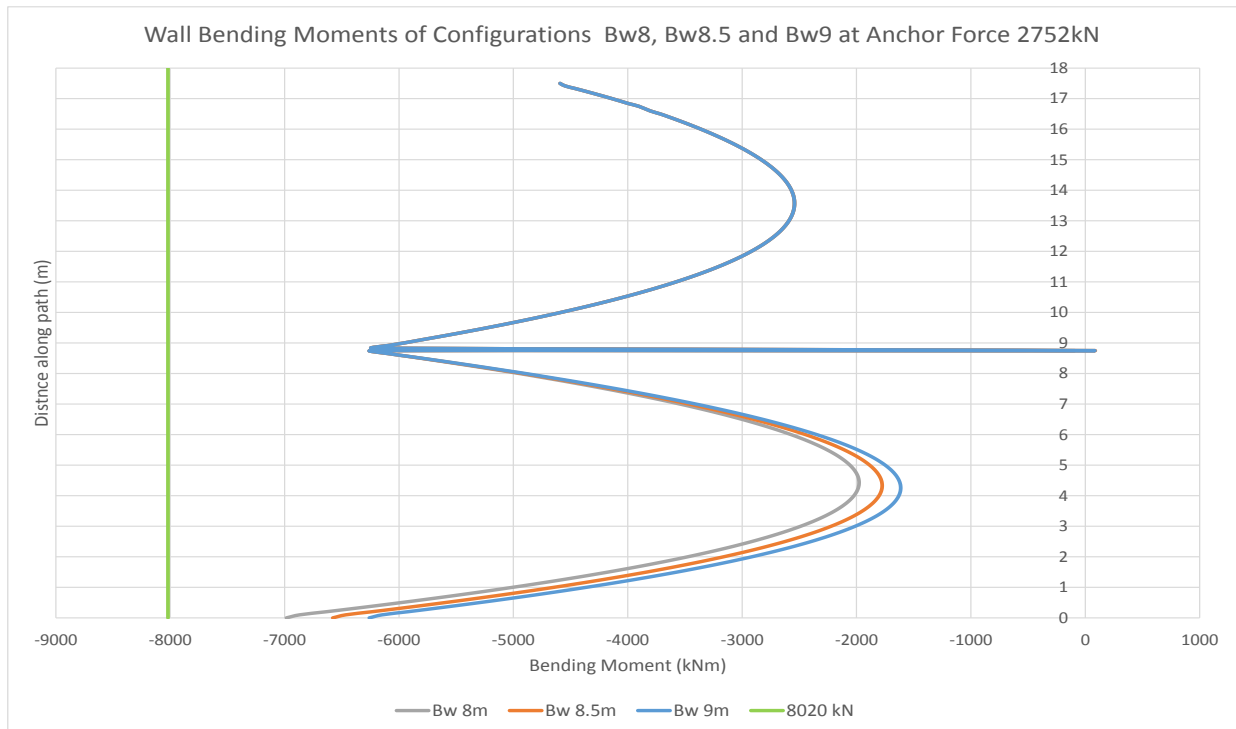


Figure 7.13: Comparative Wall Bending Moments of Configurations Bw8, Bw8.5 and Bw9 at Anchor Force 2752kN

From Figure 7.13 the bending moment above the tie was determined to be roughly equivalent. Table 7.7 provides a summary of the critical moments within the wall, from these results the moment at midspan varies in a range  $\pm 5$  kNm while the moment at the base of the wall varies  $\pm 405$  kNm between configurations Bw8 and Bw8.5 and varies  $\pm 320$  kNm for configurations Bw8.5 and Bw9.

Table 7.7: Bending Moments Summary at Anchor Force 2752kN for Layouts Bw8, Bw8.5 and Bw9 in Wall

Base Projection (m)	Base Bending Moment (kNm)	Midspan Bending Moment (kNm)
8	$\pm 6985$	$\pm 6246$
8.5	$\pm 6580$	$\pm 6245$
9	$\pm 6260$	$\pm 6250$

From Figure 7.14 it can be seen that there is no discernible pattern to the bending moments in the base projections of the layouts. As the largest of the bending moments, as given in Table 7.8, equates to 51.7% of the maximum allowable bending moment in the section, this lack of pattern can be ignored as the possible maximum bending moment for layouts between those computed will not exceed the maximum allowable bending moment.

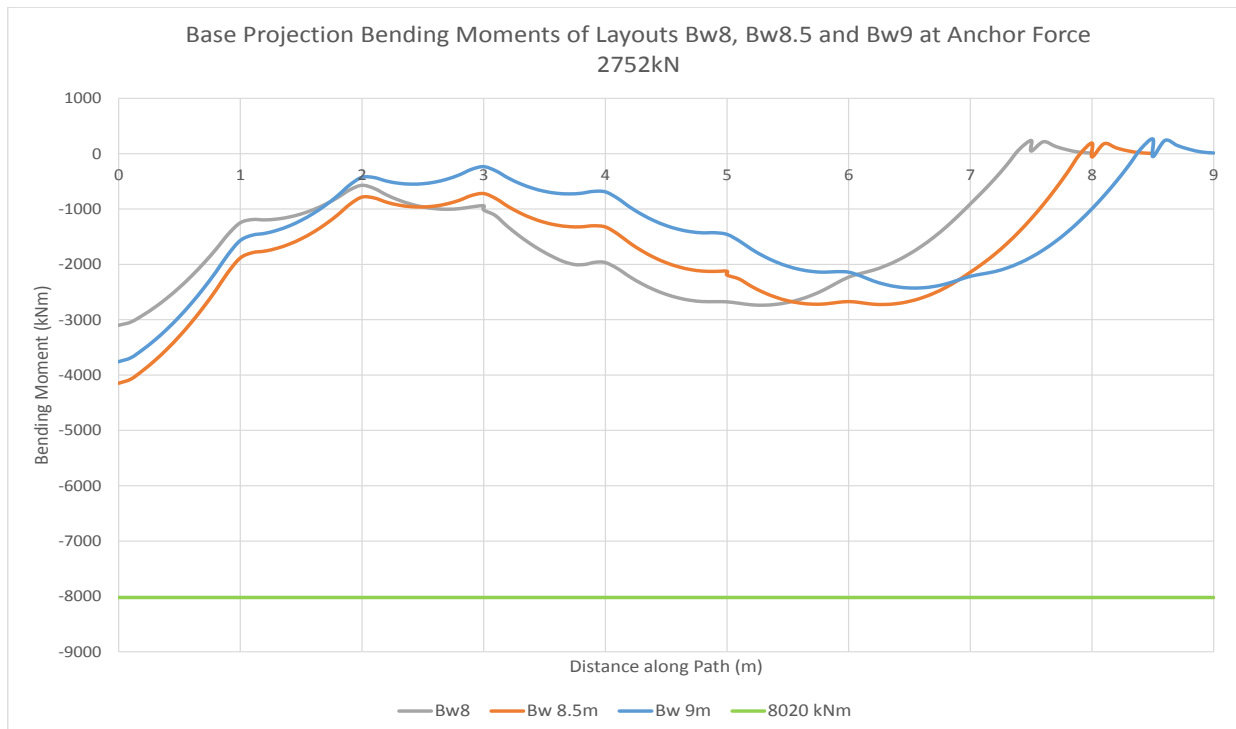


Figure 7.14: Comparative Base Projection Bending Moments of Layouts Bw8, Bw8.5 and Bw9 at Anchor Force 2752kN

Table 7.8: Maximum Bending Moments at Anchor Force 2752kN for Layouts Bw8, Bw8.5 and Bw9 in the Base Projection

Structural Configuration	Max Bending Moment (kNm)
Bw8	$\pm 3100$
Bw8.5	$\pm 4150$
Bw9	$\pm 3760$

## 7.6 Cost Optimisation

Due to the similarity in bending moments of the Bw8 and Bw9 configurations as well as with the possible configurations between them, a further phase of optimisation was required. The chosen method for the next phase of optimisation was the indicative cost of each configuration.

### 7.6.1 Material Costs

This section will be detailing the known cost of the three primary material components of the design namely the concrete, steel reinforcement and bar anchors.

#### 7.6.1.1 Concrete

A cost of R2500 per  $m^3$  was assumed as the cost of the 45MPa concrete mix as used in the original structure. The price of the exact concrete mix was not included in the case study and thus an indicative price for a modern equivalent products was used.

#### 7.6.1.2 Steel Reinforcement

The price per ton of steel reinforcement was taken as R15 000 for the optimisation, this is as the price of reinforcement for the original project was not included in the case study thus an equivalent price was used.

#### 7.6.1.3 Bar Anchors

A quoted price of R70 000 for a single ASDO500 M100/76 bar of length 15m was provided by a quantity surveyor at PRDW. This quoted price was for a project tendered in 2014.

It was recommended to use the quoted price for the ASDO500 M100/76 bar to determine a cost per ton of the same grade material that could be used to determine the cost of various other bar sizes. This was deemed sufficient by the quantity surveyor for estimated bar costs.

Table 7.9: Calculated Cost per Ton of ASDO500 grade material

<b>Bar Parameters</b>		
<b>Parameter</b>	<b>Value</b>	<b>Unit</b>
Diameter of Bar	76	mm
Length of Bar	15	m
Cost per Bar	70 000	Rand
<b>Calculated Values</b>		
<b>Parameter</b>	<b>Value</b>	<b>Unit</b>
Bar Volume	0.068	$m^3$
Bar Mass	534.2	kg
Resulting Cost per ton	131 045	Rand

The cost per ton as calculated in Table 7.9 was then increased to match the average South African inflation in the period of January 2014 until December 2017. The values given in Table 7.10, provided by inflation.eu (2018) were used to calculate the inflated price per ton. The bars are imported and thus would be subject to exchange rate fluctuations but these were ignored as the inflated cost were used to provide indicative final costs per bars rather than exact costs. Thus the final cost per ton of ASDO500 grade material used from here forward in this thesis is R162 954 as of December 2017.

Table 7.10: Cost per Ton of ASDO500 grade material due to inflation in South African Rand

<b>Year</b>	<b>Inflation</b>	<b>Inflated South African Rand Price per Ton</b>
2014	6.12%	R139 065
2015	4.51%	R145 337
2016	6.59%	R154 914
2017	5.19%	R162 954

Using the calculated cost per ton an estimated cost of various other diameter bars was determined all with a length of 15m. These are provided in Table 7.11 along with each bars working tensile capacity. The tensile capacities were obtained from Appendix I which is taken from Anker Schroeder (2015).

Table 7.11: Cost of ASDO500 Bars with tensile working capacity

Anchor Code	Bar Diameter (mm)	Mass (kg)	Tensile Strength (kN)	Cost per bar
M64/48	48	213	848	R 34 722
M72/52	52	250	1062	R 40 750
M76/56	56	290	1232	R 47 260
M80/60	60	333	1376	R 54 252
M85/65	64	379	1559	R 61 727
M90/68	68	428	1771	R 69 684
M95/72	72	479	1987	R 78 124
M100/76	76	534	2216	R 87 045
M105/80	80	592	2457	R 96 449
M110/85	85	668	2710	R 108 882
M120/90	90	749	2976	R 122 068
M125/95	95	835	3544	R 136 008
M130/100	100	925	3849	R 150 701
M135/105	105	1020	4164	R 166 148
M140/110	110	1119	4492	R 182 349
M150/115	115	1223	5186	R 199 302
M160/125	125	1445	5551	R 235 471

ASDO do provide a higher grade material for use in ground anchors known as ASDO700. These bars have a higher tensile working capacity than the ASDO500 bars and thus lighter profiles could be used for construction.

## 7.6.2 Optimisation Process

This section details the process used in the cost optimisation of the Bw8, Bw8.5 and Bw9 configurations using the bending moments obtained in Section 7.5.2.

### 7.6.2.1 Steel Reinforcement

Using the bending moments computed in Section 7.5.3 and SABS 0100-1 the exact volume of steel reinforcement for each of the configurations was determined for both the wall and base projection. Only in plane bending moments were used for this optimisation as the out of plane bending moments were unknown at the point in the design and they were determined to be very similar as a result of the patterning of the structural components, such as the ties shown in Figure 7.2, these are consistent between each of the configurations. If no compression reinforcement was required in the section, the minimum required steel reinforcement according to SABS 0100-1 was added.

Both the height of the wall and length of the base projection were divided into 4 sections, such that no section exceeded 5m. This was done to allow for greater optimisation of the rebar in the section and to allow for easier construction such that no single length

of rebar exceeded 6m. Table 7.12 provides the bending moments in the wall used for this design in each of the 4 sections for each of the analysed configurations. Table 7.13 provides the cost of the required steel reinforcement in configurations Bw8, Bw8.5 and Bw9.

Table 7.12: Design Bending Moments in each Section

Configuration	Sections			
	0-5m kNm	5-10m kNm	10-14m kNm	14-18 kNm
Bw8	± 6985	± 6245	± 4586	± 4592
Bw8.5	± 6579	± 6246	± 4586	± 4592
Bw9	± 6260	± 6247	± 4586	± 4592

Table 7.13: Cost of Steel Reinforcement for Listed Configurations

Configuration	Cost (R)
Bw8	177 722
Bw8.5	181 546
Bw9	171 172

### 7.6.2.2 Concrete

The difference in the cost of concrete between the Bw8 and Bw9 configurations is R7 375, with the total costs given in Table 7.14. This equates to a 3.85% decrease in concrete cost between the larger Bw9 and the smaller Bw8 configurations.

Table 7.14: Cost of Concrete for Listed Configurations

Configuration	Cost (R)
Bw8	184 375
Bw8.5	188 063
Bw9	191 750

### 7.6.2.3 Bar Anchors

All configurations make use of the same twin anchor set-up to produce the required 2752kN anchor force. The resulting cost of the twin ASDO500 M80/60 anchors is R108 505.

### 7.6.3 Total Cost of Each Configuration

The resulting total costs of the Bw8, Bw8.5 and Bw9 configurations are R 470 602, R 478 114 and R 471 427 respectively. The resulting difference in total price between the smallest and largest configuration is R825 or a 0.18% increase of the total cost of the configuration. The increase in the cost of the Bw8.5 configuration is due to the increased bending moment within the base projection along with the additional material required for the 0.5m of steel rebar required per length of rebar along with the additional concrete volume.

### 7.6.4 Additional Cost Influence: Reinforcing ties

The three ties that were added to reinforce the structure in Section 7.3 would also impact the overall cost of the structure. The exact cost of the UB 254x146x37 section selected for the tie is unknown as of writing this thesis. The Bw9 configuration requires a tie length of  $\pm 12.2\text{m}$ , the Bw8.5 configuration requires  $\pm 11.9\text{m}$  and the Bw8 configuration requires  $\pm 11.5\text{m}$ . The resulting difference for all three ties is a total reduction in tie length of  $\pm 2.1\text{m}$  between the Bw8 and Bw9 configurations, this would further impact the cost difference between the configurations, the weight difference between the ties is negligible as UB 254x146x37 sections weigh 37kg/m.

### 7.6.5 Cost Optimisation Conclusion

With the total cost for the Bw8 configuration being 0.18% cheaper than the Bw9 configuration for the aspects focused on in Section 7.6 ignoring the effect of possible cost differences resulting from the ties. The difference in weight of the two configurations is 7.35 tons with the Bw8 configuration having a total weight, including tie weight, of 185.7 tons while the Bw9 configuration has a weight of 193.1 tons. The difference in weight equates to 3.83% of the total weight of the structure. With the primary aim of this research to produce the lightest most optimised section and as the cost difference between the sections is negligible, for further optimisation the cost of each structural configuration will be ignored.



## 7.7 Optimisation Conclusion

From the recommendations made in Section 7.6 a further analysis was selected to determine the lightest possible configuration of the configurations with base projections between 7.6m and 7.9m that would result in a suitable sections. From this it was found that the **Bw7.6** configuration (**Wt0.5\_Bw7.6\_Bt0.5\_Ah17.5\_Aa0**) was suitable with a bending moment in the base of the wall of  $\pm 7420\text{kNm}$  and a bending moment at midspan of  $\pm 6245\text{kNm}$  along with a maximum bending moment in the base projection of  $\pm 3510\text{kNm}$ . The total weight of the precast structure using this configuration is 182.6 tons this includes the weight of the supporting ties, this equate to 55.3% of the total weight of the as built structure given in Chapter 4, the weight reduction equates to a 44.67% of the as built structures original mass.

## Chapter 8

# Conclusion and Recommendations

### 8.1 Conclusion

The incorporation of ground anchors in the design of cantilever type quay walls can reduce the total weight of the precast segment. The final configuration for the structural optimisation performed for the case study of the Port of Saldanha does provide a proof of concept for the use of tensioned ground anchors to support precast cantilever type walls.

Through the use of tensioned ground anchors as replacement elements for reinforced concrete counterforts of the cantilever type wall, the mass of the precast segment is reduced while still maintaining global stability of the entire quay wall along with the structural integrity of the precast elements.

It was found that the required anchor tension was not determined by the required anchor force during the working states design of global system stability but rather the internal forces within the precast section at the ultimate limit state. While the working states design anchor force is not the governing factor for the determination of the required ground anchor tension it does provide a good basis from which to begin the optimisation process.

## 8.2 Recommendations for Further Research On Optimisation

The final configuration of the wall structure determined in this research could be further optimised through a full 3D finite element analysis to determine the out of plane stress and bending moments in the concrete compared to the simple 2D frame model used in this thesis. This would allow for a reduction in the concrete in certain areas of the section or localised thickening of concrete for areas of higher stress. This would also allow for a more optimised section when compared to the basic rectangular section as used in the 2D frame model.

With the required marine plant for lifting the precast element not always available, a bigger item of marine plant might be necessary for any given planned port development project. This piece of marine plant could have a lifting capacity greater than the 182.6 tons required for the 5.9m section with the final structural configuration determined for this study. The length of the section could then be increased from 5.9m to optimise the usage of the lifting capacity of the marine plant along with the reduction in the number of elements to be cast and placed for an equivalent length of quay side. This could result in larger savings on the overall cost of the port development project

# Appendices

## Appendix A

### List of Definitions

<b>Astronomical Tide</b>	The tidal levels and character which would result from gravitational effects, eg. of the Earth, Sun and Moon, without any atmospheric influences.
<b>Bed</b>	The bottom of a watercourse, or any body of water.
<b>Berth</b>	A facility where a vessel may be safely moored and loaded or unloaded.
<b>Breakwater</b>	A man-made structure protecting a shore area, harbour, anchorage, or basin from waves.
<b>Chart Datum</b>	The plane or level to which soundings (or elevations) or tide heights are referenced (usually <b>Low Water Datum</b> ). The surface is called a tidal datum when referred to a certain phase of tide. To provide a safety factor for navigation, some level lower than <b>Mean Sea Level</b> is generally selected for hydrographic charts, such as <b>Mean Low Water</b> or <b>Mean Lower Low Water</b> .
<b>Cofferdam</b>	A temporary watertight structure enclosing all or part of the construction area so that construction can proceed in the dry.
<b>Controlling Depth</b>	The least depth in the navigable parts of a waterway, governing the maximum draft of vessels that can enter.
<b>Cope</b>	The waterside top edge of a quay wall.
<b>Dead Weight Tonnage</b>	The total carrying capacity of the ship for cargo, fuel, water and other supplies, measured in long tons of 1016 kg.

<b>Dock</b>	The slip or waterway between two piers, or cut into the land, for the reception of ships.
<b>Draught</b>	The greatest depth between the waterline and the bottom of the keel at any point along the ship's hull. The draft varies according to the loaded condition of the ship.
<b>Harbour</b>	Any protected water area affording a place of safety for vessels. See also <b>Port</b> . A harbour may be natural or man-made.
<b>High Tide</b>	The maximum elevation reached by each rising tide.
<b>Jetty</b>	(1)(United States usage) On open seacoasts, a structure extending into a body of water, which is designed to prevent shoaling of a channel by littoral materials and to direct and confine the stream or tidal flow. Jetties are built at mouths of rivers or tidal inlets to help deepen and stabilize the channel.(2) (British Usage) <b>Wharf</b> or <b>Pier</b> .
<b>Length overall</b>	The length of a ship measured horizontally between the outermost points of its stem and stern.
<b>Low Tide</b>	The minimum elevation reached by each falling tide.
<b>Mean Seas Level</b>	The average height of the surface of the sea for all stages of the tide over a 19-year period, ususally determined from hourly height readings. Not necessarily equal to <b>Mean Tide Level</b> . It is also the average water level that would exist in the absence of tides.
<b>Meteorological Tides</b>	Tidal constituents having their origin in the daily or seasonal variation in weather conditions which may occur with some degree of periodicity.
<b>Pier</b>	A structure, usually of open construction, extending out into the water from the shore, to serve as a landing place, recreational facility etc, rather than to afford coastal protection or affect the movement of water. Is often improperly applied to jetties.
<b>Plimsoll Mark</b>	The maximum draught indicator on a vessel also called the Plimsoll line.
<b>Port</b>	A place where vessels may discharge or receive cargo. It may be the entire harbour including its approaches

and anchorages or only the commercial portion of a harbour where the **Quays**, **Wharves**, facilities for transfer of cargo, docks and repair shops are situated. Protection may be provided the artificial or natural features.

**Quay (pronounced Key)** (1)A stretch of paved bank or a solid artificial landing place parallel to the navigable waterway, for use in loading and unloading vessels.(2) One or more berths continuously bordering on and in contact with a land or dock area. The quay apron reaches the quay front over the entire length of the berth.

**Slip** A berthing space between two piers.

**Spring Tide** A tide that occurs at or near the time of new or full moon and which rises highest and falls lowest from the mean sea level.

**Storm Surge** A rise above normal water level on the open coast due to the action of wind stress on the water surface.

**TEU** TEU stands for Twenty Foot Equivalent Unit, which is the space taken by a standard container of the following dimensions:

<i>Length</i>	= 20ft	= 6.03m
<i>Height</i>	= 8ft	= 2.44m
<i>Width</i>	= 8ft	= 2.44m
<i>Volume</i>	= 6.03x2.44x2.44	= 35.9m <sup>3</sup>

**Water Depth** Distance between the still water level and the seabed.

**Wharf** The same as a **Quay**, but is most commonly used when referring to an open structure on piles.

## Appendix B

# Foundation Profiles



## B.1 Chainages 0 to 175m; 350 to 620m

Layer Thickness (m)	$\gamma_{sub}$ (kN/m)	$\phi'$	C' (kPa)	E (MPa)	$\mu$	Mv (m <sup>2</sup> /kN)	Cv (m <sup>2</sup> /min)	K (m/s)	U.C.S. (MPa)
5,5	9,5	35°	0	30	-	-	-	$1,5 \times 10^{-8}$	-
6,0	9,8	25°	10	10	1	$2,57 \times 10^{-4}$	$1,18 \times 10^{-5}$	$4,95 \times 10^{-10}$	0,15
18,5	10,3	30°	10	15	1	$2,4 \times 10^{-4}$	$3,68 \times 10^{-6}$	$1,44 \times 10^{-10}$	0,2

Figure B.1: Foundation Profile Design Parameters (Chainages 0 to 175m &amp; 350 to 620m)

## B.2 Chainage 225m

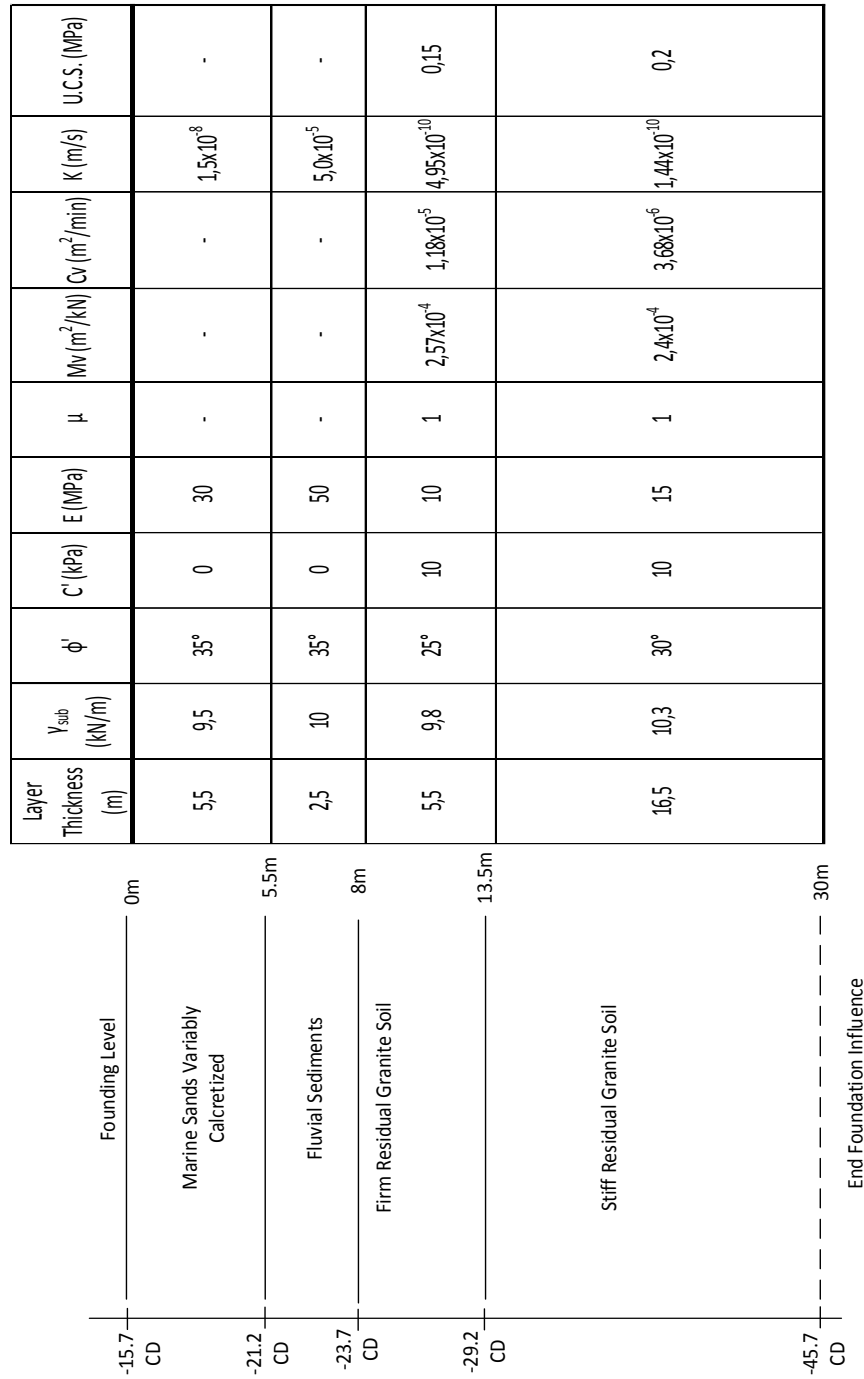


Figure B.2: Foundation Profile Design Parameters (Chainage 225m)

### B.3 Chainage 375m

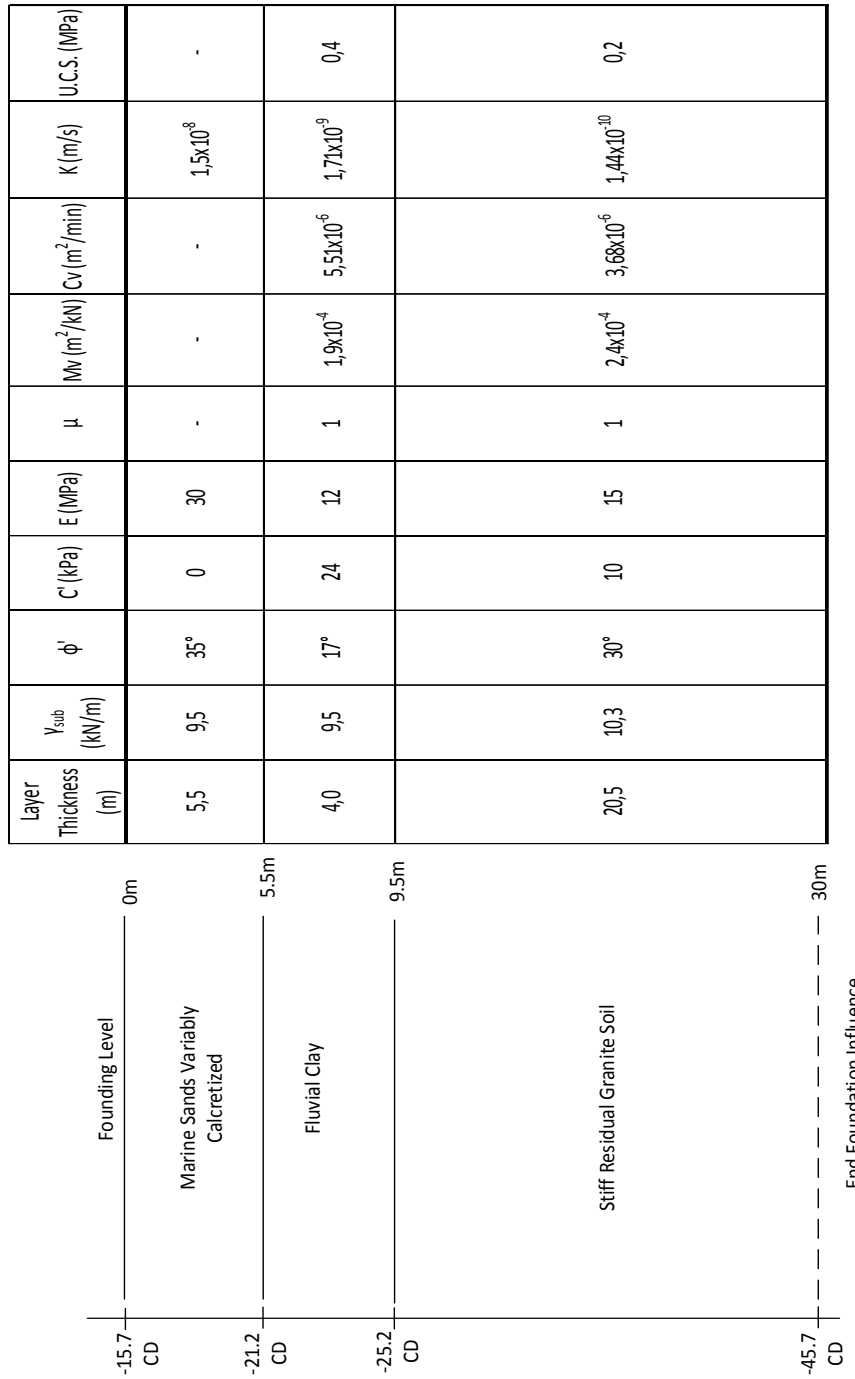


Figure B.3: Foundation Profile Design Parameters (Chainage 375m)

## B.4 Chainage 620m

Layer Thickness (m)	$V_{sub}$ (kN/m)	$\phi'$	C' (kPa)	E (MPa)	K (m/s)	U.C.S. (MPa)
1,2	10	40°	100	500	$1 \times 10^{-12}$	15
0,5	9,5	35°	0	30	$1,5 \times 10^{-8}$	-
2,0	10	40°	100	500	$1 \times 10^{-12}$	15
1,1	9,5	35°	0	30	$1,5 \times 10^{-8}$	-
25,2	10,3	30°	10	15	$1,44 \times 10^{-10}$	0,2

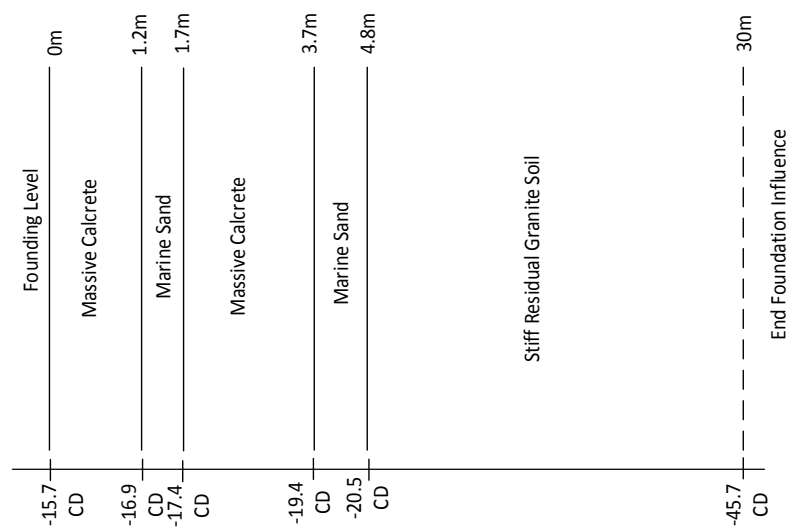


Figure B.4: Foundation Profile Massively Calcretised Marine Sands (Chainage 620m)

## Appendix C

# Geotechnical Material Description and Properties

### C.1 Marine Sands (Variably Calcretised)

Marine Sand was found in all the boreholes (Figure 4.3) and constitutes the immediate foundation from the dredged foundation level of -15.7m CD with a thickness range of 4.8m to 6.2m. This layer comprises of alternating sequences of variably dense, variably graded and layered, fine to medium grained, shell rich sands with hardened calcrete layers. Occasional layers of coarse shell fragments also occur and most likely in a lens-like distribution. There is no obvious continuity of specific hardened layers of calcretisation between adjacent boreholes. In addition in areas of more complete 'honeycomb' calcretisation will most definitely manifest in localised areas, this material is very delicate and thus successfully obtaining a undisturbed sample is not attainable. This 'honeycomb' material comprised 33% of the calcrete at the Moss gas jacket site where calcrete constituted 60% of the total volume of material dredged where the boreholes had only suggested that calcrete would compose around 20% of the material.

The borehole data at face value suggests that the immediate foundation of the quay wall is mainly comprises of uncemented, fine sand rather than harden calcrete with boreholes 7 and 9 being exceptions to this. Much of this material could in fact be 'honeycomb' cemented with a material strength in the range of 1 to 2 MPa. This can not be verified and not all material would be cemented thus to ensure safety of the structure it is deemed prudent to design using foundation parameters of the poorest foundation conditions, such the foundation profile found in boreholes 3,6 and 36 that found no layers of cemented hardened calcrete. There is no case for varying the design parameters of this material along the length of the quay wall, thus demonstrating stability for the weakest case is advised.

Continuous S.P.T. 'N' values from all the boreholes revealed that the 'poorest' conditions were found in borehole 1 where a medium dense soil condition was found with 'N' values

APPENDIX C. GEOTECHNICAL MATERIAL DESCRIPTION AND PROPERTIES **95**

in the range of 15 to 20. Accordingly, the geotechnical properties of a medium density, poorly graded, fine to medium grained sand with rounded grains the are considered appropriate for design input are:

- Submerged Unit Weight :  $9.5 \text{ kN/m}^3$  \*
- Elastic Modulus (E) : 30 MPa \*
- $\phi'$  :  $35^\circ$
- $c'$  : 0 kPa
- Coefficient of Permeability (k) :  $1.5 \times 10^{-9} \text{ m/s}$  \*
- S.P.T. 'N' value : 20

**Note:** \* denotes estimated value, all others as per Protekon tests on undisturbed samples.

## C.2 Residual Granite Soil

The properties of the residual granite heavy soil is relatively uniform along the entire length of the quay foundation and the soil stiffens with depth consistently such that two distinct layers have been identified for design purposes. These two layers consist of the upper layer having a firm consistence while the lower layer has a stiff consistency. Two of the boreholes shown in Figure 4.3 revealed evidence of very stiff conditions at a greater depth than the the other two layers although there is insufficient data from elsewhere on the site to include a third layer of this consistency in the design of the quay walls.

The soil material comprises a moderately cohesive sandy, silty, clay mix with index parameters as follows:

- % Clay : av  $\pm$  30% ; Max 39% ; Min 24%
- % Silt : av  $\pm$  40% ; Max 51% ; Min 31%
- % Sand : av  $\pm$  30% ; Max 45% ; Min 17%
- Liquid Limit : av  $\pm$  40% ; Max 47% ; Min 38%
- Plasticity Limit : av  $\pm$  10% ; Max 24% ; Min 6%

The two distinct layers are identified as follows:

- An upper firm consistency layer with thickness of 6.0 meters.
- A lower stiff consistency layer with a thickness that extends beyond the foundation influence.

Soil parameters for design purposes for these two layers are given below.

APPENDIX C. GEOTECHNICAL MATERIAL DESCRIPTION AND PROPERTIES **96****C.2.1 Firm Residual Granite Soil (6m thick Layer)**

- Saturated Density : 2000 kg/m<sup>3</sup> \* (95% Mod.AASHO)
- Submerged Unit Weight : 9.8 kN/m<sup>3</sup> \*
- Initial Soil Modulus (Ei) : 10 MPa
- $\phi'$  : 25° Considered most
- $c'$  : 10 kPa appropriate of lab results
- Quick Undrained Strength Cu : 75 kPa \*
- U.C.S. : 150 kPa \*
- Coefficient of Permeability (k) : 4.95x10<sup>-10</sup> m/s
- Coefficient of Volume Decrease (Mv) : 2.57x10<sup>-4</sup> m<sup>2</sup>/kN (Mod.Compressible)
- Coefficient of Consolidation (Cv) : 1.18x10<sup>-5</sup> m<sup>2</sup>/min
- Pore Pressure Coefficient (A) : 1.0 \*
- $\mu$  value (Skempton) : 1.0 \*

**Note:** \* denotes estimated value, all others as per Protekon tests on undisturbed samples.

**C.2.2 Stiff Residual Granite Soil (to bottom depth of foundation influence)**

- Saturated Density : 2050 kg/m<sup>3</sup> \* (99% Mod.AASHO)
- Submerged Unit Weight : 10.3 kN/m<sup>3</sup> \*
- Initial Soil Modulus (Ei) : 15 MPa
- $\phi'$  : 30°
- $c'$  : 10 kPa
- Quick Undrained Strength Cu : 100 kPa \*
- U.C.S. (Jacket Site) : 200 kPa \*
- Coefficient of Permeability (k) : 1.44x10<sup>-10</sup> m/s
- Coefficient of Volume Decrease (Mv) : 2.4x10<sup>-4</sup> m<sup>2</sup>/kN (Mod.Compressible)
- Coefficient of Consolidation (Cv) : 3.68x10<sup>-5</sup> m<sup>2</sup>/min
- Pore Pressure Coefficient (A) : 1.0 \*

APPENDIX C. GEOTECHNICAL MATERIAL DESCRIPTION AND PROPERTIES **97**

- $\mu$  value (Skempton) : 1.0 \*

**Note:** \* denotes estimated value, all others as per Protekon tests on undisturbed samples.

### C.3 Fluvial Sediments

Fluvial sediments were only located between chainages 175m and 350m in Figure 4.3 where it was located between the residual granite soil and the overlying marine sediments found in Appendix C.1 and Appendix C.2. Of the boreholes sampled only three revealed these sediments and each of these boreholes found different conditions. BH4 revealed a 3m thick layer of stiff clay, BH5 found a composite stratification of both clay and sand with a 1.5m thick layer of clay and a 2.5m thick layer of sand. BH6 found a 2.5m thick layer of dense sand. Thus three typical sections were deemed appropriate.

#### C.3.1 Fluvial Clay

This soil type comprises a cohesive sandy clay with a stiff consistency with index parameters:

- % Clay : 44 - 51%
- % Silt : 2 - 14%
- % Sand : 42 - 47%
- Liquid Limit : 50 - 54%
- Plasticity Index : 19 - 35 %

Soil parameters for design purposes are as follows

- Saturated Density : 1995 kg/ $m^3$  \* (99% Mod.AASHO)
- Submerged Unit Weight : 9.5 kN/ $m^3$  \*
- Initial Soil Modulus ( $E_i$ ) : 12 MPa
- $\phi'$  : 17°
- $c'$  : 24 kPa
- Quick Undrained Strength  $C_u$  : 200 kPa \*
- U.C.S. (Jacket Site) : 400 kPa \*
- Coefficient of Permeability ( $k$ ) :  $1.71 \times 10^{-9}$  m/s
- Coefficient of Volume Decrease ( $M_v$ ) :  $1.9 \times 10^{-4}$   $m^2/kN$  (Mod.Compressible)



## APPENDIX C. GEOTECHNICAL MATERIAL DESCRIPTION AND PROPERTIES 98

- Coefficient of Consolidation ( $C_v$ ) :  $5.51 \times 10^{-5} \text{ m}^2/\text{min}$
- Pore Pressure Coefficient (A) : 1.0 \*
- $\mu$  value (Skempton) : 1.0 \*

**Note:** \* denotes estimated value, all others as per Protekon tests on undisturbed samples.

### C.3.2 Fluvial Sand

This material is comprised of a granular, cohesionless, dense, well graded, medium grained sand with the following parameters:

- % Clay : 6%
- % Silt : 2%
- % Sand : 92%
- % Gravel : 0%
- Liquid Limit : 0%
- Plasticity Index : 0%

Soil parameters for design purposes are as follows

- Saturated Density :  $2000 \text{ kg/m}^3$  \* (99% Mod.AASHO)
- Submerged Unit Weight :  $10 \text{ kN/m}^3$  \*
- Elastic Modulus (E) : 50 MPa \*
- $\phi'$  :  $35^\circ$  \*
- $c'$  : 0 kPa \*
- Coefficient of Permeability (k) :  $1.71 \times 10^{-9} \text{ m/s}$  \*

**Note:** \* estimated, no test values available.

## Appendix D

# As Built Counterfort Design

APPENDIX D. AS BUILT COUNTERFORT DESIGN

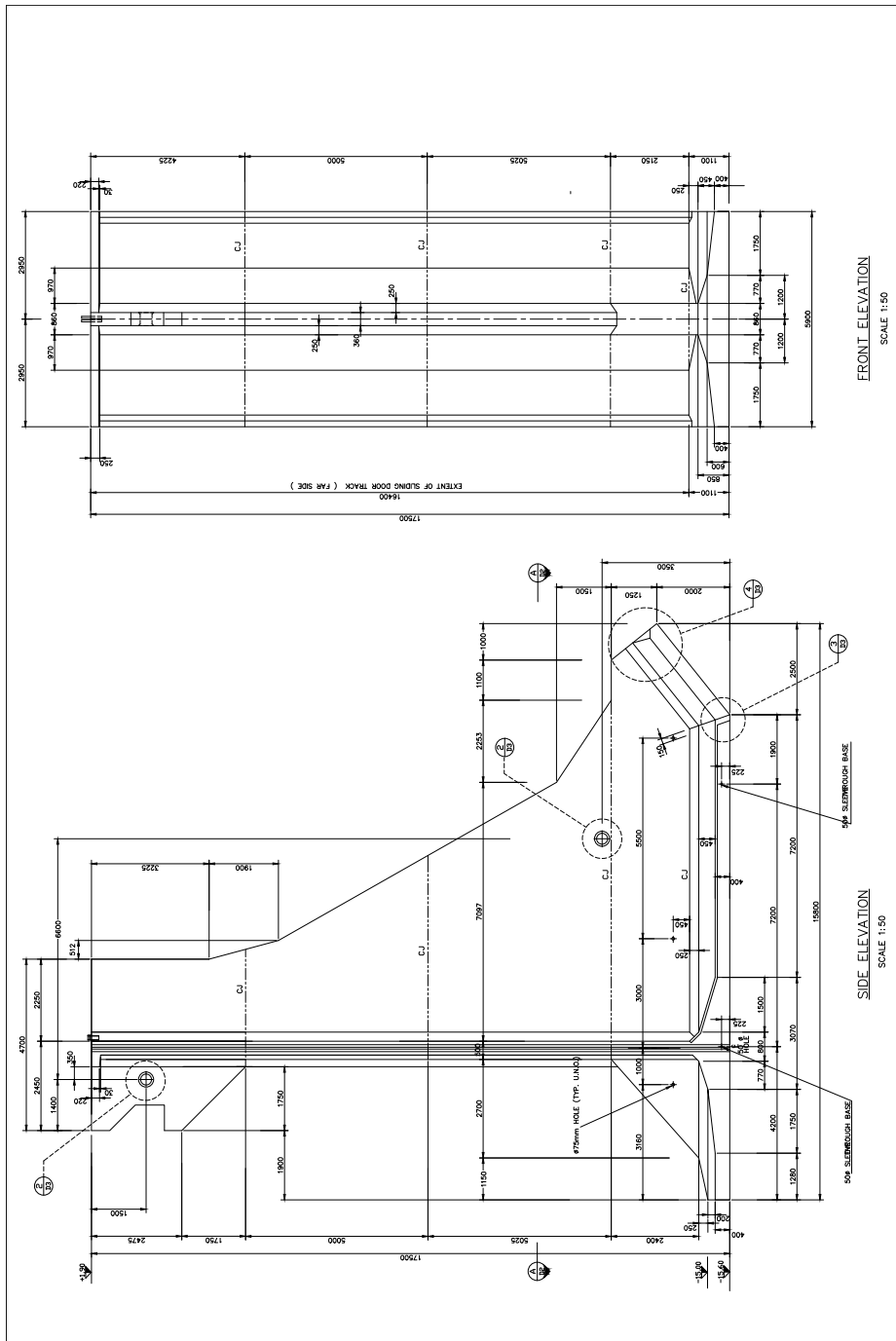


Figure D.1: As Built Precast Element Design



## Appendix E

# MATLAB Script Input Example

Table E.1: Phase 1 Input Example

Designation of Structural Configuration	Wall Thickness (m)	Base Width (m)	Base Thickness (m)	Anchor Height (m)	Anchor Angle (°)
Wt1_Bw3.5_Bt1_Ah17.5_Aa0	1.00	3.50	1	17.50	0.00
Wt1_Bw3.5_Bt1_Ah17.5_Aa5	1.00	3.50	1	17.50	5.00
Wt1_Bw3.5_Bt1_Ah17.5_Aa10	1.00	3.50	1	17.50	10.00
Wt1_Bw3.5_Bt1_Ah17.5_Aa15	1.00	3.50	1	17.50	15.00
Wt0.8_Bw3.5_Bt1_Ah17.5_Aa0	0.80	3.50	1	17.50	0.00
Wt0.8_Bw3.5_Bt1_Ah17.5_Aa5	0.80	3.50	1	17.50	5.00
Wt0.8_Bw3.5_Bt1_Ah17.5_Aa10	0.80	3.50	1	17.50	10.00
Wt0.8_Bw3.5_Bt1_Ah17.5_Aa15	0.80	3.50	1	17.50	15.00
Wt0.6_Bw3.5_Bt1_Ah17.5_Aa0	0.60	3.50	1	17.50	0.00
Wt0.6_Bw3.5_Bt1_Ah17.5_Aa5	0.60	3.50	1	17.50	5.00
Wt0.6_Bw3.5_Bt1_Ah17.5_Aa10	0.60	3.50	1	17.50	10.00
Wt0.6_Bw3.5_Bt1_Ah17.5_Aa15	0.60	3.50	1	17.50	15.00
Wt0.5_Bw3.5_Bt1_Ah17.5_Aa0	0.50	3.50	1	17.50	0.00
Wt0.5_Bw3.5_Bt1_Ah17.5_Aa5	0.50	3.50	1	17.50	5.00
Wt0.5_Bw3.5_Bt1_Ah17.5_Aa10	0.50	3.50	1	17.50	10.00
Wt0.5_Bw3.5_Bt1_Ah17.5_Aa15	0.50	3.50	1	17.50	15.00
Wt1_Bw3.6_Bt1_Ah17.5_Aa0	1.00	3.60	1	17.50	0.00
Wt1_Bw3.6_Bt1_Ah17.5_Aa5	1.00	3.60	1	17.50	5.00
Wt1_Bw3.6_Bt1_Ah17.5_Aa10	1.00	3.60	1	17.50	10.00
Wt1_Bw3.6_Bt1_Ah17.5_Aa15	1.00	3.60	1	17.50	15.00
Wt0.8_Bw3.6_Bt1_Ah17.5_Aa0	0.80	3.60	1	17.50	0.00
Wt0.8_Bw3.6_Bt1_Ah17.5_Aa5	0.80	3.60	1	17.50	5.00
Wt0.8_Bw3.6_Bt1_Ah17.5_Aa10	0.80	3.60	1	17.50	10.00
Wt0.8_Bw3.6_Bt1_Ah17.5_Aa15	0.80	3.60	1	17.50	15.00
Wt0.6_Bw3.6_Bt1_Ah17.5_Aa0	0.60	3.60	1	17.50	0.00
Wt0.6_Bw3.6_Bt1_Ah17.5_Aa5	0.60	3.60	1	17.50	5.00
Wt0.6_Bw3.6_Bt1_Ah17.5_Aa10	0.60	3.60	1	17.50	10.00
Wt0.6_Bw3.6_Bt1_Ah17.5_Aa15	0.60	3.60	1	17.50	15.00
Wt0.5_Bw3.6_Bt1_Ah17.5_Aa0	0.50	3.60	1	17.50	0.00
Wt0.5_Bw3.6_Bt1_Ah17.5_Aa5	0.50	3.60	1	17.50	5.00
Wt0.5_Bw3.6_Bt1_Ah17.5_Aa10	0.50	3.60	1	17.50	10.00
Wt0.5_Bw3.6_Bt1_Ah17.5_Aa15	0.50	3.60	1	17.50	15.00

## Appendix F

# MATLAB Scripts

### F.1 Simplified Model Script

```

clear all
clc
format compact
tic
syms hwall twall bwidth bthick aheight acangle designation tension real
%constant variables
Cdensity = 2500 ; %kg/m3
SegmentLength = 5.9 ;%m (Temp)
Hwall = 17.5; %m (remains constant for all iteration)
CopeHeight = 3.2; %m (provides lever arm for bollard loads)
OperationSurcharge = 40E3; %N/m2 vertical operational surcharge
ConstructionSurcharge = 10E3; %N/m2 vertical construction surcharge
Tidallag = 10E3; %N/m2 uniform horizontal load
g = 9.81; %m/s2 gravity
FrictionCoeef_Concrete = 0.5; %conservative from pg467 (Handbook of Port and Harbour Engineering 2nd Edition, Tsinker)

%Ship Anchor Loads
BL = 800E3 ;%N horizontal bollard pull
BLangles = [-30 -15 0 15 30]'; %degree angles of bollard load applied
ShipAnchorLoads = sumShipAnchor(BL,BLangles);
VerticalBollardLoads = [BL*sin(deg2rad(BLangles(1))) BL*sin(deg2rad(BLangles(2))) BL*sin(deg2rad(BLangles(3))) BL*sin(deg2rad(BLangles(4))) BL*sin(deg2rad(BLangles(5)))]';

%Backfill Materials Parameters
%above MSL
Gammabulk_AboveMSL = 20E3; %N/m3 bulk density
Omegadash_AboveMSL = 34; %degrees
LayerThick_AboveMSL = 4.2; %m Layer Thickness

%below MSL
Gammabulk_BelowMSL = 8.5E3; %N/m3 bouyantdensity
Omegadash_BelowMSL = 27; %degrees
LayerThick_BelowMSL = 16.6; %m Layer Thickness

%Foundation Parameters
Omegadash_Foundation = 35; %
Cdash_Foundation = 0;
Gamma_Foundation = 9.5E3; %kN/m3
FoundationDepth = 0; %m

%Tidal Lag Effects
TidalLagHorifinal = Tidallag*SegmentLength*Hwall;
TidalLagMomentfinal = -TidalLagHorifinal*(Hwall/2)

%variables to be read in
InputOutputFile = 'CorrectionInput2.xlsx';
Designation = table2array(readtable(InputOutputFile,'Sheet','Input','Range','A:A'));%code of combination
Twall = table2array(readtable(InputOutputFile,'Sheet','Input','range','B:B')) ; %Thickness of wall
Bwidth = table2array(readtable(InputOutputFile,'Sheet','Input','range','C:C')) ; %length of base
Bthick = table2array(readtable(InputOutputFile,'Sheet','Input','range','D:D')) ; %thickness of base
Aheight = table2array(readtable(InputOutputFile,'Sheet','Input','range','E:E')) ; %height of anchor cable from bottom of structure
ACangle = table2array(readtable(InputOutputFile,'Sheet','Input','range','F:F')) ; %angle of anchor cable
Looplength = length(Designation)

%Empty output arrays
UnitMass_Output = zeros(LoopLength,1);
SlidingConstruction_Output = zeros(LoopLength,1);
BearingConstruction_Output = zeros(LoopLength,1);
Tension_MaxOutput = zeros(LoopLength,1);
Tension_SlidingOutput = zeros(LoopLength,1);
Tension_BearingOutput = zeros(LoopLength,1);

count = 1;
while (count<=LoopLength)
    Designation(count);
    %Backfill Forces Construction
    EarhandSurchargePressures_construction = Muller_Breslau_Con(Omegadash_BelowMSL,Gammabulk_BelowMSL,LayerThick_BelowMSL,ConstructionSurcharge,Bwidth(count));
    EarthPressureHoriCon = EarhandSurchargePressures_construction(3,1)*SegmentLength;
    EarthPressureVertCon = EarhandSurchargePressures_construction(4,1)*SegmentLength;
    SurchargeHoriCon = EarhandSurchargePressures_construction(1,1)*SegmentLength;
    SurchargeVertCon = EarhandSurchargePressures_construction(2,1)*SegmentLength;
    %Backfill Moments Construction
    SurchargeHoriCon_Moment = SurchargeHoriCon*EarhandSurchargePressures_construction(1,2);
    SurchargeVertCon_Moment = SurchargeVertCon*(EarhandSurchargePressures_construction(2,2)-Bwidth(count)/2);
    EarthPressureHoriCon_Moment = EarthPressureHoriCon*EarhandSurchargePressures_construction(3,2);
    EarthPressureVertCon_Moment = EarthPressureVertCon*(EarhandSurchargePressures_construction(4,2)-Bwidth(count)/2);

    %Backfill Forces Final
    EarhandSurchargePressures_Final = Muller_Breslau_Final(Omegadash_AboveMSL,Gammabulk_AboveMSL,LayerThick_AboveMSL,Omegadash_BelowMSL,Gammabulk_BelowMSL,LayerThick_BelowMSL,OperationSurcharge,1);
    %EarhandSurchargePressures_Final2 = EarhandSurchargePressures_Final/(1E5)
    EarthPressureHoriFinal_AboveMSL = EarhandSurchargePressures_Final(3,1)*SegmentLength;
    EarthPressureVertFinal_AboveMSL = EarhandSurchargePressures_Final(4,1)*SegmentLength;
    SurchargeHoriFinal_AboveMSL = EarhandSurchargePressures_Final(1,1)*SegmentLength;
    SurchargeVertFinal_AboveMSL = EarhandSurchargePressures_Final(2,1)*SegmentLength;
    EarthPressureHoriFinal_BelowMSL = EarhandSurchargePressures_Final(7,1)*SegmentLength;
    EarthPressureVertFinal_BelowMSL = EarhandSurchargePressures_Final(8,1)*SegmentLength;
    SurchargeHoriFinal_BelowMSL = EarhandSurchargePressures_Final(5,1)*SegmentLength;
    SurchargeVertFinal_BelowMSL = EarhandSurchargePressures_Final(6,1)*SegmentLength;
    EarthPressureHoriFinalAdditional_BelowMSL = EarhandSurchargePressures_Final(9,1)*SegmentLength;
    EarthPressureVertFinalAdditional_BelowMSL = EarhandSurchargePressures_Final(10,1)*SegmentLength;
    %Backfill Moments Final
    SurchargeHoriFinal_AboveMSL_Moment = -SurchargeHoriFinal_AboveMSL*(EarhandSurchargePressures_Final(1,2)+ LayerThick_BelowMSL)
    EarhandSurchargePressures_Final(2,2)
    SurchargeVertFinal_AboveMSL_Moment = SurchargeVertFinal_AboveMSL*((Bwidth(count)/2)-(Bwidth(count)- EarhandSurchargePressures_Final(2,2)))
    EarthPressureHoriFinal_AboveMSL_Moment = -EarthPressureHoriFinal_AboveMSL*(EarhandSurchargePressures_Final(3,2)+ LayerThick_BelowMSL)
    EarthPressureVertFinal_AboveMSL_Moment = EarthPressureVertFinal_AboveMSL*((Bwidth(count)/2)-(Bwidth(count)- EarhandSurchargePressures_Final(4,2)))
    SurchargeHoriFinal_BelowMSL_Moment = -SurchargeHoriFinal_BelowMSL*(EarhandSurchargePressures_Final(5,2)
    SurchargeVertFinal_BelowMSL_Moment = SurchargeVertFinal_BelowMSL*((Bwidth(count)/2)-(Bwidth(count)- EarhandSurchargePressures_Final(6,2)))
    EarthPressureHoriFinal_BelowMSL_Moment = -EarthPressureHoriFinal_BelowMSL*(EarhandSurchargePressures_Final(7,2)
    EarthPressureVertFinal_BelowMSL_Moment = EarthPressureVertFinal_BelowMSL*((Bwidth(count)/2)-(Bwidth(count)- EarhandSurchargePressures_Final(8,2)))
    EarthPressureHoriFinalAdditional_BelowMSL_Moment = -EarthPressureHoriFinalAdditional_BelowMSL*(EarhandSurchargePressures_Final(9,2)
    EarthPressureVertFinalAdditional_BelowMSL_Moment = EarthPressureVertFinalAdditional_BelowMSL*((Bwidth(count)/2)-(Bwidth(count)- EarhandSurchargePressures_Final(10,2)))

    %Vertical Loads
    WallMass_Bouyant = (Hwall*Twall(count)*SegmentLength)*(Cdensity-1000)*g; %N bouyant mass vertical wall
    BaseMass_Bouyant = ((Bwidth(count)-Twall(count))*Bthick(count)*SegmentLength)*(Cdensity-1000)*g ;%N bouyant mass base
    Verticalgroundanchorload = tension*sin(deg2rad(ACangle(count)));
    Bouancy = 0;

    %Vertical Surcharge Loads
    VerticalOperationSurcharge = OperationSurcharge*SegmentLength*(Bwidth(count)-Twall(count));
    TotalVerticalOperationSurcharge = VerticalOperationSurcharge+SurchargeVertFinal_AboveMSL+ SurchargeVertFinal_BelowMSL;
    VerticalConstructionSurcharge = ConstructionSurcharge*SegmentLength*(Bwidth(count)-Twall(count));
    TotalVerticalConstructionSurcharge = VerticalConstructionSurcharge+SurchargeVertCon;

    %Vertical Earth Loads
    Soil_AboveMSLMass = (Bwidth(count)-Twall(count))*LayerThick_AboveMSL*SegmentLength)*Gammabulk_AboveMSL; %N mass backfill above MSL
    Soil_BelowMSLMass = (Bwidth(count)-Twall(count))*LayerThick_BelowMSL*SegmentLength)*Gammabulk_BelowMSL; %N mass backfill below MSL
    VerticalEarthPressuresCon = EarthPressureVertCon;
    VerticalEarthPressuresFinal = EarthPressureVertFinal_AboveMSL+EarthPressureVertFinal_BelowMSL+EarthPressureVertFinalAdditional_BelowMSL;

    %Horizontal Loads
    Horizontalgroundanchorload = tension*cos(deg2rad(ACangle(count)));

    %Moments taken around centroid of base
    WallMass_Moment = WallMass_Bouyant*((Bwidth(count)/2)-(Bwidth(count)-Twall(count)/2)) %
    BaseMass_Moment = BaseMass_Bouyant*((Bwidth(count)/2)-((Bwidth(count)-Twall(count))/2)) %Nm Moment from weight of section base
    Soil_AboveMSL_Moment = Soil_AboveMSLMass*((Bwidth(count)/2)-((Bwidth(count)-Twall(count))/2)) %Nm Moment from weight of soil above MSL
    Soil_BelowMSL_Moment = Soil_BelowMSLMass*((Bwidth(count)/2)-((Bwidth(count)-Twall(count))/2)); %Nm Moment from weight of soil below MSL
    Tension_Moment_Horizontal = Horizontalgroundanchorload*Aheight(count); %Nm Moment inducted by ground anchor
    Tension_Moment_Vertical = Verticalgroundanchorload*((Bwidth(count)/2)-(Bwidth(count)-Twall(count)/2));

```

```

OperationSurchargeVertical_Moment = VerticalOperationSurcharge*((Bwidth(count)/2)-((Bwidth(count)-Twall(count))/2)); %Nm Moment from surcharge
ConstructionSurchargeVertical_Moment = VerticalConstructionSurcharge*((Bwidth(count)/2)-((Bwidth(count)-Twall(count))/2));

%Consolidated Loads (Construction);
SumV_Construction = WallMass_Bouyant+BaseMass_Bouyant+Soil_BelowMSLMass+TotalVerticalConstructionSurcharge+VerticalEarthPressuresCon;
SumH_Construction = EarthPressureHoriCon+SurchargeHoriCon;
Mr_Construction = BaseMass_Moment+Soil_BelowMSL_Moment+ConstructionSurchargeVertical_Moment+SurchargeVertCon_Moment+EarthPressureVertCon_Moment;
Mo_Construction = EarthPressureHoriCon_Moment + SurchargeHoriCon_Moment + WallMass_Moment;

%Consolidated Loads (Final)
SumV_Final = WallMass_Bouyant+BaseMass_Bouyant+Soil_AboveMSLMass+Soil_BelowMSLMass+TotalVerticalOperationSurcharge-Verticalgroundanchorload+VerticalEarthPressuresFinal; %correct
SumH_Final = EarthPressureHoriFinal_AboveMSL+EarthPressureHoriFinal_BelowMSL+SurchargeHoriFinal_AboveMSL+ EarthPressureHoriFinalAdditional_BelowMSL+SurchargeHoriFinal_BelowMSL+TidalLagHoriFin;
Bouyancy = 0;
StructureMoments = vpa(BaseMass_Moment+WallMass_Moment,4);
SoilMassMoments = vpa(Soil_BelowMSL_Moment+Soil_AboveMSL_Moment,4);
SurchargeMoments = vpa(OperationSurchargeVertical_Moment+SurchargeVertFinal_AboveMSL_Moment+SurchargeVertFinal_BelowMSL_Moment+SurchargeHoriFinal_AboveMSL_Moment+SurchargeHoriFinal_BelowMSL_M;
EarthPressureMoments = EarthPressureVertFinal_AboveMSL_Moment+EarthPressureVertFinal_BelowMSL_Moment+EarthPressureVertFinalAdditional_BelowMSL_Moment+EarthPressureHoriFinal_AboveMSL_Moment+Ear;
TensionMoment = Tension_Moment_Horizontal+Tension_Moment_Vertical;
SumM_Final = StructureMoments+SoilMassMoments+SurchargeMoments+EarthPressureMoments+TidalLagMomentfinal+TensionMoment;

%Construction stability checks
SlidingConstruction_Output(count,1) = sliding_construction(SumV_Construction,Bouyancy,FrictionCoef_Concrete,SumH_Construction);
BearingConstruction_Output(count,1) = bearing_construction(SumH_Construction,SumV_Construction, Mo_Construction,Mo_Construction,SegmentLength,Bwidth(count),OmegaDash_Foundation,FoundationDepth);

if(SlidingConstruction_Output(count,1) >= 1.2 && BearingConstruction_Output(count,1) >= 1.75)
%Zero Vectors for results
Tensions = zeros(2,1); %zeros vectors to store tension for each different static tests
Tensions_Sliding = zeros(length(BLAngles),1);
Tensions_Bearing = zeros(length(BLAngles),1);

count_Sliding = 1;
while( count_Sliding <= length(BLAngles))
sV = SumV_Final - ShipAnchorLoads(count_Sliding,1);
sH = SumH_Final - ShipAnchorLoads(count_Sliding,2);
Tensions_Sliding(count_Sliding) = Sliding(sV,Bouyancy,sH,FrictionCoef_Concrete);
count_Sliding = count_Sliding+1;
end
Tension_KN_Sliding = max(Tensions_Sliding)
Tensions(1,1) = Tension_KN_Sliding;
Tension_SlidingOutput(count,1) = Tension_KN_Sliding;

%Bearing Failure
count_Bearing = 1;
while(count_Bearing <= length(BLAngles))
M = SumM_Final + ((ShipAnchorLoads(count_Bearing,1)*((Bwidth(count)/2)-(Twall(count)/2)))+ ((ShipAnchorLoads(count_Bearing,2)*(Hwall+CopeHeight)));
sV = SumV_Final - ShipAnchorLoads(count_Bearing,1);
sH = SumH_Final - ShipAnchorLoads(count_Bearing,2);
Tensions_Bearing(count_Bearing) = Bearing5(sH,sV, M,SegmentLength,Bwidth(count),OmegaDash_Foundation,FoundationDepth,Cdash_Foundation,Gamma_Foundation);
count_Bearing = count_Bearing+1;
end
Tension_KN_Bearing = max(Tensions_Bearing)
Tensions(2,1) = Tension_KN_Bearing;
Tension_BearingOutput(count,1) = Tension_KN_Bearing;

%Outputs
WallMass = (Hwall*Twall(count)*SegmentLength)*Cdensity*g; %N mass vertical wall
BaseMass = ((Bwidth(count)-Twall(count))*Bthick(count)*SegmentLength)*Cdensity*g; %N mass base
Unitmass = (WallMass + BaseMass)/(9.81*1000)
UnitMass_Output(count,1) = Unitmass;
Tension_MaxOutput(count,1) = max(Tensions);
count = count+1
else
count = count+1
end
end
%writes outputs from all layouts
xlwrite(InputOutputFile,Designation,'Output','A1')
xlwrite(InputOutputFile,UnitMass_Output,'Output','B1')
xlwrite(InputOutputFile,SlidingConstruction_Output,'Output','C1')
xlwrite(InputOutputFile,BearingConstruction_Output,'Output','D1')
xlwrite(InputOutputFile,Tension_SlidingOutput,'Output','E1')
xlwrite(InputOutputFile,Tension_BearingOutput,'Output','F1')
xlwrite(InputOutputFile,Tension_MaxOutput,'Output','G1')
toc

%All additional functions required for computations are given below.

%Determination of Ship Loads at Various Angles
function shipLoads = sumShipAnchor(BL,BLAngles)
shipLoads = zeros(length(BLAngles),2);
count = 1;
while(count <= length(BLAngles))
shipLoads(count,1) = BL*sin(deg2rad(BLAngles(count))); %vertical loads
shipLoads(count,2) = BL*cos(deg2rad(BLAngles(count))); %horizontal loads
count = count+1;
end
end

%Surcharge Forces
%Horizontal Surcharge Forces for Final Load Case
function SurchargeHoriFinal = SurchargeHoriFinal(Surcharge, Ka_aboveMSL,LT_aboveMSL, Ka_belowMSL, LT_belowMSL, segmentwidth)
PressureAboveMSL = Surcharge*Ka_aboveMSL;
PressureBelowMSL = Surcharge*Ka_belowMSL;
ForceAboveMSL = (segmentwidth*LT_aboveMSL)*PressureAboveMSL;
ForceBelowMSL = segmentwidth*LT_belowMSL*PressureBelowMSL;
SurchargeHoriFinal = ForceAboveMSL + ForceBelowMSL;
end

%Horizontal Surcharge Forces for Constuction Load Case
function SurchargeHoriConst = SurchargeHoriConst(Surcharge, Ka_belowMSL, LT_belowMSL, segmentwidth)
PressureBelowMSL = Surcharge*Ka_belowMSL;
ForceBelowMSL = segmentwidth*LT_belowMSL*PressureBelowMSL;
SurchargeHoriConst = ForceBelowMSL;
end

%Surcharge Moments for Final Load Case
function SurchargeMomentFinal = SurchargeMomentFinal(Surcharge, Ka_aboveMSL,LT_aboveMSL, Ka_belowMSL, LT_belowMSL, segmentwidth)
PressureAboveMSL = Surcharge*Ka_aboveMSL;
PressureBelowMSL = Surcharge*Ka_belowMSL;
ForceAboveMSL = (segmentwidth*LT_aboveMSL)*PressureAboveMSL;
ForceBelowMSL = segmentwidth*LT_belowMSL*PressureBelowMSL;
MomentAboveMSL = ForceAboveMSL*(LT_belowMSL+(0.5*LT_aboveMSL));
MomentBelowMSL = ForceBelowMSL*(LT_belowMSL/2);
SurchargeMomentFinal = MomentAboveMSL + MomentBelowMSL;
end

%Surcharge Moments for Constuction Load Case
function SurchargeMomentConst = SurchargeMomentConst(Surcharge, Ka_belowMSL, LT_belowMSL, segmentwidth)
PressureBelowMSL = Surcharge*Ka_belowMSL;
ForceBelowMSL = segmentwidth*LT_belowMSL*PressureBelowMSL;
MomentBelowMSL = ForceBelowMSL*(LT_belowMSL/2);
SurchargeMomentConst =MomentBelowMSL;
end

%Earth Pressure Calculations
%Muller-Breslau Pressures for Final Load Case
function muller_Breslau_Final = Muller_Breslau_Final(Omegadash_AboveMSL,Gammabulk_AboveMSL,LayerThick_AboveMSL,Omegadash_BelowMSL,Gammabulk_BelowMSL,LayerThick_BelowMSL,Surcharge,Bwidth)
%in degrees
muller_Breslau_Final = zeros(10,2);
alpha = 90; %wall inclination
beta = 0; %backfill slope
phid_AboveMSL = Omegadash_AboveMSL;
phid_BelowMSL = Omegadash_BelowMSL; %angle of soil friction
deltad_AboveMSL = (2/3)*phid_AboveMSL;

```



```

deltad_BelowMSL = (2/3)*phid_BelowMSL; %wall friction
gamma_AboveMSL = Gammabulk_AboveMSL;
gamma_BelowMSL = Gammabulk_BelowMSL; %backfill density
Height = LayerThick_BelowMSL + LayerThick_AboveMSL;
alpha = deg2rad(alphad);
beta = deg2rad(betad);

% Calculation of Q BelowMSL (relavance)
phi_BelowMSL = deg2rad(phid_BelowMSL);
delta_BelowMSL = deg2rad(deltad_BelowMSL);
Comp1_BelowMSL = (sin(alpha+phi_BelowMSL)^2)*cos(delta_BelowMSL);
Comp2_BelowMSL = sin(alpha)*(sin(alpha-delta_BelowMSL));
Comp3_BelowMSL = sin(phi_BelowMSL+delta_BelowMSL)*sin(phi_BelowMSL-beta);
Comp4_BelowMSL = sin(alpha-delta_BelowMSL)/sin(alpha+beta);
Comp5_BelowMSL = (Comp3_BelowMSL/Comp4_BelowMSL)^0.5;
Comp6_BelowMSL = (Comp5_BelowMSL+1)^2;
f_1_BelowMSL = Comp1_BelowMSL/Comp2_BelowMSL/Comp6_BelowMSL;
Q_a_BelowMSL = 0.5*gamma_BelowMSL*(Height^2)*f_1_BelowMSL/sin(alpha)/cos(delta_BelowMSL);
Alpha = 90-alpha;

%Calculation of Active horizontal pressure (Kah) BelowMSL
Kah_C1_BelowMSL = cosd(phid_BelowMSL+Alpha)^2;
Kah_C2_BelowMSL = sind(phid_BelowMSL+deltad_BelowMSL)*sind(phid_BelowMSL-betad);
Kah_C3_BelowMSL = cosd(Alpha-deltad_BelowMSL)*cosd(Alpha+betad);
Kah_C4_BelowMSL = (Kah_C2_BelowMSL/Kah_C3_BelowMSL)^0.5;
Kah_C5_BelowMSL = (cosd(Alpha)^2)*(1+Kah_C4_BelowMSL)^2;
Kah_BelowMSL = Kah_C1_BelowMSL/Kah_C5_BelowMSL;
ActiveForceaboveHori_BelowMSL = alphad+90+deltad_BelowMSL;

%Calculation of Active horizontal pressure (Kah) AboveMSL
Kah_C1_AboveMSL = cosd(phid_AboveMSL+Alpha)^2;
Kah_C2_AboveMSL = sind(phid_AboveMSL+deltad_AboveMSL)*sind(phid_AboveMSL-betad);
Kah_C3_AboveMSL = cosd(Alpha-deltad_AboveMSL)*cosd(Alpha+betad);
Kah_C4_AboveMSL = (Kah_C2_AboveMSL/Kah_C3_AboveMSL)^0.5;
Kah_C5_AboveMSL = (cosd(Alpha)^2)*(1+Kah_C4_AboveMSL)^2;
Kah_AboveMSL = Kah_C1_AboveMSL/Kah_C5_AboveMSL;
ActiveForceaboveHori_AboveMSL = alphad+90+deltad_AboveMSL;

%aboveMSL
muller_Breslau_Final(1,1) = Kah_AboveMSL*LayerThick_AboveMSL*Surcharge;
muller_Breslau_Final(2,1) = muller_Breslau_Final(1,1)*tand(ActiveForceaboveHori_AboveMSL);
muller_Breslau_Final(3,1) = Kah_AboveMSL*(LayerThick_AboveMSL^2/2)*gamma_AboveMSL;
muller_Breslau_Final(4,1) = muller_Breslau_Final(3,1)*tand(ActiveForceaboveHori_AboveMSL);
muller_Breslau_Final(1,2) = LayerThick_AboveMSL/2;
muller_Breslau_Final(3,2) = LayerThick_AboveMSL/3;
muller_Breslau_Final(2,2) = xCoord(muller_Breslau_Final(1,2),LayerThick_AboveMSL,Bwidth);
muller_Breslau_Final(4,2) = xCoord(muller_Breslau_Final(3,2),LayerThick_AboveMSL,Bwidth);
%belowMSL
muller_Breslau_Final(5,1) = (Kah_BelowMSL*LayerThick_BelowMSL*Surcharge); %surcharge effect
muller_Breslau_Final(6,1) = muller_Breslau_Final(5,1)*tand(ActiveForceaboveHori_BelowMSL);
muller_Breslau_Final(7,1) = Kah_BelowMSL*(LayerThick_BelowMSL^2/2)*gamma_BelowMSL;
muller_Breslau_Final(8,1) = muller_Breslau_Final(7,1)*tand(ActiveForceaboveHori_BelowMSL);
muller_Breslau_Final(9,1) = (Kah_BelowMSL*LayerThick_AboveMSL*gamma_BelowMSL)*Kah_BelowMSL*LayerThick_BelowMSL; %additional earth pressure from soil above MSL
muller_Breslau_Final(10,1) = muller_Breslau_Final(9,1)*tand(ActiveForceaboveHori_BelowMSL);
muller_Breslau_Final(5,2) = LayerThick_BelowMSL/2;
muller_Breslau_Final(6,2) = xCoord(muller_Breslau_Final(5,2),LayerThick_BelowMSL,Bwidth);
muller_Breslau_Final(7,2) = LayerThick_BelowMSL/3;
muller_Breslau_Final(8,2) = xCoord(muller_Breslau_Final(7,2),LayerThick_BelowMSL,Bwidth);
muller_Breslau_Final(9,2) = LayerThick_BelowMSL/2;
muller_Breslau_Final(10,2) = xCoord(muller_Breslau_Final(9,2),LayerThick_BelowMSL,Bwidth);
end
%Muller-Breslau Pressures for Construction Load Case
function muller_Breslau_const = Muller_Breslau_Con(Omegadash_BelowMSL,Gammabulk_BelowMSL,LayerThick_BelowMSL,Surcharge,Bwidth)
%in degrees
muller_Breslau_const = zeros(4,2);
alphad = 90; %wall inclination
betad = 0; %backfill slope
phid = Omegadash_BelowMSL; %angle of soil friction
sigd = (2/3)*phid; %wall friction
gamma = Gammabulk_BelowMSL; %backfill density
Height = LayerThick_BelowMSL;
alpha = deg2rad(alphad);
beta = deg2rad(betad);
phi = deg2rad(phid);
sig = deg2rad(sigd);
Comp1 = (sin(alpha+phi)^2)*cos(sig);
Comp2 = sin(alpha)*(sin(alpha-sig));
Comp3 = sin(phi+sig)*sin(phi-beta);
Comp4 = sin(alpha-sig)/sin(alpha+beta);
Comp5 = (Comp3/Comp4)^0.5;
Comp6 = (Comp5+1)^2;
f_1 = Comp1/Comp2/Comp6;
Q_a = 0.5*gamma*(Height^2)*f_1/sin(alpha)/cos(sig);
Alpha = 90-alpha;
Kah_C1 = cosd(phid+Alpha)^2;
Kah_C2 = sind(phid+sigd)*sind(phid-betad);
Kah_C3 = cosd(Alpha-sigd)*cosd(Alpha+betad);
Kah_C4 = (Kah_C2/Kah_C3)^0.5;
Kah_C5 = (cosd(Alpha)^2)*(1+Kah_C4)^2;
Kah = Kah_C1/Kah_C5;
ActiveForceaboveHori = alphad+90+sigd;
muller_Breslau_const(1,1) = Kah*Height*Surcharge;
muller_Breslau_const(2,1) = muller_Breslau_const(1,1)*tand(ActiveForceaboveHori);
muller_Breslau_const(3,1) = Kah*(Height^2/2)*gamma;
muller_Breslau_const(4,1) = muller_Breslau_const(3,1)*tand(ActiveForceaboveHori);
muller_Breslau_const(1,2) = Height/2;
muller_Breslau_const(3,2) = Height/3;
muller_Breslau_const(2,2) = xCoord(muller_Breslau_const(1,2),Height,Bwidth);
muller_Breslau_const(4,2) = xCoord(muller_Breslau_const(3,2),Height,Bwidth);
end
%Determination of Vertical Component Location for Muller-Breslau Calculation
function xcoord = xCoord(Ycoord,Hwall,Bwidth)
m = -(Hwall/Bwidth);
xcoord = (Ycoord-Hwall)/m;
end
%Horizontal Earth Pressure for Final Load Case
function EarthPressureHoriFinal = EPHoriFinal(Ka_aboveMSL,LT_aboveMSL,Density_aboveMSL,Ka_belowMSL,LT_belowMSL,Density_belowMSL,segmentwidth)
PressureAboveMSL = LT_aboveMSL*Density_aboveMSL*Ka_aboveMSL;
PressureBelowMSL1 = LT_aboveMSL*Density_belowMSL*Ka_belowMSL;
PressureBelowMSL2 = LT_belowMSL*Density_belowMSL*Ka_belowMSL;
ForceAboveMSL = 0.5*(segmentwidth*LT_aboveMSL)*PressureAboveMSL;
ForceBelowMSL1 = segmentwidth*LT_belowMSL*PressureBelowMSL1;
ForceBelowMSL2 = 0.5*(segmentwidth*LT_belowMSL)*(PressureBelowMSL2-PressureBelowMSL1);
EarthPressureHoriFinal = ForceAboveMSL + ForceBelowMSL1+ForceBelowMSL2;
end
%Horizontal Earth Pressure for Construction Load Case
function EarthPressureHoriCon = EPHoriCon(Ka_belowMSL,LT_belowMSL,Density_belowMSL,segmentwidth)
PressureBelowMSL = LT_belowMSL*Density_belowMSL*Ka_belowMSL;
ForceBelowMSL = 0.5*(segmentwidth*LT_belowMSL)*(PressureBelowMSL);
EarthPressureHoriCon = ForceBelowMSL;
end
%Earth Pressure Moments for Final Load Case
function EarthPressureMomentFinal = EPMomentFinal(Ka_aboveMSL,LT_aboveMSL,Density_aboveMSL,Ka_belowMSL,LT_belowMSL,Density_belowMSL,segmentwidth)
PressureAboveMSL = LT_aboveMSL*Density_aboveMSL*Ka_aboveMSL;
PressureBelowMSL1 = LT_aboveMSL*Density_belowMSL*Ka_belowMSL;
PressureBelowMSL2 = LT_belowMSL*Density_belowMSL*Ka_belowMSL;
ForceAboveMSL = 0.5*(segmentwidth*LT_aboveMSL)*PressureAboveMSL;
ForceBelowMSL1 = segmentwidth*LT_belowMSL*PressureBelowMSL1;
ForceBelowMSL2 = 0.5*(segmentwidth*LT_belowMSL)*(PressureBelowMSL2-PressureBelowMSL1);
MomentAboveMSL = ForceAboveMSL*(LT_belowMSL+(1/3)*LT_aboveMSL);
MomentBelowMSL1 = ForceBelowMSL1*(LT_belowMSL/2);
MomentBelowMSL2 = ForceBelowMSL2*(LT_belowMSL/3);

```

```

EarthPressureMomentFinal = MomentAboveMSL + MomentBelowMSL1+MomentBelowMSL2;
end
%Earth Pressure Moments for Construction Load Case
function EarthPressureMomentCon = EPMomentCon(Ka_belowMSL, LT_belowMSL, Density_belowMSL, segmentwidth)
PressureBelowMSL = LT_belowMSL*Density_belowMSL*Ka_belowMSL;
ForceBelowMSL = 0.5*(segmentwidth*LT_belowMSL)*(PressureBelowMSL);
EarthPressureMomentCon = ForceBelowMSL*(LT_belowMSL/3);
end

%Sliding FOS check
%Sliding FOS check for Construction Load Case
function Sliding_Construction = sliding_construction(sV,sU,f,sH)
Sliding_Construction = ((sV)*f)/sH;
end
%Sliding FOS check for Final Load Case
function Tension_KN_Sliding = sliding(sV,sU,sH,f)
syms tension real
Fsl = ((sV-sU)*f)/sH == 2.0;
Tension_Sliding = vpa(solve(Fsl,tension),4); %N
Tension_KN_Sliding = vpa(Tension_Sliding/1E3,3);
end

%Bearing Capacity Calculations
%Bearing Capacity Calculation for Construction Load Case
function Bearing_Construction = bearing_construction(sH,sV,mO,mR,SegmentLength,BaseWidth, foundationphi, foundationdepth,cdash, foundationGamma)
% i = rad2deg(atan(sH/sV));
i = atan(sH/sV);
I = 90-i;
e = (mR-mO)/sV;
B_dash = BaseWidth-(2*e);
L = SegmentLength;
%Capacity Factors
Nq = (exp(pi*tand(foundationphi)))*(tand(45+(foundationphi/2))^2);
Nc = (Nq-1)*cotd(foundationphi);
Ngamma = (Nq-1)*tand(1.4*foundationphi);
%Shape Function
Sc = 1+0.2*(B_dash/L)*(tand(45+foundationphi/2))^2;
Sq = 1+0.1*(B_dash/L)*(tand(45+foundationphi/2))^2;
Sgamma = Sq;
%Depth Factors
dc = 1+0.2*(foundationdepth/L)*(tand(45+foundationphi/2));
dq = 1+0.1*(foundationdepth/L)*(tand(45+foundationphi/2));
dgamma = dq;
%Inclination Factors
ic = (1-((2*I)/180))^2;
iq = ic;
igamma = (1-(I/foundationphi))^2;
%Max Bearing Capacity
qf = (cdash*Nc*Sc*dc*ic)+(foundationGamma*foundationdepth*Nq*Sq*dq*iq)+(0.5*foundationGamma*B_dash*Ngamma*Sgamma*dgamma*igamma);
q = sV/(B_dash*L);
Bearing_Construction = qf/q;
end
%Bearing Capacity Calculation for Final Load Case
function Tension_KN_Bearing = Bearing5(sH,sV,sM,SegmentLength,BaseWidth, foundationphi, foundationdepth,cdash, foundationGamma)
syms tension real
qf = 0.00001;
q = 0.00001;
e = sM/sV == -(BaseWidth/2)-.01;
tension1 = vpa(solve(e,tension),4);
L = SegmentLength;
%Capacity Factors
Nq = (exp(pi*tand(foundationphi)))*(tand(45+(foundationphi/2))^2);
Nc = (Nq-1)*cotd(foundationphi);
Ngamma = 2*(Nq-1)*tand(foundationphi);
%Depth Factors
dc = 1+0.2*(foundationdepth/L)*(tand(45+foundationphi/2));
dq = 1+0.1*(foundationdepth/L)*(tand(45+foundationphi/2));
dgamma = dq;

tension2 = tension1;
while(subs(qf/q) <= 2.0)
SH = subs(sH,tension2);
SV = subs(sV,tension2);
SM = subs(sM,tension2);
shsv = SH/SV;
i = vpa(atan(shsv)*(180/pi),4);
I = 90-i;
e = SM/SV;
B_dash = vpa(BaseWidth-abs(2*e),4);

%Shape Function
Sc = 1+0.2*(B_dash/L)*(tand(45+foundationphi/2))^2;
Sq = 1+0.1*(B_dash/L)*(tand(45+foundationphi/2))^2;
Sgamma = Sq;
%Inclination Factors
ic = ((1-((2*I)/180))^2);
iq = ic;
igamma = (1-(I/foundationphi))^2;
%Max Bearing Capacity
qf = (cdash*Nc*Sc*dc*ic)+(foundationGamma*foundationdepth*Nq*Sq*dq*iq)+(0.5*foundationGamma*B_dash*Ngamma*Sgamma*dgamma*igamma);
%qf = vpa(qf,5)
q = SV/(B_dash*L);
%Q = vpa(q,5)
tension2 = tension2+25000;
end
Tension_KN_Bearing = vpa(tension2/1E3,3);
end

```

## **F.2 Simplified Model Output Analytics**

```

clear all
clc
format compact
tic
%Reading in of Outputs from Excel
Designation_175 = table2array(readtable('BasicShape_17_5.xlsx','Sheet','Output','Range','A:A'));
Unitmass_175 = table2array(readtable('BasicShape_17_5.xlsx','Sheet','Output','Range','B:B'));
Tension_175 = table2array(readtable('BasicShape_17_5.xlsx','Sheet','Output','Range','G:G'));

Designation_1725 = table2array(readtable('BasicShape_17_25.xlsx','Sheet','Output','Range','A:A'));
Unitmass_1725 = table2array(readtable('BasicShape_17_25.xlsx','Sheet','Output','Range','B:B'));
Tension_1725 = table2array(readtable('BasicShape_17_25.xlsx','Sheet','Output','Range','G:G'));

Designation_17 = table2array(readtable('BasicShape_17.xlsx','Sheet','Output','Range','A:A'));
Unitmass_17 = table2array(readtable('BasicShape_17.xlsx','Sheet','Output','Range','B:B'));
Tension_17 = table2array(readtable('BasicShape_17.xlsx','Sheet','Output','Range','G:G'));

Designation_1675 = table2array(readtable('BasicShape_16_75.xlsx','Sheet','Output','Range','A:A'));
Unitmass_1675 = table2array(readtable('BasicShape_16_75.xlsx','Sheet','Output','Range','B:B'));
Tension_1675 = table2array(readtable('BasicShape_16_75.xlsx','Sheet','Output','Range','G:G'));

Designation_165 = table2array(readtable('BasicShape_16_5.xlsx','Sheet','Output','Range','A:A'));
Unitmass_165 = table2array(readtable('BasicShape_16_5.xlsx','Sheet','Output','Range','B:B'));
Tension_165 = table2array(readtable('BasicShape_16_5.xlsx','Sheet','Output','Range','G:G'));
%Determination of Required length of array
Length_175 = length(Designation_175);
Length_1725 = length(Designation_1725);
Length_17 = length(Designation_17);
Length_1675 = length(Designation_1675);
Length_165 = length(Designation_165);
TotalLength = Length_175 + Length_1725 + Length_17 + Length_1675 + Length_165;

%Zero matrices for all outputs
Designation_all = strings(TotalLength,1);
UnitMass_all = zeros(TotalLength,1);
Tension_all = zeros(TotalLength,1);

%combining arrays
Designation_all = [Designation_175; Designation_1725; Designation_17; Designation_1675; Designation_165];
UnitMass_all = [Unitmass_175; Unitmass_1725; Unitmass_17; Unitmass_1675; Unitmass_165];
Tension_all = [Tension_175; Tension_1725; Tension_17; Tension_1675; Tension_165];

%Outputs of passed layouts
%computing number of passed layouts
count1 = 1;
countpass = 0;
while(count1<=TotalLength)
    if(UnitMass_all(count1)>0)
        countpass = countpass+1;
        count1 = count1+1;
    else
        count1 = count1+1;
    end
end

%Blank arrays for passed layouts
Designation_pass = strings(countpass,1);
Unitmass_pass = zeros(countpass,1);
Tension_pass = zeros(countpass,1);

%creating arrays of passed layouts
sortedCount = 1;
count2 = 1;
while(count2<=TotalLength)
    if(UnitMass_all(count2)>0)
        Designation_pass(sortedCount,1) = Designation_all(count2,1);
        Unitmass_pass(sortedCount,1) = UnitMass_all(count2,1);
        Tension_pass(sortedCount,1) = Tension_all(count2,1);
        sortedCount = sortedCount+1;
        count2 = count2+1;
    else
        count2 = count2+1;
    end
end

%Matrix To Sort
ToSort = [Designation_pass,Unitmass_pass,Tension_pass];

%sorting matrix by mass
MassSorted = sortrows(ToSort,2);
[temp,RankedMasses] = ismember(MassSorted(:,2), unique(MassSorted(:,2)));
RankedMassSorted = [MassSorted,RankedMasses];
DesignationSorted_Mass = sortrows(RankedMassSorted,1);

%sorting matrix by tension
TensionSorted = sortrows(ToSort,3);
[temp,RankedTensions] = ismember(str2double(TensionSorted(:,3)), unique(str2double(TensionSorted(:,3))));
RankedTensionSorted = [TensionSorted,RankedTensions];
DesignationSorted_Tension = sortrows(RankedTensionSorted,1);

%developing Final Marray and dertermining final ranking
CombinedRanking = (str2double(DesignationSorted_Mass(:,4)))+(str2double(DesignationSorted_Tension(:,4))); %combining ranking of each layout together
CombinedRanking_unsorted = cellstr([DesignationSorted_Mass(:,1),DesignationSorted_Mass(:,2),DesignationSorted_Mass(:,3),CombinedRanking]); %adding combined ranking to each designation
[~,ii] = sort(str2double(CombinedRanking_unsorted(:,4)));
FinalRanking = CombinedRanking_unsorted(ii,:);

%writing outputs of sorting
OutputFile = 'AnalyticsOutput_Final.xlsx';
xlswrite(OutputFile,RankedMassSorted(:,1),'MassRanked','A1')
xlswrite(OutputFile,RankedMassSorted(:,2),'MassRanked','B1')
xlswrite(OutputFile,RankedMassSorted(:,3),'MassRanked','C1')
xlswrite(OutputFile,RankedMassSorted(:,4),'MassRanked','D1')
xlswrite(OutputFile,RankedTensionSorted(:,1),'TensionRanked','A1')
xlswrite(OutputFile,RankedTensionSorted(:,2),'TensionRanked','B1')
xlswrite(OutputFile,RankedTensionSorted(:,3),'TensionRanked','C1')
xlswrite(OutputFile,RankedTensionSorted(:,4),'TensionRanked','D1')
xlswrite(OutputFile,CombinedRanking_unsorted(:,1),'CombinedRanking','A1')
xlswrite(OutputFile,CombinedRanking_unsorted(:,2),'CombinedRanking','B1')
xlswrite(OutputFile,CombinedRanking_unsorted(:,3),'CombinedRanking','C1')
xlswrite(OutputFile,CombinedRanking_unsorted(:,4),'CombinedRanking','D1')
xlswrite(OutputFile,FinalRanking(:,1),'FinalRanking','A1')
xlswrite(OutputFile,FinalRanking(:,2),'FinalRanking','B1')
xlswrite(OutputFile,FinalRanking(:,3),'FinalRanking','C1')
xlswrite(OutputFile,FinalRanking(:,4),'FinalRanking','D1')
toc

```

## Appendix G

# Full Output of Phase 1

Table G.1: Phase 1 Outputs

Designation	Mass (t)	Construction Phase		Final Phase Tensile Force (kN)		
		Sliding FOS	Bearing FOS	Sliding	Bearing	Maximum
Wt0.5_Bw5.3_Bt0.5_Ah16.5_Aa0	164.5	1.209	5.553	2231.4	1231.7	2231.4
Wt0.5_Bw5.3_Bt0.5_Ah16.75_Aa0	164.5	1.209	5.553	2231.4	1205.1	2231.4
Wt0.5_Bw5.3_Bt0.5_Ah17.25_Aa0	164.5	1.209	5.553	2231.4	1177.1	2231.4
Wt0.5_Bw5.3_Bt0.5_Ah17.5_Aa0	164.5	1.209	5.553	2231.4	1175.6	2231.4
Wt0.5_Bw5.3_Bt0.5_Ah17_Aa0	164.5	1.209	5.553	2231.4	1203.6	2231.4
Wt0.5_Bw5.4_Bt0.5_Ah16.5_Aa0	165.2	1.228	5.812	2191.2	1199.5	2191.2
Wt0.5_Bw5.4_Bt0.5_Ah16.75_Aa0	165.2	1.228	5.812	2191.2	1173.8	2191.2
Wt0.5_Bw5.4_Bt0.5_Ah17.25_Aa0	165.2	1.228	5.812	2191.2	1147.4	2191.2
Wt0.5_Bw5.4_Bt0.5_Ah17.5_Aa0	165.2	1.228	5.812	2191.2	1146.7	2191.2
Wt0.5_Bw5.4_Bt0.5_Ah17_Aa0	165.2	1.228	5.812	2191.2	1173.1	2191.2
Wt0.5_Bw5.5_Bt0.5_Ah16.5_Aa0	165.9	1.247	6.077	2151.0	1166.4	2151.0
Wt0.5_Bw5.5_Bt0.5_Ah16.75_Aa0	165.9	1.247	6.077	2151.0	1141.5	2151.0
Wt0.5_Bw5.5_Bt0.5_Ah17.25_Aa0	165.9	1.247	6.077	2151.0	1116.7	2151.0
Wt0.5_Bw5.5_Bt0.5_Ah17.5_Aa0	165.9	1.247	6.077	2151.0	1091.9	2151.0
Wt0.5_Bw5.5_Bt0.5_Ah17_Aa0	165.9	1.247	6.077	2151.0	1116.6	2151.0
Wt0.5_Bw5.6_Bt0.5_Ah16.5_Aa0	166.7	1.265	6.346	2110.9	1132.2	2110.9
Wt0.5_Bw5.6_Bt0.5_Ah16.75_Aa0	166.7	1.265	6.346	2110.9	1108.2	2110.9
Wt0.5_Bw5.6_Bt0.5_Ah17.25_Aa0	166.7	1.265	6.346	2110.9	1085.2	2110.9
Wt0.5_Bw5.6_Bt0.5_Ah17.5_Aa0	166.7	1.265	6.346	2110.9	1061.1	2110.9
Wt0.5_Bw5.6_Bt0.5_Ah17_Aa0	166.7	1.265	6.346	2110.9	1084.2	2110.9
Wt0.5_Bw5.7_Bt0.5_Ah16.5_Aa0	167.4	1.284	6.621	2070.7	1072.1	2070.7
Wt0.5_Bw5.7_Bt0.5_Ah16.75_Aa0	167.4	1.284	6.621	2070.7	1074.0	2070.7
Wt0.5_Bw5.7_Bt0.5_Ah17.25_Aa0	167.4	1.284	6.621	2070.7	1052.7	2070.7

*Continue on next page*

Table G.1: All Permutations for Phase 2 (cont.).

Designation	Mass (t)	Construction Phase		Final Phase Tensile Force (kN)		
		Sliding FOS	Bearing FOS	Sliding	Bearing	Maximum
Wt0.5_Bw5.7_Bt0.5_Ah17.5_Aa0	167.4	1.284	6.621	2070.7	1029.4	2070.7
Wt0.5_Bw5.7_Bt0.5_Ah17_Aa0	167.4	1.284	6.621	2070.7	1050.9	2070.7
Wt0.5_Bw5.8_Bt0.5_Ah16.5_Aa0	168.2	1.303	6.901	2030.5	1036.0	2030.5
Wt0.5_Bw5.8_Bt0.5_Ah16.75_Aa0	168.2	1.303	6.901	2030.5	1038.9	2030.5
Wt0.5_Bw5.8_Bt0.5_Ah17.25_Aa0	168.2	1.303	6.901	2030.5	1019.3	2030.5
Wt0.5_Bw5.8_Bt0.5_Ah17.5_Aa0	168.2	1.303	6.901	2030.5	996.8	2030.5
Wt0.5_Bw5.8_Bt0.5_Ah17_Aa0	168.2	1.303	6.901	2030.5	1016.6	2030.5
Wt0.5_Bw5.9_Bt0.5_Ah16.5_Aa0	168.9	1.321	7.185	1990.3	999.0	1990.3
Wt0.5_Bw5.9_Bt0.5_Ah16.75_Aa0	168.9	1.321	7.185	1990.3	1002.7	1990.3
Wt0.5_Bw5.9_Bt0.5_Ah17.25_Aa0	168.9	1.321	7.185	1990.3	959.9	1990.3
Wt0.5_Bw5.9_Bt0.5_Ah17.5_Aa0	168.9	1.321	7.185	1990.3	963.3	1990.3
Wt0.5_Bw5.9_Bt0.5_Ah17_Aa0	168.9	1.321	7.185	1990.3	981.4	1990.3
Wt0.5_Bw6_Bt0.5_Ah16.5_Aa0	169.6	1.340	7.475	1950.1	961.0	1950.1
Wt0.5_Bw6_Bt0.5_Ah16.75_Aa0	169.6	1.340	7.475	1950.1	965.6	1950.1
Wt0.5_Bw6_Bt0.5_Ah17.25_Aa0	169.6	1.340	7.475	1950.1	924.6	1950.1
Wt0.5_Bw6_Bt0.5_Ah17.5_Aa0	169.6	1.340	7.475	1950.1	928.9	1950.1
Wt0.5_Bw6_Bt0.5_Ah17_Aa0	169.6	1.340	7.475	1950.1	945.2	1950.1
Wt0.5_Bw6.1_Bt0.5_Ah16.5_Aa0	170.4	1.359	7.770	1909.9	922.0	1909.9
Wt0.5_Bw6.1_Bt0.5_Ah16.75_Aa0	170.4	1.359	7.770	1909.9	927.6	1909.9
Wt0.5_Bw6.1_Bt0.5_Ah17.25_Aa0	170.4	1.359	7.770	1909.9	888.4	1909.9
Wt0.5_Bw6.1_Bt0.5_Ah17.5_Aa0	170.4	1.359	7.770	1909.9	893.6	1909.9
Wt0.5_Bw6.1_Bt0.5_Ah17_Aa0	170.4	1.359	7.770	1909.9	908.1	1909.9
Wt0.5_Bw6.2_Bt0.5_Ah16.5_Aa0	171.1	1.377	8.069	1869.7	882.0	1869.7
Wt0.5_Bw6.2_Bt0.5_Ah16.75_Aa0	171.1	1.377	8.069	1869.7	863.6	1869.7
Wt0.5_Bw6.2_Bt0.5_Ah17.25_Aa0	171.1	1.377	8.069	1869.7	851.2	1869.7
Wt0.5_Bw6.2_Bt0.5_Ah17.5_Aa0	171.1	1.377	8.069	1869.7	832.3	1869.7
Wt0.5_Bw6.2_Bt0.5_Ah17_Aa0	171.1	1.377	8.069	1869.7	870.0	1869.7
Wt0.5_Bw6.3_Bt0.5_Ah16.5_Aa0	171.8	1.396	8.374	1829.5	841.0	1829.5
Wt0.5_Bw6.3_Bt0.5_Ah16.75_Aa0	171.8	1.396	8.374	1829.5	823.6	1829.5
Wt0.5_Bw6.3_Bt0.5_Ah17.25_Aa0	171.8	1.396	8.374	1829.5	813.2	1829.5
Wt0.5_Bw6.3_Bt0.5_Ah17.5_Aa0	171.8	1.396	8.374	1829.5	795.1	1829.5
Wt0.5_Bw6.3_Bt0.5_Ah17_Aa0	171.8	1.396	8.374	1829.5	831.0	1829.5
Wt0.5_Bw6.4_Bt0.5_Ah16.5_Aa0	172.6	1.415	8.683	1789.4	799.1	1789.4
Wt0.5_Bw6.4_Bt0.5_Ah16.75_Aa0	172.6	1.415	8.683	1789.4	782.7	1789.4
Wt0.5_Bw6.4_Bt0.5_Ah17.25_Aa0	172.6	1.415	8.683	1789.4	774.1	1789.4
Wt0.5_Bw6.4_Bt0.5_Ah17.5_Aa0	172.6	1.415	8.683	1789.4	757.0	1789.4
Wt0.5_Bw6.4_Bt0.5_Ah17_Aa0	172.6	1.415	8.683	1789.4	791.0	1789.4

*Continue on next page*

Table G.1: All Permutations for Phase 2 (cont.).

Designation	Mass (t)	Construction Phase		Final Phase Tensile Force (kN)		
		Sliding FOS	Bearing FOS	Sliding	Bearing	Maximum
Wt0.5_Bw6.5_Bt0.5_Ah16.5_Aa0	173.3	1.433	8.997	1749.2	756.2	1749.2
Wt0.5_Bw6.5_Bt0.5_Ah16.75_Aa0	173.3	1.433	8.997	1749.2	740.8	1749.2
Wt0.5_Bw6.5_Bt0.5_Ah17.25_Aa0	173.3	1.433	8.997	1749.2	734.2	1749.2
Wt0.5_Bw6.5_Bt0.5_Ah17.5_Aa0	173.3	1.433	8.997	1749.2	718.0	1749.2
Wt0.5_Bw6.5_Bt0.5_Ah17_Aa0	173.3	1.433	8.997	1749.2	750.1	1749.2
Wt0.5_Bw6.6_Bt0.5_Ah16.5_Aa0	174.1	1.452	9.316	1709.0	712.3	1709.0
Wt0.5_Bw6.6_Bt0.5_Ah16.75_Aa0	174.1	1.452	9.316	1709.0	698.0	1709.0
Wt0.5_Bw6.6_Bt0.5_Ah17.25_Aa0	174.1	1.452	9.316	1709.0	693.3	1709.0
Wt0.5_Bw6.6_Bt0.5_Ah17.5_Aa0	174.1	1.452	9.316	1709.0	678.0	1709.0
Wt0.5_Bw6.6_Bt0.5_Ah17_Aa0	174.1	1.452	9.316	1709.0	708.3	1709.0
Wt0.5_Bw6.7_Bt0.5_Ah16.5_Aa0	174.8	1.471	9.639	1668.8	667.5	1668.8
Wt0.5_Bw6.7_Bt0.5_Ah16.75_Aa0	174.8	1.471	9.639	1668.8	654.1	1668.8
Wt0.5_Bw6.7_Bt0.5_Ah17.25_Aa0	174.8	1.471	9.639	1668.8	651.5	1668.8
Wt0.5_Bw6.7_Bt0.5_Ah17.5_Aa0	174.8	1.471	9.639	1668.8	637.2	1668.8
Wt0.5_Bw6.7_Bt0.5_Ah17_Aa0	174.8	1.471	9.639	1668.8	665.5	1668.8
Wt0.5_Bw6.8_Bt0.5_Ah16.5_Aa0	175.5	1.489	9.967	1628.6	621.6	1628.6
Wt0.5_Bw6.8_Bt0.5_Ah16.75_Aa0	175.5	1.489	9.967	1628.6	609.4	1628.6
Wt0.5_Bw6.8_Bt0.5_Ah17.25_Aa0	175.5	1.489	9.967	1628.6	608.7	1628.6
Wt0.5_Bw6.8_Bt0.5_Ah17.5_Aa0	175.5	1.489	9.967	1628.6	595.4	1628.6
Wt0.5_Bw6.8_Bt0.5_Ah17_Aa0	175.5	1.489	9.967	1628.6	621.7	1628.6
Wt0.5_Bw6.9_Bt0.5_Ah16.5_Aa0	176.3	1.508	10.300	1588.4	574.8	1588.4
Wt0.5_Bw6.9_Bt0.5_Ah16.75_Aa0	176.3	1.508	10.300	1588.4	563.7	1588.4
Wt0.5_Bw6.9_Bt0.5_Ah17.25_Aa0	176.3	1.508	10.300	1588.4	565.1	1588.4
Wt0.5_Bw6.9_Bt0.5_Ah17.5_Aa0	176.3	1.508	10.300	1588.4	552.7	1588.4
Wt0.5_Bw6.9_Bt0.5_Ah17_Aa0	176.3	1.508	10.300	1588.4	577.1	1588.4
Wt0.5_Bw7_Bt0.5_Ah16.5_Aa0	177.0	1.527	10.637	1548.2	527.1	1548.2
Wt0.5_Bw7_Bt0.5_Ah16.75_Aa0	177.0	1.527	10.637	1548.2	517.0	1548.2
Wt0.5_Bw7_Bt0.5_Ah17.25_Aa0	177.0	1.527	10.637	1548.2	520.5	1548.2
Wt0.5_Bw7_Bt0.5_Ah17.5_Aa0	177.0	1.527	10.637	1548.2	509.1	1548.2
Wt0.5_Bw7_Bt0.5_Ah17_Aa0	177.0	1.527	10.637	1548.2	531.4	1548.2
Wt0.5_Bw7.1_Bt0.5_Ah16.5_Aa0	177.7	1.545	10.979	1508.0	478.3	1508.0
Wt0.5_Bw7.1_Bt0.5_Ah16.75_Aa0	177.7	1.545	10.979	1508.0	494.3	1508.0
Wt0.5_Bw7.1_Bt0.5_Ah17.25_Aa0	177.7	1.545	10.979	1508.0	474.9	1508.0
Wt0.5_Bw7.1_Bt0.5_Ah17.5_Aa0	177.7	1.545	10.979	1508.0	464.6	1508.0
Wt0.5_Bw7.1_Bt0.5_Ah17_Aa0	177.7	1.545	10.979	1508.0	484.8	1508.0
Wt0.5_Bw7.2_Bt0.5_Ah16.5_Aa0	178.5	1.564	11.326	1467.9	428.6	1467.9
Wt0.5_Bw7.2_Bt0.5_Ah16.75_Aa0	178.5	1.564	11.326	1467.9	445.7	1467.9

*Continue on next page*

Table G.1: All Permutations for Phase 2 (cont.).

Designation	Mass (t)	Construction Phase		Final Phase Tensile Force (kN)		
		Sliding FOS	Bearing FOS	Sliding	Bearing	Maximum
Wt0.5_Bw7.2_Bt0.5_Ah17.25_Aa0	178.5	1.564	11.326	1467.9	428.5	1467.9
Wt0.5_Bw7.2_Bt0.5_Ah17.5_Aa0	178.5	1.564	11.326	1467.9	419.1	1467.9
Wt0.5_Bw7.2_Bt0.5_Ah17_Aa0	178.5	1.564	11.326	1467.9	437.3	1467.9
Wt0.5_Bw7.3_Bt0.5_Ah16.5_Aa0	179.2	1.583	11.677	1427.7	402.9	1427.7
Wt0.5_Bw7.3_Bt0.5_Ah16.75_Aa0	179.2	1.583	11.677	1427.7	396.2	1427.7
Wt0.5_Bw7.3_Bt0.5_Ah17.25_Aa0	179.2	1.583	11.677	1427.7	381.0	1427.7
Wt0.5_Bw7.3_Bt0.5_Ah17.5_Aa0	179.2	1.583	11.677	1427.7	372.7	1427.7
Wt0.5_Bw7.3_Bt0.5_Ah17_Aa0	179.2	1.583	11.677	1427.7	388.9	1427.7
Wt0.5_Bw7.4_Bt0.5_Ah16.5_Aa0	180.0	1.601	12.033	1387.5	351.2	1387.5
Wt0.5_Bw7.4_Bt0.5_Ah16.75_Aa0	180.0	1.601	12.033	1387.5	345.6	1387.5
Wt0.5_Bw7.4_Bt0.5_Ah17.25_Aa0	180.0	1.601	12.033	1387.5	332.7	1387.5
Wt0.5_Bw7.4_Bt0.5_Ah17.5_Aa0	180.0	1.601	12.033	1387.5	325.5	1387.5
Wt0.5_Bw7.4_Bt0.5_Ah17_Aa0	180.0	1.601	12.033	1387.5	339.4	1387.5
Wt0.5_Bw7.5_Bt0.5_Ah16.5_Aa0	180.7	1.620	12.393	1347.3	298.6	1347.3
Wt0.5_Bw7.5_Bt0.5_Ah16.75_Aa0	180.7	1.620	12.393	1347.3	294.1	1347.3
Wt0.5_Bw7.5_Bt0.5_Ah17.25_Aa0	180.7	1.620	12.393	1347.3	283.4	1347.3
Wt0.5_Bw7.5_Bt0.5_Ah17.5_Aa0	180.7	1.620	12.393	1347.3	277.3	1347.3
Wt0.5_Bw7.5_Bt0.5_Ah17_Aa0	180.7	1.620	12.393	1347.3	289.1	1347.3
Wt0.5_Bw7.6_Bt0.5_Ah16.5_Aa0	181.4	1.639	12.757	1307.1	245.0	1307.1
Wt0.5_Bw7.6_Bt0.5_Ah16.75_Aa0	181.4	1.639	12.757	1307.1	241.7	1307.1
Wt0.5_Bw7.6_Bt0.5_Ah17.25_Aa0	181.4	1.639	12.757	1307.1	233.2	1307.1
Wt0.5_Bw7.6_Bt0.5_Ah17.5_Aa0	181.4	1.639	12.757	1307.1	228.1	1307.1
Wt0.5_Bw7.6_Bt0.5_Ah17_Aa0	181.4	1.639	12.757	1307.1	237.8	1307.1
Wt0.5_Bw7.7_Bt0.5_Ah16.5_Aa0	182.2	1.657	13.126	1266.9	190.4	1266.9
Wt0.5_Bw7.7_Bt0.5_Ah16.75_Aa0	182.2	1.657	13.126	1266.9	188.3	1266.9
Wt0.5_Bw7.7_Bt0.5_Ah17.25_Aa0	182.2	1.657	13.126	1266.9	182.1	1266.9
Wt0.5_Bw7.7_Bt0.5_Ah17.5_Aa0	182.2	1.657	13.126	1266.9	178.1	1266.9
Wt0.5_Bw7.7_Bt0.5_Ah17_Aa0	182.2	1.657	13.126	1266.9	185.5	1266.9
Wt0.5_Bw7.8_Bt0.5_Ah16.5_Aa0	182.9	1.676	13.500	1226.7	134.8	1226.7
Wt0.5_Bw7.8_Bt0.5_Ah16.75_Aa0	182.9	1.676	13.500	1226.7	133.9	1226.7
Wt0.5_Bw7.8_Bt0.5_Ah17.25_Aa0	182.9	1.676	13.500	1226.7	130.0	1226.7
Wt0.5_Bw7.8_Bt0.5_Ah17.5_Aa0	182.9	1.676	13.500	1226.7	127.1	1226.7
Wt0.5_Bw7.8_Bt0.5_Ah17_Aa0	182.9	1.676	13.500	1226.7	132.3	1226.7
Wt0.5_Bw7.9_Bt0.5_Ah16.5_Aa0	183.6	1.695	13.877	1186.5	78.3	1186.5
Wt0.5_Bw7.9_Bt0.5_Ah16.75_Aa0	183.6	1.695	13.877	1186.5	78.6	1186.5
Wt0.5_Bw7.9_Bt0.5_Ah17.25_Aa0	183.6	1.695	13.877	1186.5	77.1	1186.5
Wt0.5_Bw7.9_Bt0.5_Ah17.5_Aa0	183.6	1.695	13.877	1186.5	75.2	1186.5

*Continue on next page*



Table G.1: All Permutations for Phase 2 (cont.).

Designation	Mass (t)	Construction Phase		Final Phase Tensile Force (kN)		
		Sliding FOS	Bearing FOS	Sliding	Bearing	Maximum
Wt0.5_Bw7.9_Bt0.5_Ah17_Aa0	183.6	1.695	13.877	1186.5	78.2	1186.5
Wt0.5_Bw8_Bt0.5_Ah16.5_Aa0	184.4	1.713	14.259	1146.4	20.8	1146.4
Wt0.5_Bw8_Bt0.5_Ah16.75_Aa0	184.4	1.713	14.259	1146.4	22.3	1146.4
Wt0.5_Bw8_Bt0.5_Ah17.25_Aa0	184.4	1.713	14.259	1146.4	23.1	1146.4
Wt0.5_Bw8_Bt0.5_Ah17.5_Aa0	184.4	1.713	14.259	1146.4	22.4	1146.4
Wt0.5_Bw8_Bt0.5_Ah17_Aa0	184.4	1.713	14.259	1146.4	23.1	1146.4
Wt0.5_Bw8.1_Bt0.5_Ah16.5_Aa0	185.1	1.732	14.646	1106.2	-12.7	1106.2
Wt0.5_Bw8.1_Bt0.5_Ah16.75_Aa0	185.1	1.732	14.646	1106.2	-34.9	1106.2
Wt0.5_Bw8.1_Bt0.5_Ah17.25_Aa0	185.1	1.732	14.646	1106.2	-31.7	1106.2
Wt0.5_Bw8.1_Bt0.5_Ah17.5_Aa0	185.1	1.732	14.646	1106.2	-31.3	1106.2
Wt0.5_Bw8.1_Bt0.5_Ah17_Aa0	185.1	1.732	14.646	1106.2	-32.9	1106.2
Wt0.5_Bw8.2_Bt0.5_Ah16.5_Aa0	185.9	1.751	15.036	1066.0	-72.2	1066.0
Wt0.5_Bw8.2_Bt0.5_Ah16.75_Aa0	185.9	1.751	15.036	1066.0	-68.1	1066.0
Wt0.5_Bw8.2_Bt0.5_Ah17.25_Aa0	185.9	1.751	15.036	1066.0	-87.5	1066.0
Wt0.5_Bw8.2_Bt0.5_Ah17.5_Aa0	185.9	1.751	15.036	1066.0	-85.9	1066.0
Wt0.5_Bw8.2_Bt0.5_Ah17_Aa0	185.9	1.751	15.036	1066.0	-64.9	1066.0
Wt0.5_Bw8.3_Bt0.5_Ah16.5_Aa0	186.6	1.769	15.431	1025.8	-132.6	1025.8
Wt0.5_Bw8.3_Bt0.5_Ah16.75_Aa0	186.6	1.769	15.431	1025.8	-127.3	1025.8
Wt0.5_Bw8.3_Bt0.5_Ah17.25_Aa0	186.6	1.769	15.431	1025.8	-119.2	1025.8
Wt0.5_Bw8.3_Bt0.5_Ah17.5_Aa0	186.6	1.769	15.431	1025.8	-116.5	1025.8
Wt0.5_Bw8.3_Bt0.5_Ah17_Aa0	186.6	1.769	15.431	1025.8	-122.8	1025.8
Wt0.5_Bw8.4_Bt0.5_Ah16.5_Aa0	187.3	1.788	15.830	985.6	-194.0	985.6
Wt0.5_Bw8.4_Bt0.5_Ah16.75_Aa0	187.3	1.788	15.830	985.6	-187.4	985.6
Wt0.5_Bw8.4_Bt0.5_Ah17.25_Aa0	187.3	1.788	15.830	985.6	-176.9	985.6
Wt0.5_Bw8.4_Bt0.5_Ah17.5_Aa0	187.3	1.788	15.830	985.6	-172.9	985.6
Wt0.5_Bw8.4_Bt0.5_Ah17_Aa0	187.3	1.788	15.830	985.6	-181.7	985.6
Wt0.5_Bw8.5_Bt0.5_Ah16.5_Aa0	188.1	1.806	16.234	945.4	-256.4	945.4
Wt0.5_Bw8.5_Bt0.5_Ah16.75_Aa0	188.1	1.806	16.234	945.4	-248.5	945.4
Wt0.5_Bw8.5_Bt0.5_Ah17.25_Aa0	188.1	1.806	16.234	945.4	-235.5	945.4
Wt0.5_Bw8.5_Bt0.5_Ah17.5_Aa0	188.1	1.806	16.234	945.4	-230.3	945.4
Wt0.5_Bw8.5_Bt0.5_Ah17_Aa0	188.1	1.806	16.234	945.4	-241.5	945.4
Wt0.5_Bw8.6_Bt0.5_Ah16.5_Aa0	188.8	1.825	16.642	905.2	-319.8	905.2
Wt0.5_Bw8.6_Bt0.5_Ah16.75_Aa0	188.8	1.825	16.642	905.2	-310.5	905.2
Wt0.5_Bw8.6_Bt0.5_Ah17.25_Aa0	188.8	1.825	16.642	905.2	-295.0	905.2
Wt0.5_Bw8.6_Bt0.5_Ah17.5_Aa0	188.8	1.825	16.642	905.2	-288.6	905.2
Wt0.5_Bw8.6_Bt0.5_Ah17_Aa0	188.8	1.825	16.642	905.2	-302.3	905.2
Wt0.5_Bw8.7_Bt0.5_Ah16.5_Aa0	189.5	1.844	17.053	865.0	-359.1	865.0

*Continue on next page*

Table G.1: All Permutations for Phase 2 (cont.).

Designation	Mass (t)	Construction Phase		Final Phase Tensile Force (kN)		
		Sliding FOS	Bearing FOS	Sliding	Bearing	Maximum
Wt0.5_Bw8.7_Bt0.5_Ah16.75_Aa0	189.5	1.844	17.053	865.0	-373.5	865.0
Wt0.5_Bw8.7_Bt0.5_Ah17.25_Aa0	189.5	1.844	17.053	865.0	-355.5	865.0
Wt0.5_Bw8.7_Bt0.5_Ah17.5_Aa0	189.5	1.844	17.053	865.0	-347.9	865.0
Wt0.5_Bw8.7_Bt0.5_Ah17_Aa0	189.5	1.844	17.053	865.0	-364.0	865.0
Wt0.5_Bw8.8_Bt0.5_Ah16.5_Aa0	190.3	1.862	17.470	824.9	-424.4	824.9
Wt0.5_Bw8.8_Bt0.5_Ah16.75_Aa0	190.3	1.862	17.470	824.9	-412.5	824.9
Wt0.5_Bw8.8_Bt0.5_Ah17.25_Aa0	190.3	1.862	17.470	824.9	-416.8	824.9
Wt0.5_Bw8.8_Bt0.5_Ah17.5_Aa0	190.3	1.862	17.470	824.9	-408.0	824.9
Wt0.5_Bw8.8_Bt0.5_Ah17_Aa0	190.3	1.862	17.470	824.9	-426.6	824.9
Wt0.5_Bw8.9_Bt0.5_Ah16.5_Aa0	191.0	1.881	17.890	784.7	-490.7	784.7
Wt0.5_Bw8.9_Bt0.5_Ah16.75_Aa0	191.0	1.881	17.890	784.7	-477.4	784.7
Wt0.5_Bw8.9_Bt0.5_Ah17.25_Aa0	191.0	1.881	17.890	784.7	-479.2	784.7
Wt0.5_Bw8.9_Bt0.5_Ah17.5_Aa0	191.0	1.881	17.890	784.7	-469.1	784.7
Wt0.5_Bw8.9_Bt0.5_Ah17_Aa0	191.0	1.881	17.890	784.7	-465.2	784.7
Wt0.5_Bw9_Bt0.5_Ah16.5_Aa0	191.8	1.900	18.314	744.5	-558.0	744.5
Wt0.5_Bw9_Bt0.5_Ah16.75_Aa0	191.8	1.900	18.314	744.5	-543.3	744.5
Wt0.5_Bw9_Bt0.5_Ah17.25_Aa0	191.8	1.900	18.314	744.5	-517.4	744.5
Wt0.5_Bw9_Bt0.5_Ah17.5_Aa0	191.8	1.900	18.314	744.5	-531.1	744.5
Wt0.5_Bw9_Bt0.5_Ah17_Aa0	191.8	1.900	18.314	744.5	-529.8	744.5

## Appendix H

# Example Calculation for Moment Equilibrium

Table H.1: Permutation Input Parameters

<b>Inputs</b>		
Base Width (BW)	9	m
Wall Thickness (Wt)	0.5	m
Effective Base Width	8.5	m
Anchor Height (Ah)	17.5	m
Base Thickness (Bt)	0.5	m
Required Anchor Force For Global	744.48	kN
Anchor Force	0	kN

Table H.2: Load Factors

<b>Load Factors ULS (BS)</b>		
Permanent Loads	Self Weight	1.35
	Soil parameters	1.35
	Prestressing	1
Variable Loads	Imposed Loads	1.5
	Loads from fluids that vary with time	1.5

Table H.3: System Forces at ULS and Moment Arms

Forces				
Force Label	Force	Unit	Moment Arm	Unit
Horizontal Earth Force Below MSL	-2.96E+06	N	5.5	m
Additional Earth Force Below MSL	-4.76E+05	N	8.3	m
Surcharge Force Below MSL	-1.87E+06	N	8.3	m
Horizontal Earth Force Above MSL	-3.30E+05	N	18	m
Surcharge Force Above MSL	-3.49E+05	N	18.7	m
Tidal Lag	-1.55E+06	N	8.75	m
Anchor Force	0.00E+00	N	17.5	m
Bollard Load	-1.20E+06	N	20.8	m
Soil Weight	1.52E+07	N	4.25	m
Vertical Surcharge	3.01E+06	N	4.25	m
Vertical Component Surcharge BelowMSL	6.06E+05	N	4.25	m
Vertical Component Earth BelowMSL	9.63E+05	N	5.67	m
Additional Vertical Component Earth BelowMSL	1.55E+05	N	4.25	m
Vertical Component Surcharge AboveMSL	1.46E+05	N	4.25	m
Vertical Component Earth AboveMSL	1.38E+05	N	5.67	m
Base Weight	5.08E+05	N	4.25	m
Wall Weight	1.05E+06	N	0.25	m

Table H.4: System Moments at ULS

Moments		
Moment Label	Magnitude	Unit
Horizontal Earth Force Below MSL	-1.64E+07	Nm
Additional Earth Force Below MSL	-3.95E+06	Nm
Surcharge Force Below MSL	-1.55E+07	Nm
Horizontal Earth Force Above MSL	-5.93E+06	Nm
Surcharge Force Above MSL	-6.52E+06	Nm
Tidal Lag	-1.36E+07	Nm
Anchor	0.00E+00	Nm
Bollard Load	-2.50E+07	Nm
Soil Weight	6.48E+07	Nm
Vertical Surcharge	1.28E+07	Nm
Vertical Component Surcharge BelowMSL	2.58E+06	Nm
Vertical Component Earth BelowMSL	5.46E+06	Nm
Additional Vertical Component Earth BelowMSL	6.58E+05	Nm
Vertical Component Surcharge AboveMSL	6.19E+05	Nm
Vertical Component Earth AboveMSL	7.80E+05	Nm
Base Weight	2.16E+06	Nm
Wall Weight	2.61E+05	Nm

Table H.5: Moment Equilibrium Result

Moment STR					
Equilibrium around Base	3259761	Nm	=	3259.761	kNm

# Appendix I

## ASDO Bars

# ASDO ANCHOR DESIGN CAPACITIES

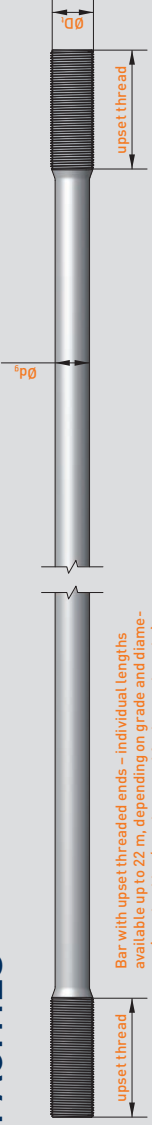


Table 2 – Anchors with upset forged threads

Nominal upset thread diameter Thread tensile stress area Shaft diameters available*	ØD <sub>1</sub> A <sub>1</sub> All grades	Metric	ASD0355 – Tensile resistance (EN1993-5)																																							
			M64/L48	M68/52	M72/56	M76/60	M80/64	M85/68	M90/72	M95/75	M100/80	M105/85	M110/90	M115/95	M120/100	M125/105	M130/110	M135/115	M140/120	M145/125																						
ØD <sub>2</sub>	64	mm	48	52	56	60	64	68	72	75	80	85	90	95	100	105	110	115	120	125	130	135	140	145	150	155	160	165	170	175	180	185	190	195	200	205	210	215	220			
A <sub>2</sub>	2,676	mm <sup>2</sup>	1,810	2,124	2,463	2,827	3,217	3,632	4,072	4,536	5,027	5,545	6,092	6,668	7,275	7,915	8,589	9,298	10,044	10,828	11,651	12,515	13,421	14,370	15,364	16,404	17,492	18,630	19,820	21,063	22,360	23,715	25,130	26,606	28,145	29,749	31,420	32,155	33,947	35,863		
F <sub>y</sub>	642	kN	754	874	1,004	1,142	1,289	1,445	1,568	1,784	2,014	2,258	2,516	2,788	3,074	3,376	3,694	4,028	4,378	4,746	5,132	5,538	5,965	6,414	6,886	7,383	7,907	8,459	9,041	9,654	10,299	10,976	11,687	12,434	13,218	14,041	14,905	15,810	16,758	17,752	18,794	
F <sub>ult</sub>	923	kN	1,083	1,256	1,442	1,641	1,852	2,076	2,294	2,564	2,894	3,244	3,615	4,006	4,416	4,847	5,297	5,768	6,259	6,771	7,305	7,861	8,439	9,041	9,668	10,321	11,001	11,709	12,447	13,216	14,017	14,851	15,720	16,626	17,571	18,557	19,585	20,658	21,778	22,947	24,167	
F <sub>res</sub>	642	kN	748	847	952	1,063	1,171	1,289	1,369	1,536	1,712	1,899	2,094	2,258	2,426	2,600	2,781	2,969	3,165	3,369	3,581	3,799	4,026	4,261	4,504	4,756	5,017	5,287	5,566	5,854	6,152	6,460	6,778	7,106	7,445	7,794	8,154	8,525	8,907	9,299	9,704	10,123

\*Note: The above sizes are standardised, other shaft and thread ratios can be adapted to suit your project requirements, e.g. for sacrificial steel requirements or smaller design loads. design resistance calculated as per EN1993-5 with  $\gamma_{M2} = 1.0$  &  $\gamma_{M3} = 1.25$  and k as noted.

## Appendix J

# History of Port Structures

Maritime transports history dates back to before 3500 BC. Over the centuries, the systems used to transport goods and people over the oceans has evolved in line with the demands of world trade and advances in ship design and cargo handling. Since the earliest days of the human race, mankind has been fascinated by the possibility of travelling across the rivers and oceans that they encountered. The earliest forms of maritime transport involved small vessels travelling short distances (primarily on river networks), as ocean going vessels had not yet been developed. These early vessels made use of crude river mooring locations. Around these small river moorings towns and villages began to appear and grow. Over time, these mooring locations developed into ports and the towns grew into hubs for trade and the sharing of knowledge and skills (Centre for Civil Engineering Research and Codes, 2005). As the technology of a civilization improved, larger vessels could be constructed and along with improvements in navigation allowed the merchants to travel greater and greater distances to trade with other civilizations. As maritime traffic increased the ability of these small river ports to handle the volume of ship traffic and cargo was exceeded. Thus the ports needed to be expanded to handle the greater volume of ship traffic and cargo while ensuring that the river channel was not blocked by these structures. This led to the development of piers along the river banks along which a greater number of ships could dock and unload while leaving the main river channel unobstructed. This is viewed as the beginning of the development of port infrastructure (Tsinker, 1998).

After this period, the ever-increasing demand for trade resulted in an expansion of ports to the coast and construction of the first open water ports. Many of the first open water ports were built along the Mediterranean coastline. In turn, this led to the development of what became known as a "breakwater" which was used to protect the ships docked in the ports. Inside the area protected by the breakwater, the design of the structures was similar to those used for the river ports. Since this time there have been many advances in materials used to build both ports and the vessels that dock within them. As the material and construction technology improved ships began increasing in size. The most significant increase in size was in the draught of the vessels. A ships draught



is how far below the waterline the ship extends. As the draft increased, ports had to be built out further from the coast as ships could not reach the piers where they once had unloaded due to how shallow old ports and harbours were. This led to an increase in cost of construction for these sorts of ports due to the additional complexity of design due to the construction of these structures further from shore and the requirement to backfill and reclaim all the land behind the .

The first written record that provides details on how port structures were built is provided in Vitruvius' *De Architectura* which dates from the first century B.C.E. Very little written proof on the subject of port construction from between the 1st century B.C.E. until around the 18th century exists due to the fact that the majority of historians that study maritime transport during this period focus on the trade itself, rather than the structures that made this trade possible (Jarvis, 1998). As a result of all this development, ports not only had significant influences of trade and industry , but also on human prosperity and an increased understanding in the fields of technology and building materials (Centre for Civil Engineering Research and Codes, 2005).

During the 1960s it came to the attention of the various engineering disciplines that the shipping industry was going through rapid changes. These rapid changes were going to result in the near-total extinction of the traditional general cargo vessel primarily as a result of the introduction of the shipping container (Jarvis, 1998). During the 1950s the container had been introduced for the transport of general cargo by rail and road across the USA, its use for maritime transport was the next logical step but due to socio-economic complications the use of containers was limited to the coastline of the USA until 1966 when the first container arrived in the port of Rotterdam. Over the last 5 decades container shipping has spread across the world and become the primary form for maritime transportation of general cargo around the world (Ligteringen and Velsink, 2012).

## Appendix K

# Maritime Transportation Vessel Details

### K.0.1 Transport Capacity

A ship's tonnage is an indication of the cargo capacity that the vessel is able to transport. Various ways exist to express the tonnage of a vessel, this is dependant on the vessel type, its country of origin, or the purpose for which the tonnage is to be used, eg: harbour duties. The primary methods of expressing tonnage are:

1. Gross Register Tonnage (GRT)
2. Net Register Tonnage (NRT)
3. Dead Weight Tonnage (DWT)

The relationship between these parameters is not fixed as they are dependant on the type of vessel concerned. There are certain rules of thumb that can be used to obtain a basic first assumption:

**General Cargo Ships**  $DWT \approx 1.5GRT \approx 2.5NRT$

**Very Large Crude Carriers**  $DWT \approx 2.0GRT \approx 2.6NRT$

The definitions of the tonnages are as follows:

**GRT** is the total volume of all permanently enclosed space above and below decks, with certain exceptions, such as the wheel house, chart room, radio and other specific spaces above deck. GRT is expressed in tons, in which one ton is equal to  $100 \text{ ft}^3 = 2.83 \text{ m}^3$ . GRT is normally used as the basis for calculation of port duties.

**NRT** is the total of all space used for cargo, expressed in units of  $2.83 \text{ m}^3$ . The NRT is equal to GRT minus the crew's accommodation, workshops, engine room etc.

**DWT** is the difference between light and load displacement, in which:

- **Light Displacement** is the mass of the ship's hull, engines, spares and all other items necessary for normal working performance.
- **Load Displacement** is the ship's mass when full loaded, this includes the ships hull, engines, cargo, crew etc. Fully loaded means the ship sinks into the water down to its Plimsoll Mark.

As a result the DWT provides the mass of cargo, fuel, crew, passengers etc expressed in metric tons.

The following units are used to describe a ships tonnage:

- Metric ton (t = 1000 kg)
- English or Long ton (ts = 1016 kg)
- Short ton (sts = 907 kg)
- Port tons/ Shipping tons: Port or shipping tons are used to determine maritime transport charges. A port or shipping ton is equal to  $1 m^3$  when the specific weight of cargo is smaller than  $1 t/m^3$  and equal to 1 t when the specific weight of cargo is bigger than  $1 t/m^3$ .

For certain specialised ships the cargo carrying capacity is not only expressed in terms of GRT, NRT or DWT but also in other units, for a specific type of vessel.

- **TEU**  
This unit is normally used to express the capacity for container storage on board of a vessel.
- $m^3$   
The carrying capacity of liquefied gas tankers is usually expressed in  $m^3$ .
- **Street/Lane Length**  
This dimensions is often used for so-called Ro/Ro vessels. It expresses the total loading length with standardised width of 2.50 m, available on board of the vessel. It is expressed in meters.

### K.0.2 Vessel Vertical Dimensions

The maximum distance between the waterline and the keel of a vessel is known as the draught, as shown in Figure K.1. The vessel's displacement tonnage is calculated in respect of the draught and the stationary freeboard, both of these are indicated on the side of the vessel.

## SHIP DIMENSIONS

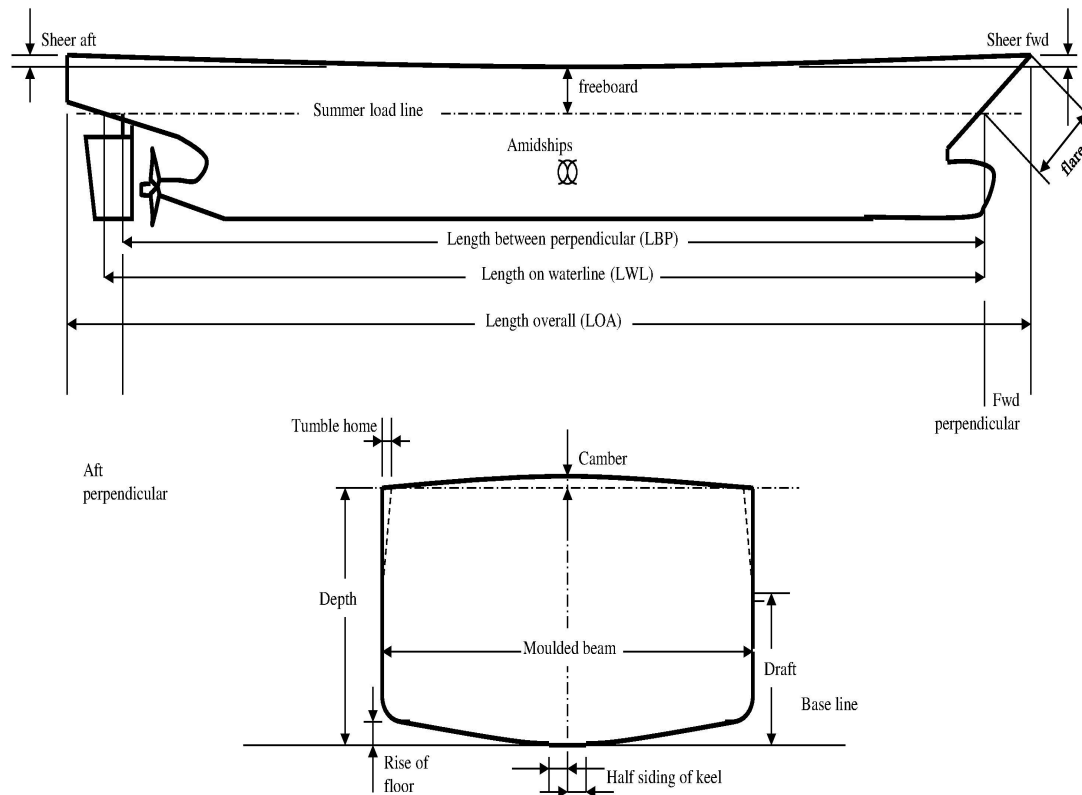


Figure K.1: All Dimensions of Maritime Vessels (Marine Study, 2016)

The maximum draught is indicated by the so-called Plimsoll Mark, an example of which is given in Figure K.2. This mark is comprised of a circle with a horizontal line overlying the circle with two letters on either side of the circle. The letters stand for the classification society of the Plimsoll Mark. These societies issue binding conditions for sizes and quality of materials to be used in construction, tests to be carried out etc. A vessel without this "classification" is virtually uninsurable. This classification is most commonly done by Lloyd Register (Letters: LR) in England, Bureau Veritas (Letters: BV) in France and the American Bureau of Shipping (Letters: AB) in the USA.

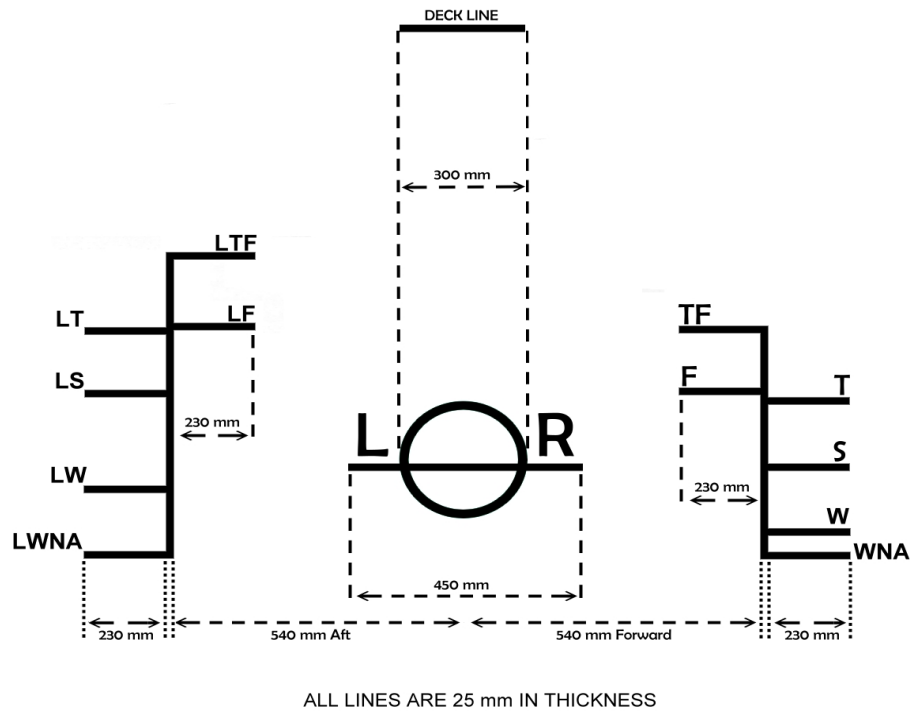


Figure K.2: Layout of Plimsoll Mark (MarineWiki, 2010)

The draught of a vessel varies as it is dependant on the density of the water that the vessel is travelling through or docked in. The density of the water does not remain constant throughout the year, the density also changes with latitude and longitude. An example of this is that a vessel will sit deeper in the water in the summer near the equator than in the North Atlantic during winter. Along the right-hand side of the Plimsoll Mark is a second indicator this indicates the maximum allowable draft under various conditions (Ligteringen and Velsink, 2012). These conditions are:

**TF** = Tropical Fresh Water

**F** = Fresh Water

**T** = Tropical Salt Water

**S** = Summer Salt Water

**W** = Winter Salt Water

**WNA** = Winter Salt Water on the North Atlantic

These draught markings all include a certain factor of safety. These draught markings are painted at the bow, in the middle and at the stern of the vessel on both sides, this is to ensure that the vessel is not overloaded in a particular quadrant of the vessel.

### K.0.3 Vessel Horizontal Dimensions

#### K.0.3.1 Length

The length of a vessel can be expressed in two ways:

- **LBP** Length Between Perpendiculars
- **LOA** Length Over All

Both lengths are given in Figure K.1. With the definitions of the lengths given as:

**LBP** LBP is the horizontal distance in meters between the points of intersection of the ship's bow and the summer salt water line when fully loaded and the vertical line through the axis of the ships rudder.

**LOA** LOA is the horizontal distance between two vertical lines, one tangential to the ship's bow and one to the ship's stern.

LOA is normally used for dimensioning of harbour basins and ship berths, unless specified a ships length is given by LOA.

#### K.0.3.2 Beam

The beam or breadth of a vessel is the maximum distance in meters between the two sides of the ship as shown in Figure K.1.

## K.1 Commodities and Types of Maritime Transportation Vessels

The flow of cargo around the world is classified using two separate classifications. These are classification by type of cargo and classification by method of transportation.

The first classification follows an internationally agreed upon division of cargo into 10 main groups. This is known as the NSTR (Nomenclature uniforme des marchandises pour les Statistiques de Transport, Révisée). The main groups are:

1. Agricultural products and livestock.
2. Other food products and fodder.
3. Solid mineral fuels (eg. coals, cokes etc.)
4. Oil and oil products.
5. Iron, ore and metal scrap.
6. Iron, Steel and non-Ferro metals.
7. Raw minerals; construction materials.

8. Fertilisers.
9. Chemical Products.
10. Vehicles, machinery and other such goods.

This standardisation of cargo categories allowed for the determination of accurate cargo statistics for each individual port and from this the international flow of cargo is obtained, this allows for easier forecasting for future development. As discussed in (Ligteringen and Velsink, 2012), port planning begins by using these forecasts.

The second classification of cargo is of greater importance than the first classification for the actual design of the terminal. As each of the different methods of transportation require different berth side infrastructure. The following divisions are made regarding the methods of transport:

1. Dry Bulk
2. Liquid Bulk
3. Container
4. Roll-on/Roll-off
5. Other

The category "Other" fills the role of traditional general cargo vessels which primarily involves break-bulk cargo and bagged goods. Ligteringen and Velsink (2012) Chapter 2 covers any vessels not given below that are used for international maritime transport.

### K.1.1 Conventional Cargo Vessels

General cargo vessels carry various kinds of break-bulk cargo, with break-bulk being defined as boxes, sacks, bags, drum, machine parks and refrigerated goods. Table K.1 details the different methods of cargo handling for the various break-bulk cargo types.

Table K.1: Types of Break-Bulk Cargo and their Handling Methods. (Ligteringen and Velsink, 2012)

Category of Break Bulk	Shape or packing	Cargo Handling Method
1. Bagged Goods	Undefined Shape	Ropes, on pallets
2. Normal Break-Bulk	Crates,boxes,drums	Ropes,hooks,pallets
3. Neo Bulk	Steel plates, bars and wire, lumber, paper	Ropes and hooks,cassettes

Each piece of cargo is either handled separately or smaller items can be assembled together and handled as a unit. These are then lifted out of the vessel using either shore

based cranes or cranes aboard the vessel.

The capacity of these vessels range from 5000 to 25 000 DWT, with the cargo distributed between the vessels holds, usually either 4 or 5 per vessel. The older style of general cargo vessels can easily be identified by its many deck cranes, this is so that each hold can be serviced by two cranes. The draft of this vessel type is usually small ranging from 7.5m to 10m, allowing these vessels to serve most ports worldwide, an example of such a vessel is given in Figure K.3.



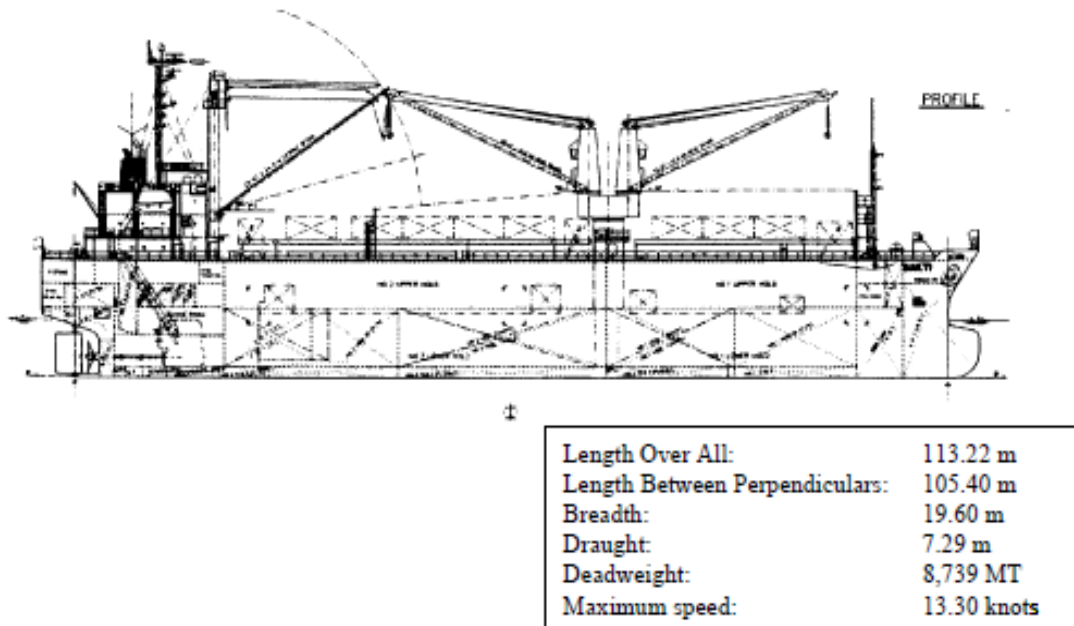


Figure K.3: General Cargo Vessel 'Sakti' (Ligteringen and Velsink, 2012)

Over the past few decades, the reduction in turnaround time of ships has become of greater importance. This has led to new developments in ship design and cargo handling methods. An example is the Unit Load Concept (ULC) where cargo that was once transported on pallets is now transported using a different method such as large cassettes of paper. This has led to changes of the port side infrastructure that is used to handle this cargo.

The general cargo vessel is the original form of cargo vessel with all specialised vessels originating from the vessel type.

### K.1.2 Bulk Cargo Vessels

These style of vessels are best suited for the transportation of large volumes of homogeneous, unpacked cargo such as liquids (Oil, liquid natural gas), chemical products (fertiliser), cement, iron ore, coal and agricultural products (rice, grain). As a result of the homogeneous nature of this cargo, it can be handled in a more or less continuous manner. The handling of different bulk goods is done using different methods such as pumping for liquids, sucking for grains and cereals and a combination of grabber cranes and conveyor belts for coal and ores.

Bulk cargo vessels are mainly divided into two primary types liquid bulk carriers and dry bulk carriers. Each of these types can be further subdivided into smaller more specialised types. Table K.2 provides a breakdown of these types and the capacity ranges dependant on the type of cargo carried.

Table K.2: Bulk Carrier Types and Capacity. (Ligteringen and Velsink, 2012)

Vessel Type	Cargo Type	Capacity Range (1000 DWT)
<b>Liquid Bulk</b>		
Crude Carrier	Crude Oil	20-400
Product Tanker	Refined Products	0.5-100
Parcel Tanker	Refined Products, Chemicals	0.5-40
LNG Tanker	Liquefied Natural Gas	60-90
LPG Tanker	Liquefied Pressurised Gas	0.5-70
<b>Dry Bulk</b>		
	Ore, Coal	100-365
	Chemical	5-70
	Agricultural Products	0.5-10

#### K.1.2.1 Dry Bulk

These vessels are designed for large volumes of uniform, unpacked cargo, such as ore, coal and grains. The loading of this type of vessel is done from land based infrastructure

rather than ship based equipment. For the purpose of unloading the vessel, either of these methods can be used. The two approaches to unloading has resulted in a split in vessel design, a large number of the dry bulk fleet have no self-loading equipment and are known as "ungeared bulk carriers". Those vessels that carry self-loading equipment are known as "geared bulk carriers" and have no need for shore based infrastructure to unload.

The access to the storage areas, called the hold, of these types of vessels is through large hatches on the deck. These hatches are very wide as to provide easy access to all areas of the hold for all the cargo handling equipment being used. The largest bulk carriers are known as Very Large Ore Carriers (VLOC's) and can measure 350 000 DWT, an example of such as vessel is given in Figure K.4.

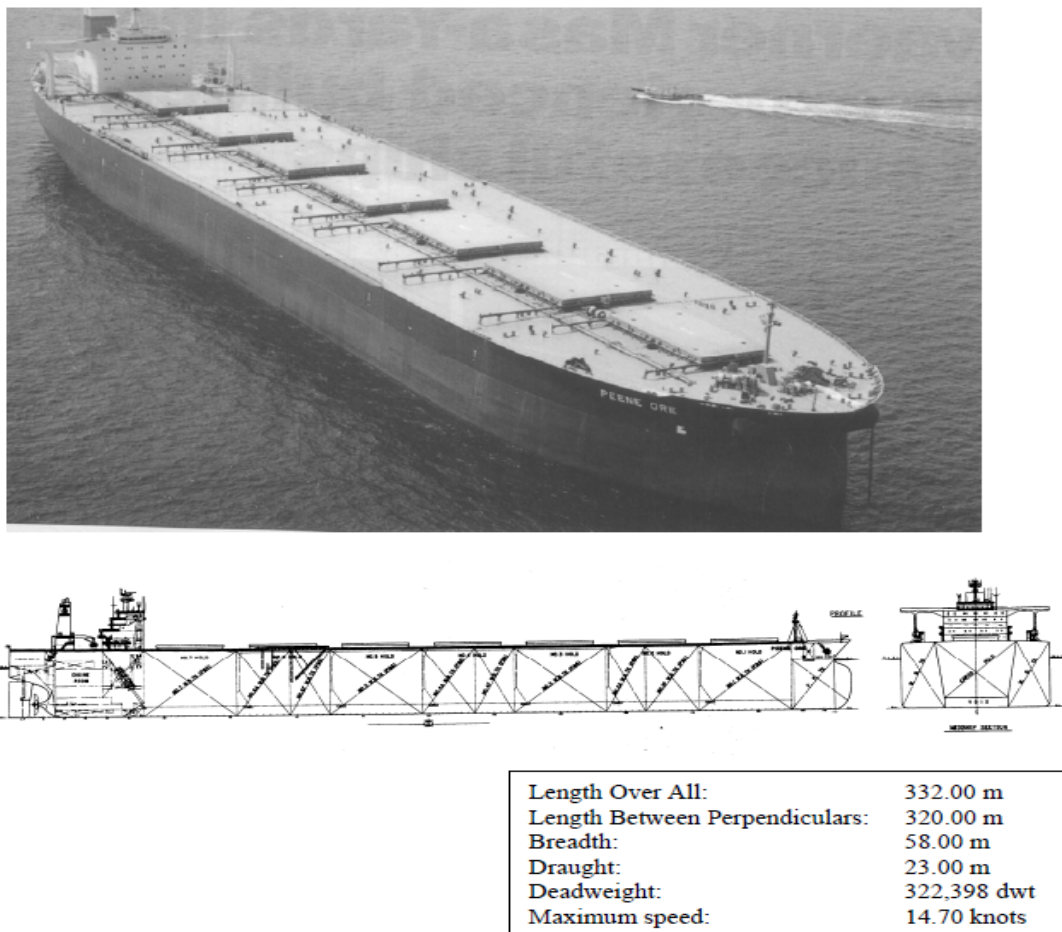


Figure K.4: Very Large Ore Carrier (VLOC) 'Peene Ore' (Ligteringen and Velsink, 2012)

### **K.1.2.2 Liquid Bulk**

The most common liquid bulk cargo vessels are those used to transport crude oil, liquid natural gas (LNG) and liquid petroleum gas (LPG). Parcel and product tankers are less common.

#### **Crude Oil Tanker**

Since the end of World War 2, the demand for crude oil has increased dramatically. This is mostly due to coal being the major source of energy prior to the war. Before WW2, oil was transported by small oil tankers, after the war these tankers were no longer able to meet the demand and thus grew larger and larger in size to become what we recognise as modern crude oil tankers. This large increase in vessel size was required to keep pace with the demand for oil and to reduce transportation costs. This led to the development of the Very Large Crude Carriers (VLCC's) and the Ultra Large Crude Carriers (ULCC's) with the ULCC's being the larger of the two. An example of a VLCC is given in Figure K.5.



Length Over All:	332.94 m
Length Between Perpendiculars:	320.00 m
Breadth:	60.00 m
Draught:	21.10 m
Deadweight:	300,058 MT
Maximum speed:	16.80 knots

Figure K.5: Very Large Crude Carrier (VLCC) 'New Vanguard' (Ligteringen and Velsink, 2012)

The intermediate size tanker (50 000 - 200 000 DWT) has returned to prominence as:

1. The levelling off or even small reduction in the world crude oil trade.
2. Increased use of the upgraded Suez Canal instead of around the Cape of Good Hope services.
3. Although VLCC's and ULCC's are able to transport larger volumes of crude oil on a single voyage they are unable to berth in many ports worldwide due to their deep draughts. As of 1992 less than 10 ULCC's were still in operation.

Crude Oil Tankers can be identified by their flat decks without hatches or cranes. These vessels do have pipelines, pumps and manifolds on deck, which are there to allow for filling and emptying of the vessel.

### Liquid Gas Tanker

These vessels carry their cargo's of gas at high pressures, low temperatures or a combination of both. The products carried by these vessels are:

- **LPG**, a mixture of propane and butane.
- **LNG**, which consists mainly of methane.
- Other types of chemical gas, like ammonia and ethylene.

The difference between LNG and LPG vessels is given in Figure K.6.



(a) LNG Tanker

(b) LPG Tanker

Figure K.6: The difference between LNG tankers and LPG tankers (Ligteringen and Velsink, 2012)

The gas is mainly transported at atmospheric pressure and at low temperatures (LPG at  $-46^{\circ}\text{C}$  and LNG at  $-162^{\circ}\text{C}$ ) in its liquid form within separate tanks in the vessels hold, this is known as cryogenic transportation. Natural gas in its liquid form retains 0.0027% of its original volume, this allows for a greater volume of gas to be transported than in its natural gaseous form. LPG can be transported at normal temperatures but only under pressure. LNG only liquefies at  $-80^{\circ}\text{C}$  even under pressure and thus cant be transported using this method. In principle LNG tankers are able to transport LPG, while LPG tankers are unable to transport LNG as this is due to the pressures and temperatures required. The capacity of these type of vessels is expressed in  $m^3$ .

LNG tankers have recently grown to a capacity of  $154\,000\ m^3$  with a length over 300m, with the largest of this type reaching capacities of  $262\,000\ m^3$ . The growth of this type of vessel is given in Figure K.7.

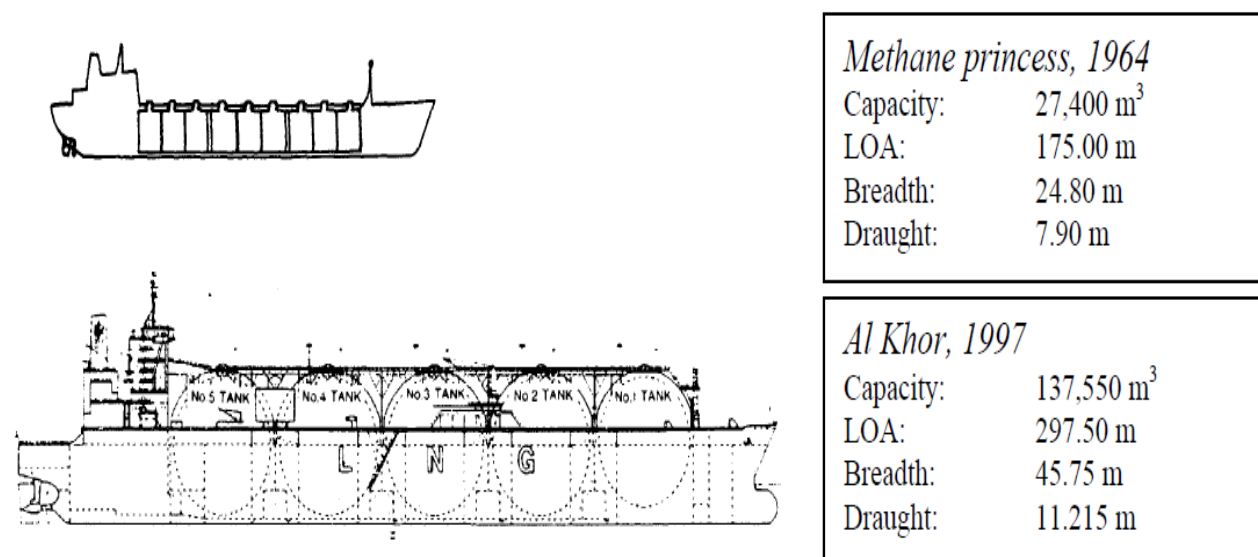


Figure K.7: The development of Liquid Gas Tankers (Ligteringen and Velsink, 2012)

### Product Tanker

A product tanker is defined as a vessel with independent tanks for the transportation of petroleum products in bulk according to Lloyd's Register. Many of these vessels have a dead weight capacity of less than 7500 tons, the international fleet of product tankers includes larger vessels with capacities of between 30 000 and 40 000 tons with the largest vessels having a capacity of 110 000 DWT.

### Parcel Tanker

This type of vessel is a specialised tanker for the transportation of refined oil products, such as diesel, paraffin and chemical liquids. The name parcel tanker is a result of the various relatively small compartments in the vessels hold that can be used separately for the transportation of various products in a single voyage.

### K.1.3 Container Vessels

Notwithstanding the introduction of the ULC into the handling of break-bulk cargo the turnaround time of cargo vessels in ports remained high. International trade increased rapidly and along with it, maritime transportation after WW2. This in turn led to heavily congested ports and extended waiting times for vessels wanting to load or unload.

The introduction of the container to international maritime transport in the 1960s led to increased productivity. This increased productivity is due to the fact that various pieces of cargo could be packed into a single container, which could then be handled in a single

lift.

The earliest containers had dimensions of 8ft by 8ft by 20ft or 2.44m by 2.44m by 6.1m. As a result of these dimensions the capacity of a container vessel or container storage yard is still expressed in Twenty Feet Equivalent Units (TEU's). This allowed for easy comparison between container vessels. Along with the standard 20ft units, 40ft units have been added for use by the container fleet. Along with these containers various specialised containers exist of specific purposes such as refrigeration containers for the transportation of temperature sensitive cargo.

The earliest container vessels were converted general cargo vessels that were converted to carry containers and are known as "first generation" container vessels. Since this "first generation" several additional classes of container vessels have been built with increasing dimensions and capacities, see Table K.3 an example of a Jumbo container vessel is given in Figure K.8.

Table K.3: Container Vessel Characteristics. (Ligteringen and Velsink, 2012)

Class	TEU Capacity	DWT (average)	Length(m)	Draught(m)	Beam(m)
1 <sup>st</sup> generation	750-1100	14 000	180-200	9	27
2 <sup>nd</sup> generation	1500-1800	30 000	225-240	11.5	30
3 <sup>rd</sup> generation	2400-3000	45 000	275-300	12.5	32
4 <sup>th</sup> generation	4000-4500	57 000	290-310	12.5	32.3
Post Panamax	4300-5000	54 000	270-300	12	38-40
Jumbo	6000-9000	90 000	310-350	14	43
Mega	13000+	157 000	400+	15.5	56



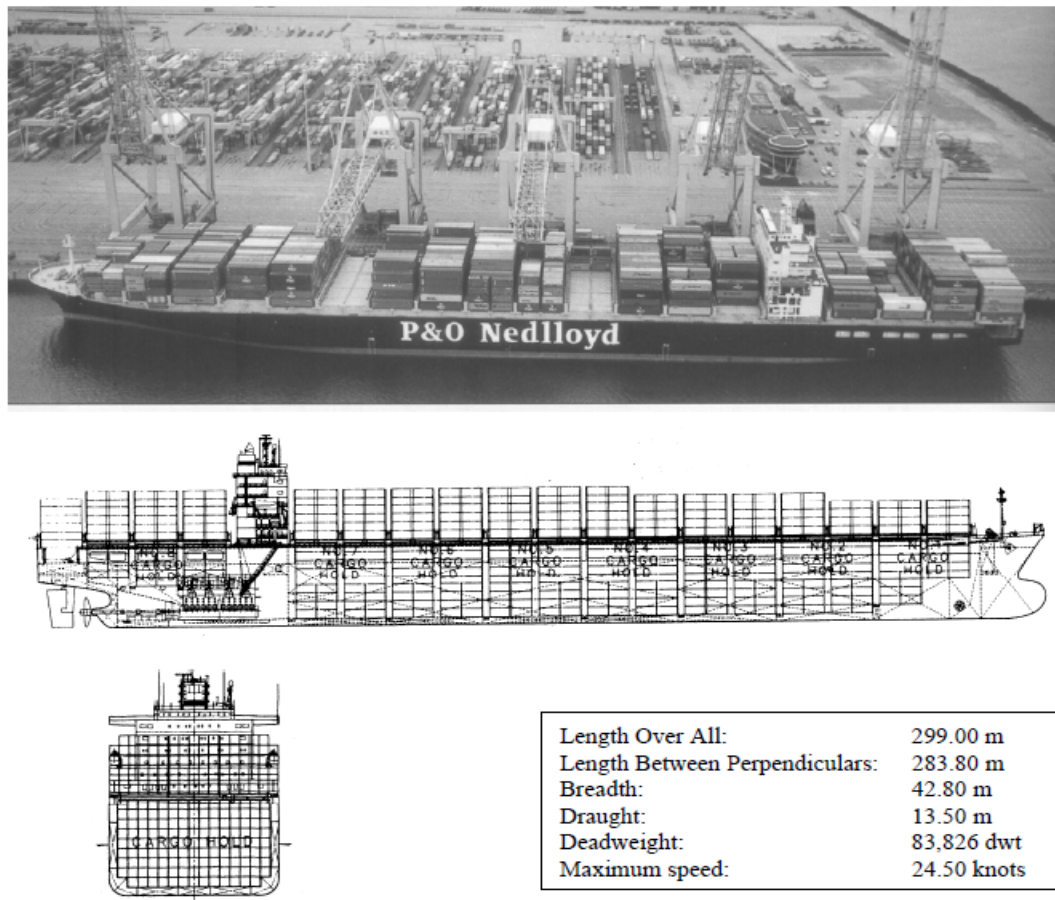


Figure K.8: Jumbo container vessel " P&O Nedlloyd Southhampton" (Ligteringen and Velsink, 2012)

# List of References

- africaports.co.za (2016). Saldanha bay.  
Available at: <https://africaports.co.za/saldanha-bay/>
- Agerschou, H., Dand, I., Ernst, T., Khoos, H., Jensen, J., Korsgaard, J., Land, J.M., McKay, T., Oumeraci, H., Petersen, J.B., Runge-Schmidt, L. and Scendsen, H.L. (2004). *Planning and Design of Ports and Marine Terminals*. 2nd edn. ThomasTelford.
- Boyce, L.W.A.T.S.L.S.S.G.M. (1996). *Slope Stability and Stabilization Methods*. ISBN 0-471-10622-4.
- BSI (1984). *British Standard Code of Practice for Maritime Structures*.
- BSI (2004). *Eurocode 7: Geotechnical Design - Part 1: General Rules*.
- Clayton, C.R., I.Woods, R., Bond, A.J. and Milititsky, J. (2014). *Earth Pressure and Earth-Retaining Structures*. 3rd edn. CRC Press Taylor & Francis. ISBN 978-1-4822-0661-6.
- Day, P. (2018). Private communication.
- GEOSLOPE (). Slope/w 2016.  
Available at: <https://www.geoslope.com/products/slope-w>
- inflation.eu (2018). Historic inflation south africa -cpi inflation.  
Available at: <http://www.inflation.eu/inflation-rates/south-africa/historic-inflation/cpi-inflation-south-africa.aspx>
- Jarvis, A. (1998). *Studies in the History of Civil Engineering: Volume 6 Port and harbour engineering*. Studies in the history of civil engineering ; v. 6. Ashgate, Aldershot [England]. ISBN 0860787559.
- Knappett, J. and Craig, R. (2012). *Craig's Soil Mechanics*. 8th edn. Spon Press. ISBN 978-0-415-56125-9.
- Ligteringen, H. and Velsink, H. (2012). *Ports and Terminals*. VSSD. ISBN 978-9065623041.
- MarineWiki (2010). Plimsoll-mark-lr.jpg.  
Available at: <http://www.marinewiki.org/index.php?title=File:Plimsoll-mark-LR.jpg>
- Meyerhof, G. (1963). Some recent research on the bearing capacity of foundations. *Canadian Geotechnical Journal*, vol. 1, no. 1.
- Meyerhof, G.G. (1951). The ultimate bearing capacity of foundations. *Geotechnique*, vol. 2, no. 4.

- SABS (2000). *Code of practice [for] the structural use of concrete (SABS 0100-1)*.
- Terzaghi, K. (1943). *Theoretical Soil Mechanics*.
- Centre for Civil Engineering Research and Codes (2005). *Handbook quay walls*. Taylor & Francis, Leiden. ISBN 0415364396.
- Anker Schroeder (2015). *Anchors for marine structures*. Tech. Rep., Anker Schroeder ASDO GmbH.
- CEN (2005). *Eurocode- Basis of Structural Design BS EN 1990:2002+A1*.
- Dassault Systems (). *Abaqus 2016*.  
Available at: <https://www.3ds.com/products-services/simulia/products/abaqus/>
- Marine Study (2016). *Definitions and ship dimensions*.  
Available at: <http://marineexam.blogspot.co.za/2016/08/ship-construction.html>
- SAICE Geotechnical Division (1989). *Lateral Support in Surface Excavations: Code of Practice*.
- Transnet National Ports Authority (2010). *Port of Saldanha*.  
Available at: <https://www.transnetnationalportsauthority.net/OurPorts/Saldanha/Pages/Overview.aspx>
- Thoresen, C.A. (2003). *Port Designer's Handbook: Recommendations and Guidelines*. Thomas-Telford. ISBN 978-08277-3228-6.
- Tsinker, G. (1998). *Handbook Of Port and Harbour Engineering: Geotechnical and Structural Aspects*. Springer-Science+Business Media, New York. ISBN 978-1-4757-0865-3.